

**MODULAR ORGANIZATION OF THE PRIMATE
CORTICOSTRIATAL SYSTEM**

by

Hemai Bharati Parthasarathy

B.A., Biophysics
The Johns Hopkins University, 1988

MIT LIBRARIES

FEB 8 1996

SCHERING

SUBMITTED TO THE DEPARTMENT OF BRAIN AND
COGNITIVE SCIENCES IN PARTIAL FULFILLMENT
OF THE REQUIREMENTS FOR THE DEGREE OF

DOCTOR OF PHILOSOPHY

at the

MASSACHUSETTS INSTITUTE OF TECHNOLOGY

February 1996

© 1996 Massachusetts Institute of Technology. All rights reserved.

Signature of Author _____

Department of Brain and Cognitive Sciences

December 8, 1995

Certified by _____

Professor Ann M. Graybiel

Thesis Advisor

Accepted by _____

Professor Gerald E. Schneider

Chairman, Department Graduate Committee

MASSACHUSETTS INSTITUTE
OF TECHNOLOGY

JAN 16 1996

SCHERING

LIBRARIES

ABSTRACT

Modular Organization of the Primate Corticostriatal System

by

Hemai Bharati Parthasarathy

Submitted to the Department of Brain and Cognitive Sciences on December 8, 1995 in
Partial Fulfillment of the Requirements for the Degree of Doctor of Philosophy in
Systems Neuroscience

The basal ganglia are a set of forebrain nuclei strongly interconnected with the cerebral cortex. The gross anatomical connections among these nuclei are fairly well understood. However, a more detailed understanding of the organization of this circuitry is clearly important for models and hypotheses of basal ganglia function. As a first step towards this understanding, we have studied the projections from relatively well-defined areas of the cerebral cortex to the striatum.

Initially, we studied the projections to the striatum from two areas of the frontal cortex, thought to code saccadic eye movements in different coordinate frames, the frontal eye field (FEF) and the supplementary eye field (SEF). We used electrical microstimulation in anesthetized macaque monkeys to identify each eye field and then placed one of two distinguishable anterograde tracers ($[^{35}\text{S}]$ methionine or WGA-HRP) in each area. Both of these eye fields sent distributed fiber projections to the striatum which converged on multiple zones (matrisomes) in the caudate nucleus and dorsolateral putamen. The existence of multiple distributed oculomotor-related matrisomes contributes to the growing notion of modularity in a seemingly homogenous striatum. Selective convergence within striatal modules could allow for novel recombination of information in the striatum.

In a second series of experiments, we demonstrated functional terminations of corticostriatal fibers in striatal matrisomes and showed a differential effect of these afferents on phenotypically defined subpopulations of striatal neurons. Taking advantage of a recently developed tracer, biotinylated dextran amine (BDA), we traced the fine arborizations and varicosities (thought to be synaptic terminations) of fibers from neurophysiologically-defined areas of squirrel monkey somatosensory cortex to modules in the striatum. Furthermore, we showed that electrical microstimulation of the primate cerebral cortex activates the expression of certain immediate early genes (IEGs) in striatal neurons within matrisomes defined by corresponding corticostriatal input. Our experiments indicate a selective influence of activity in somatosensory or motor cortex on the expression of Fos in parvalbumin-containing GABAergic interneurons and enkephalinergic projection neurons. This differential induction may be a spatial reflection of the striatal network response to cortical input.

Thesis Supervisor: Dr. Ann M. Graybiel, Walter A. Rosenblith Professor in
Neuroscience

ACKNOWLEDGEMENTS

I would like to thank Professor Ann Graybiel for the opportunity to work in her laboratory and for introducing me to the study of the basal ganglia. I would also like to thank my committee members, Professor Emilio Bizzi, Professor Peter Schiller, and Professor Jay Baraban for supervising this thesis.

For greatly easing my jumps through the hoops of graduate school, I am deeply grateful to Ms. Jan Ellertsen. For helping to coordinate the very last hurdle, I also thank Mrs. Rosalind Wood.

I would especially like to thank Dr. Robert Marini for his advice, assistance and support during my trials as a fledgeling animal surgeon. I thank him and the veterinary staff of DCM for their excellent care of our experimental animals.

I also thank Mrs. Sunsil Kim for having made Schering-Plough library such a pleasant and useful place when I first arrived at M.I.T.

For warmly welcoming me into their home and for saving me from living in my office during the final stages of my Ph.D., I thank Mr. and Mrs. Chin Lin.

For the many happy hours over many happy beers, and for sharing with me the delights of New England, I'd like to say "cheers" to Todd Holmes, Rachel Kindt, Alex Stewart, David Marshall, Eliot Charles, Bobby Dolan, Bob Snowden, Peter Brotchie, Catherine Cooper, Mary Herndon, Chris Stipp, Joe McIntyre, Nalin Vikramanayaka, Joachim Schultz, Steve Farber, Jonathan Wallach, Martha Marvin, Dan Chasman, Ai Yamamoto, Lisa Snider, Corrie Lathan, Louis Toth, Zohar Sachs, and of course, Martyn Bracewell.

In our laboratory, I thank Mr. Henry Hall for lending his photographic expertise to these experiments, for unstinting generosity particularly with regard to my favorite flavors of ice cream, and, unforgettably, for smoothly and efficiently taking charge of MRK5 on a disastrous morning. I also thank Drs. Alice Flaherty, Viveka Hillegaart, Elena Barragan, Rosario Moratalla, Mandar Jog, Chris Connolly, and Frank Eblen for stimulating comradery and advice in and out of the lab. I am especially indebted to Ms. Diane Major for being an unfailing source of valuable information about everything from TMB to afternoon tea. I am also grateful to her for her tenacious technical support, unflagging moral support, and superb companionship at the movies.

Finally, for her encouragement in the darkest of hours, for her friendship in the brightest, for teaching me countless things about the right way to do science, I owe an inestimable debt to Dr. Sabina Berretta. If my future collaborations are half as rich, I will consider myself unaccountably lucky.

And finally, finally, Thanks Mom and Dad!

INDEX

ABSTRACT	2
ACKNOWLEDGEMENTS	3
CHAPTER 1. Introduction. Functional Organization Of The Basal Ganglia	5-18
CHAPTER 2. Distributed But Convergent Ordering Of Corticostriatal Projections: analysis of the frontal eye field and the supplementary eye field in the macaque monkey	19-69
CHAPTER 3. Functional Terminations Of Cortical Afferents On Neuronal Subpopulations In Multiple Striatal Zones: cortically-driven immediate early gene expression in the squirrel monkey putamen	70-127
CHAPTER 4. Conclusions	128-130
REFERENCES	131-147
APPENDIX. Excitation Of The Motor Cortex Induces Fos, Jun B, and NGFI-A In The Rat Striatum	148-200

CHAPTER 1. Introduction. Functional Organization Of The Basal Ganglia.

The term basal ganglia unites a set of forebrain nuclei whose function is closely tied to that of the frontal lobe. The entire cerebral cortex sends a massive excitatory projection to the corpus striatum, which in turn sends GABAergic and neuropeptidergic signals to much smaller target nuclei, the globus pallidus (GP) and the substantia nigra (SN). Segments of these target nuclei send GABAergic projections to specific thalamic nuclei, which then send glutamatergic projections back to the frontal lobe. Thus the basal ganglia send information back to the cortex in what is often expressed as a cortico-basal ganglia-cortical loop (Fig. 1.1).

On this skeletal description of basal ganglia anatomy hangs a series of complex interconnections (Fig. 1.2). The substantia nigra pars compacta (SNpc) sends dopaminergic afferents to the striatum. The centromedian, parafascicular and midline thalamic nuclei are interconnected with the cerebral cortex and project to the striatum. The subthalamic nucleus (STN) is an important component of this circuitry in that it receives glutamatergic afferents from the cerebral cortex, GABAergic afferents from the external segment of the globus pallidus (GPe) and has excitatory projections to both segments of the globus pallidus, as well as to the SN and to the striatum. GPe itself sends GABAergic efferents to the internal segment of the globus pallidus (GPi), the substantia nigra pars reticulata (SNpr), and the nucleus reticularis of the thalamus (NRT). In addition to this forebrain interconnectivity, the SNpr sends a GABAergic projection to the superior colliculus; and this is the primary route for the basal ganglia influence on saccadic eye movements (Hikosaka and Wurtz, 1985). Not shown in figure 1.2 are the basal ganglia connections with the pedunculopontine nucleus or the dorsal raphe, nor are the limbic connections emphasized. (For a complete review of the anatomical connections of the basal ganglia, see Alheid et al., 1990).

At the level of the circuit as a whole, it has been argued that the basal ganglia are composed of several separable basal ganglia-thalamocortical circuits whose outputs were originally proposed to be: motor (supplementary and premotor areas), oculomotor (frontal eye field), dorsolateral prefrontal, lateral orbitofrontal, and anterior cingulate cortical

areas (Alexander et al., 1986; Alexander and Crutcher, 1990; Strick et al., 1995). Perhaps, though not necessarily, for each of these loops, there appears to be strong heuristic value in thinking of a direct pathway, from the striatum through GPi or SNpr to the thalamus, which has a net excitatory effect on the cortex (Deniau and Chevalier, 1985), and an indirect pathway, from the striatum through GPe, then STN, then to GPi, which has a net inhibitory effect on the cortex (Albin et al., 1989; Bergman et al., 1990). These two pathways may focus feed-forward excitation back to the cortex by coordinating suppression of unwanted cortical activity with facilitation of desired cortical activity (Mink and Thach, 1991; Smith et al., 1993).

Single unit electrophysiology studies in behaving monkeys have emphasized the concepts of context-dependence and preparatory set in describing the activity of neurons in the basal ganglia, particularly in the striatum (Hikosaka et al., 1989a; Hikosaka et al., 1989b; Alexander and Crutcher, 1990; Kimura, 1990; Ljungberg et al., 1992; Schultz and Romo, 1992; Jaeger et al., 1993; Aosaki et al., 1994). It appears that neuronal activity in the basal ganglia is primarily not related to direct parameters of movement execution, or even to movement initiation, but rather to associating specific motor programs to appropriate external or internal cues. For example, observed task-dependent differences in the discharge patterns of pallidal neurons during different visually-guided versus self-paced wrist-movement tasks were not related to wrist position, velocity, load or muscle activity (Mink and Thach 1991). In the striatum, premotor cortex (PMC) and supplementary motor area (SMA), similarities have been found among activity profiles during the preparatory phase of cued reaching tasks (Alexander and Crutcher, 1990). Neurons in all three areas were found to be simultaneously active throughout most of the interval between the instruction and the “go” signal.

Houk and Wise (1993) have suggested that striatal activity in response to specific patterns of convergent cortical input leads to disinhibition of thalamocortical modules. Reverberatory activity within these modules could be a mechanism for sustaining focused frontal cortical activity as a working memory (Goldman-Rakic, 1995), perhaps to be used in coordinating complex series' of actions.

A more sophisticated view of positive feedback through the basal ganglia to the cortex was put forward by Plenz and Braitenberg (1993). They argued that by virtue of their widely convergent cortical afferents, populations of striatal neurons become active with the coherent firing of cortical cell assemblies (Hebb's 'phase sequences' 1949). Sequential activation of these dynamically linked cortical units would lead to changes in the active population of striatal neurons. On the basis of arguments that GPe neurons integrate input from a larger number of striatal neurons than GPi neurons (Percheron et al. 1984) they proposed that GPe inhibits GPi neurons (directly or via the STN) until the coherent change in striatal activity exceeds the threshold established by the different integration factors. Once this minimal coherence had been exceeded, GPi neurons were proposed to facilitate thalamic afferent-recipient cortical cell assemblies in a process which would facilitate the further sequential activation of these cell assemblies.

While the aforementioned theories of basal ganglia function make some reference to dopaminergic signals as reinforcers, more explicit hypotheses of motor learning have also been advanced. Elegant studies by Wolfram Schultz and his colleagues have led them to suggest a role for learning in the basal ganglia. They have demonstrated that neurons in the substantia nigra fire optimally to unpredicted rewarding stimuli. If a conditioned stimulus predicts a reward, the response of single dopamine-containing neurons to the reward is quickly extinguished, and transferred to the conditioned stimulus (Romo and Schultz, 1990). Schultz and his colleagues have noted that contemporary learning theories depend on unpredicted rewards as key events during learning of a new behavioral response. Simultaneous dopamine release during such a reward onto the majority of striatal neurons engaged in highly differentiated neuronal processing related to a specific behavior could lead to reinforcement of that behavior (Schultz, 1995). The mechanism of reinforcement would involve both the focusing of striatal activity onto the strongest inputs (Wickens et al., 1991) and induction of long term facilitation.

A possible counterpart to this nigral activity has been found in the activity of tonically active neurons in the striatum. A coordinated pause in the activity of many of these neurons seems to be correlated with acquisition of associations between stimuli and reward. (Aosaki et al., 1994). However, in contrast to the response profiles of

dopaminergic neurons, tonically active neurons do not lose their responsiveness with overtraining. Aosaki and colleagues speculate that the striatum might maintain the record of conditioned behavior which the substantia nigra in part establishes.

In a more biochemical context, Wickens and Kötter (1995) have argued that dopamine reinforces the corticostriatal pathway by facilitating activity-dependent modification of those synapses (Calabresi et al., 1992). They have suggested that glutamate-induced elevation of intraspinal calcium allows for a window of time during which subsequent dopamine-induced elevation of cAMP can act synergistically to potentiate specific terminals via the phosphoprotein DARPP32.

Functional hypotheses concerning the basal ganglia, of which this is a representative rather than exhaustive list, must rely on the complex interaction among basal ganglia connections, the details of which are still not worked out. But the need for comparative analysis of these connections on a finer scale has been recognized and is being undertaken.

We have taken the organization of the corticostriatal system to be one of the crucial links in the functioning of the basal ganglia. The corpus striatum processes input from the cerebral cortex, the thalamus, dopaminergic and serotonergic systems. Of these afferents, the projection from the cerebral cortex is arguably the largest and perhaps the most information-specific. It has been estimated that each striatal neuron receives 10,000 synapses from the cerebral cortex (Wilson, 1995). We were interested in the degree of potential interaction among these cortical inputs within the striatum and the rules governing their convergence.

Cortical afferent fibers distribute themselves in multiple patches which span a large longitudinal extent of the striatum (Künzle, 1975; Künzle, 1977; Yeterian and Van Hoesen, 1978; Selemon and Goldman-Rakic, 1985; Cavada and Goldman-Rakic, 1991; Flaherty and Graybiel, 1991). While this distribution might be of 'incidental consequence' to developmental rules, as has been argued for facets of cortical organization itself (Purves et al., 1992), it might also be of a functionally-necessary design. Nelson and Bower (1990) described the computational usefulness of certain mapping constraints that could be applicable to the central nervous system. Patchy

afferent maps were found to be most useful for analysis which required both local and long-range interactions. Striatal neurons retrogradely labeled from GP and SN also occur in patches (Selemon and Goldman-Rakic, 1990; Flaherty and Graybiel, 1993). How these groups of input and output neurons relate to one another is still largely unknown (Percheron et al., 1994), but the computational possibilities depend on this relationship.

Unlike the cerebral cortex, the striatum, at first glance, is a homogenous mass of cells. In the primate, 75% of the striatal neurons are medium spiny neurons that project directly to striatal target nuclei (GPe, GPi, SNpr) (Graveland and DiFiglia, 1985). The remainder of the neuronal population consists of interneurons - including the large aspiny cholinergic cells, GABAergic interneurons which contain parvalbumin or calretinin, and neurons which colocalize somatostatin, neuropeptide Y, and nitric oxide synthase - that are distributed throughout the striatum (Wilson, 1990; Yelnik et al., 1991). However, within this cell mass, neurochemically distinct clusters of neurons (striosomes) were discovered which had special afferent and efferent connections, and restricted neuronal arborizations (for reviews, see Graybiel, 1990; Smith and Bolam, 1990; Gerfen, 1992). The obvious question was whether striosomes and the surrounding matrix comprised two coexisting but functionally independent systems or whether the patchy organization of striosomes afforded the opportunity of local interactions between striosome and matrix. Indeed while a large percentage of striatal projection neurons have dendritic arborizations restricted to one compartment (Walker et al., 1993), populations of interneurons send arbors between the two compartments (Cowan et al., 1990; Kawaguchi, 1992) and may thus facilitate functionally-important interactions within the striatum as a whole.

The patches delineated by the fiber projections from most cortical areas are found in the striatal matrix, and thus have been called *matrisomes* (Graybiel et al., 1993). Unlike striosomes, the neurochemically indistinct *matrisomes* may not be hard-wired, so for instance, projections from the somatosensory cortex, which is largely a continuous map of the body with some notable discontinuities (Werner, 1970), might be broken up into multiple representations within the striatum, but smoothly, such that density of striatal innervation by a given volume of cortex reflects some measure of functional-relatedness

of the cortical neurons within that volume (Fig.1.3). Such a situation is entirely speculative and in some ways analogous to the debate over whether cortical columns constitute discrete elements or blend smoothly into one another (Malach, 1994). But it seems a little easier to imagine smooth transitions than a situation in which clusters of “hand-related” neurons are completely distinct from clusters of “forearm-related” neurons, because it is difficult to know where the hand ends and the forearm begins, and it is otherwise difficult to imagine how plastic changes in the cortex (Merzenich et al., 1983) could then be meaningfully accommodated by corticostriatal projections. Furthermore, since matrisomal dimensions are often on the order of the dendritic arborization of striatal medium spiny neurons (ca. 500 μ m; Wilson, 1990), such a situation would allow for maximal diversity of dendritic sampling within the striatal population (Malach, 1994).

Despite advances in the understanding of the anatomical and chemical connectivity in the basal ganglia, significant knowledge regarding the functional corticostriatal synaptic organization is still lacking. Clearly, a detailed study of this projection system is necessary to understand the nature, organization and distribution of the information communicated by the cortex to the striatum.

We have designed experiments using traditional tract-tracing techniques to study the organization of corticostriatal projections in the primate. By using electrophysiological mapping to define cortical areas of interest, we took advantage of the available information on the organization of the cortex to aid us in understanding how such information is reorganized in the striatum. We also took advantage of multiple tracers to compare corticostriatal projections within single brains. Two such tracers, [³⁵S]methionine and wheat germ agglutinin-conjugated horseradish peroxidase (WGA-HRP), trace anterograde fibers with a relatively low resolution. The third, more recently developed anterograde tracer, biotinylated dextran amine (BDA), resolves terminal varicosities on corticostriatal fibers. Because individual variability of these connections is significant at the scale of analysis in which we are interested, cross-animal comparisons are of limited value to such studies. Thus, in Chapter 2, we study with distinguishable anterograde tracers ([³⁵S]methionine and WGA-HRP), the fiber projections to the

striatum from two oculomotor fields of the frontal cortex in individual brains of macaque monkeys.

In addition, we used the immunohistochemical detection of immediate early gene (IEG) proteins to assess the functional spatial influence of cortical afferents on striatal domains. The IEG proteins we chose, Fos and Jun B, are part of a class of transcription factor molecules which are rapidly induced in response to a variety of cellular signals (Sheng and Greenberg, 1990). These molecules, in turn, regulate the expression of so called “late response” genes in a complex cascade of transcriptional modulation. In relation to neuronal signaling, Fos and Jun B can be induced by calcium- or cAMP-dependent second-messenger cascades, which are initiated by depolarization or neurotransmitter-receptor binding (Morgan and Curran, 1991). The expression of these genes has been well-characterized in specific cell types of the rodent striatum in response to neurotransmitter analogs, and in many other parts of the brain in response to physiological stimuli (for review, see Hughes and Dragunow, 1995). In the rodent, electrical stimulation of the cortex induces the expression of Fos in the striatum, presumably by causing the release of glutamate onto striatal neurons (Fu and Beckstead, 1992; Wan et al., 1992; Besson et al., 1993; Parthasarathy et al., 1994).

We consider the use of immediate early genes in this paradigm to be a form of functional imaging. Such imaging, whether by deoxyglucose-related, cerebral-blood flow-related, or immediate-early gene induction-related methods is not without its drawbacks. Temporal information is severely compromised, if not virtually eliminated as in the case of IEG induction. Furthermore, in all cases, the exact relationship to electrophysiological activity is unclear. However, the induction of IEGs offers the possibility of transneuronal cellular resolution. Thus, in tandem with anterograde tracers, we have used electrical stimulation of the cerebral cortex to study the gross anatomical and cell-specific pattern of subsequent IEG induction in the primate striatum. In Chapter 3, we compare the distributions of corticostriatal fiber projections and terminal varicosities from the somatosensory and motor cortex of the squirrel monkey with cortically-driven immediate early gene expression in the striatum.

Finally, although the overall aim of this work is to understand the functional anatomical organization of the corticostriatal system, we wanted to examine in a little more detail the nature of the role of corticostriatal afferents in the regulation of immediate early genes. We therefore conducted experiments in the rat designed to open a window into the mechanisms by which these genes are induced in this system. These experiments are discussed in the Appendix.

Figure 1.1. Schematic illustration of selected important connections among nuclei in the basal ganglia. These pathways form a loop from cortex to striatum to target nuclei (globus pallidus and substantia nigra) to thalamus, and back to the cortex. The cerebral cortex is represented compartmentalized into its four lobes. The globus pallidus is divided into external (ext) and internal (int) segments. The substantia nigra is divided into its pars compacta (pc) and pars reticulata (pr).

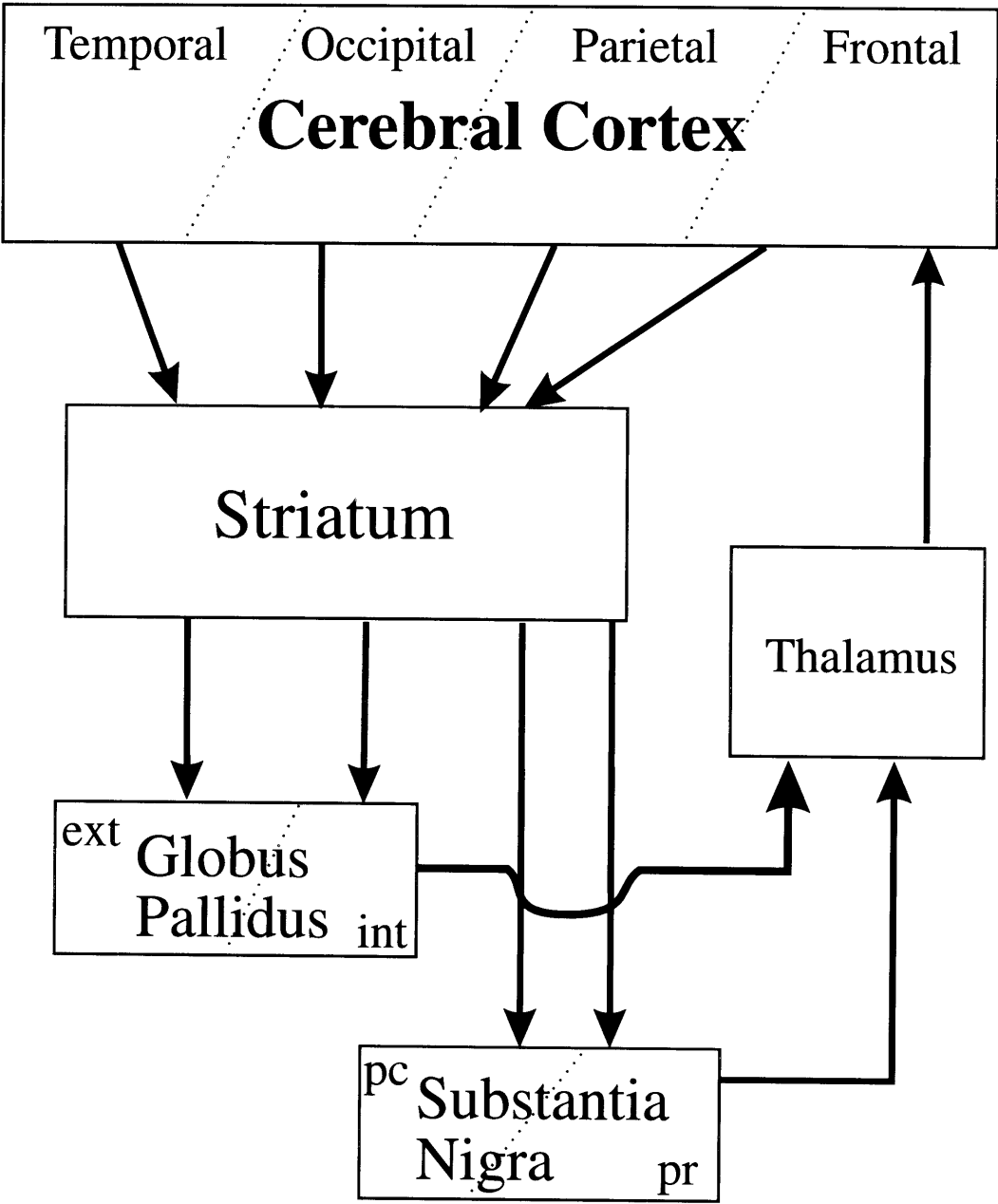


Figure 1.2. Schematic illustration of the majority of known connections among the basal ganglia nuclei. cmpf - centromedian-parafascicular nucleus complex, ext - external segment, int - internal segment, nrt - reticular nucleus of the thalamus, pc - pars compacta, pr - pars reticulata, SC superior colliculus, STN subthalamic nucleus.

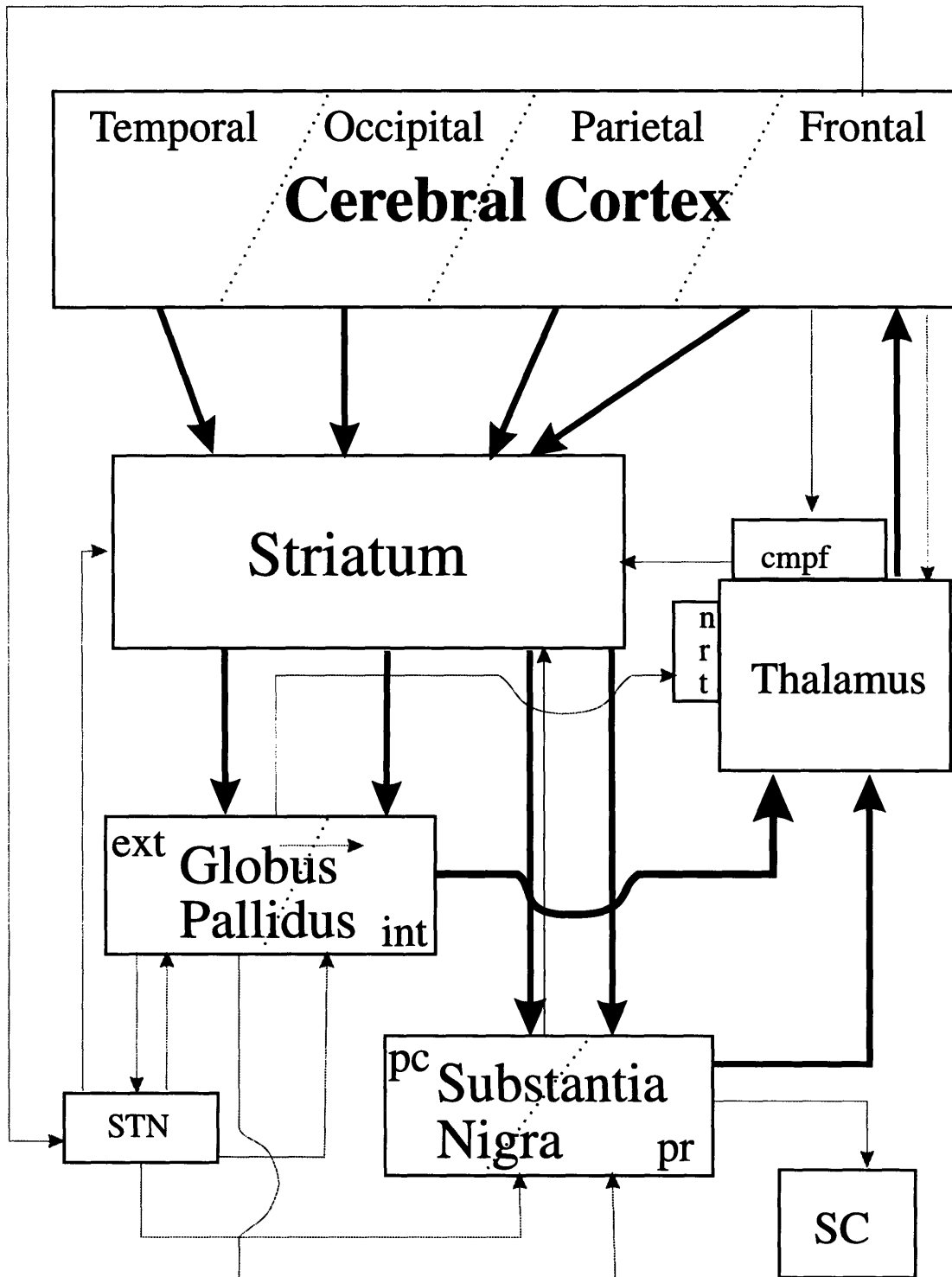
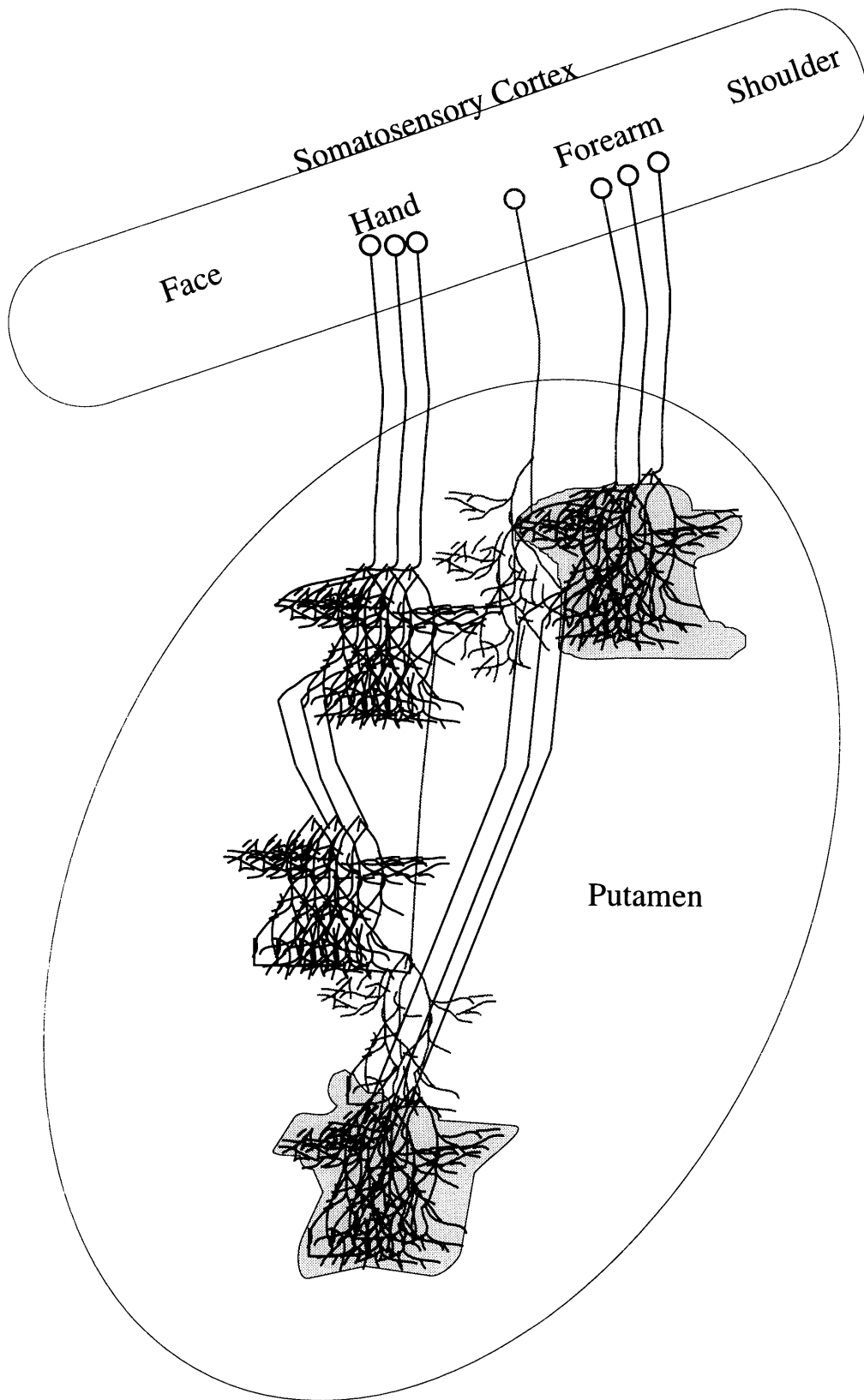


Figure 1.3. Schematic illustration of a hypothetical pattern of connectivity between somatosensory cortex and the striatum. In this diagram, corticostriatal axons arborize in two patches in the putamen. Neurons from the hand representation of somatosensory cortex send axons which largely overlap in the putamen. Similarly, corticostriatal terminals from the forearm representation of somatosensory cortex converge in multiple patches (shaded areas). Each “forearm patch” in the striatum may be continuous with a “hand patch”.



CHAPTER 2. Distributed But Convergent Ordering Of Corticostriatal Projections: Analysis Of The Frontal Eye Field And The Supplementary Eye Field In The Macaque Monkey*

ABSTRACT

The degree of parallel processing in frontal cortex-basal ganglia circuits is a central and debated issue in research on the basal ganglia. To approach this issue directly, we analyzed and compared the corticostriatal projections of two principal oculomotor areas of the frontal lobes, the frontal eye field (FEF) and the supplementary eye field (SEF). We first identified cortical regions within or adjacent to each eye field by microstimulation in macaque monkeys and then injected each site with either [³⁵S]methionine or wheatgerm agglutinin-horseradish peroxidase conjugate. We analyzed the corticostriatal projections and also the interconnections of the pairs of cortical areas.

We observed major convergence of the projections of the FEF and the SEF within the striatum, principally in the caudate nucleus. In cross-sections through the striatum, both projections were broken into a series of discontinuous input zones that seemed to be part of complex three-dimensional labyrinthes. Where the FEF and SEF projection fields were both present, they overlapped patch for patch. Thus, both inputs were dispersed within the striatum but converged with one another. Striatal afferents from cortex adjacent to the FEF and the SEF did not show convergence with SEF and FEF inputs, but did, in part, converge with one another. For all pairs of cortical areas tested, the degree of overlap in the corticostriatal projections appeared to be directly correlated with the degree of cortical interconnectivity of the areas injected. All of the corticostriatal fiber projections observed primarily avoided immunohistochemically identified striosomes. We conclude that there is convergence of oculomotor information from two distinct regions of the frontal cortex to the striatal matrix, which is known to project into pallidonigral circuits including the striato-nigro-collicular pathway of the saccadic eye movement system. Furthermore, functionally distinct premotor areas near the oculomotor fields often systematically projected to striatal zones adjacent to

* Reprinted in full from Parthasarathy et al., 1992, with permission from the publishers.

oculomotor field projections, suggesting an anatomical basis for potential interaction of these inputs within the striatum. We propose that parallel processing is not the exclusive principle of organization of forebrain circuits associated with the basal ganglia. Rather, patterns of both convergence and divergence are present and are likely to depend on multiple functional and developmental constraints.

INTRODUCTION

Theories about basal ganglia function have increasingly emphasized a parallel design of pathways emerging from the cortex, passing through the basal ganglia and returning to the cortex. Somatic motor, oculomotor, and complex loops have been distinguished for the frontal lobe's connections with the basal ganglia; and comparable parallel circuits have been hypothesized for other cortical domains (Graybiel, 1984; Alexander et al., 1986). Clear examples of convergence of corticostriatal input systems have been found (Yeterian and Van Hoesen, 1978; Flaherty and Graybiel, 1991a), and the anatomy of striatopallidal connections strongly suggests convergence of striatopallidal connections among areas of somatic sensory cortex that encode different modalities (Percheron et al., 1984). Thus, convergence may also be an important ordering principle, at least for basal ganglia circuits involving somesthesia (Flaherty and Graybiel, 1991a; Percheron and Filion 1991). In the experiments reported here, we set out to examine these issues of convergence and non-convergence by analyzing and comparing the patterns of projections to the striatum from two oculomotor fields of the frontal lobe.

The oculomotor system has major advantages as a test system for models of corticostriatal processing. First, physiological and anatomical evidence has strongly implicated regions of the striatum in the control of eye movements. In monkeys trained to perform tasks requiring saccadic eye movements, neurons in the caudate nucleus discharge in relation to intentional saccades (Hikosaka et al., 1989a); and in the substantia nigra pars reticulata, which receives input from the caudate nucleus, neuronal activity is also modulated during specific oculomotor tasks ranging from visually-triggered to memory-guided saccades (Hikosaka and Wurtz, 1983a; Hikosaka and Wurtz, 1983b). The modulation of neuronal activity in the nigral pars reticulata is an inhibition of tonic activity, that mirrors the excitation produced in the caudate nucleus. It is thought that the nigral neurons exert a tonic inhibitory effect on saccade-related neurons in the superior colliculus, and that this tonic nigrotectal inhibition can be relieved by striatal inhibition of the nigral neurons during the generation of saccades (Hikosaka and Wurtz, 1985a; Hikosaka and Wurtz, 1985b; Chevalier and Deniau, 1990). Thus, there is a discrete, functionally characterized, saccade-related circuit running through the basal ganglia with a well mapped representation in the striatum.

Second, previous work has shown that the two principal oculomotor fields of the frontal lobes, the medially located supplementary eye field (SEF) (Huerta and Kaas, 1990; Shook et al., 1991) and the laterally located frontal eye field (FEF) (Stanton et al., 1988) project strongly and discretely to a region of the caudate nucleus shown to contain units with oculomotor properties. There are important differences in the activity profiles of neurons in the two cortical fields. Microstimulation of the FEF elicits vector-coded saccades (Robinson and Fuchs, 1969; Bruce and Goldberg, 1985), whereas the SEF can be stimulated to produce saccades with amplitudes and directions that are dependent on eye position (Schlag and Schlag-Rey, 1987; Tehovnik and Lee, 1990). Recording studies in monkeys trained to make saccades have shown that in the FEF, neurons fire before, during, and after saccades of a specific direction and amplitude (Bizzi and Schiller, 1970; Bruce and Goldberg, 1985; Schall, 1991a). Furthermore, in dorsomedial cortex which probably includes supplementary motor area (SMA) as well as SEF, neurons have been found that fire during saccades to a given location in space (Schall, 1991b; Lee and Tehovnik, 1991). Thus, the cortical areas providing input to the oculomotor striatum have different processing parameters, and may even map oculomotor functions in different coordinate frames.

Third, these two oculomotor cortical fields are physically distant from one another, but are reciprocally interconnected (Huerta and Kaas, 1990; Schall et al., 1991). Thus, their corticostriatal projections provide an excellent system for testing the hypothesis that corticocortical and corticostriatal connectivity patterns are lawfully related (Yeterian and Van Hoesen, 1978).

We therefore carried out a series of experiments designed to compare the corticostriatal projections from the SEF and the FEF. To define the SEF and FEF cortex, we applied the technique of cortical microstimulation in ketamine-anesthetized monkeys. Then, combining dual-tracer tract tracing with immunohistochemistry, we examined the patterns of corticostriatal innervation with respect to each other and to the striosome-matrix compartmentalization of the striatum. In order to gain information about the more general topographic ordering of corticostriatal projections from the supplementary motor cortex and the periarculate cortex, we also made tracer injections in regions adjacent to the two eye fields.

METHODS

Cortical microstimulation and injection experiments were carried out on 8 macaque monkeys (6 *Macaca fascicularis* and 2 *Macaca mulatta*). In 6 monkeys, paired deposits of the distinguishable tracers, [³⁵S]methionine (200 uCi/ul, New England Nuclear) and wheatgerm agglutinin - horseradish peroxidase (WGA-HRP, 15% in saline; Sigma), were placed in the medial and lateral eye fields identified by stimulation, or in adjoining cortex (see Results). In one monkey, paired injections of the two tracers were made in topographically distinct regions of the FEF. In one other monkey, WGA-HRP was injected into the dorsomedial frontal cortex mapped for saccade-related activity under alert behaving conditions (Tehovnik and Lee, 1990; this animal is also monkey Q reported in Schall 1991b). Injection sites and volumes for the tracer deposits in each animal are summarized in Table 2.1.

Cortical microstimulation: Prior to surgery, each animal was tranquilized with ketamine (12 mg/kg) and anesthetized with xylazine (0.7 mg/kg). In addition, atropine (0.04 mg/kg), dexamethazone (0.1 mg/kg) and tribriassin (30 mg/kg) were administered. Anesthesia was maintained by ketamine (in doses of 5 mg/kg) and supplemented, before surgical procedures, by Xylazine (0.7 mg/kg). Lactated Ringer solution with 5% dextrose (2.3 ml/kg/hr IV) was given throughout the experiment.

In preparation for stimulation, the left frontal convexity cortex was exposed under sterile surgical conditions by removal of a bone flap. A metal post was cemented to the skull to provide painless restraint and head support without stereotaxic ear bars. The FEF and the SEF were located by monitoring eye movements visually during intracortical microstimulation. Stimulus trains (cathodal, 0.2 msec pulsewidth, 300 Hz) were delivered for 50-100 msec through low impedance (.5 - 1.0 Mohm) glass-coated platinum-iridium microelectrodes. Currents ranged from 30 to 100 μ A at most sites. Apparently because of difficulties in maintaining the same level of anaesthesia throughout the physiological mapping phase of the experiments, higher currents were sometimes needed to elicit any movements whatsoever. Such sites are indicated on the maps generated.

Sites of electrode penetrations were marked on an enlarged photograph of the exposed cortex. To locate the FEF, we stimulated along the anterior lip of the arcuate sulcus and in

adjoining cortex. To locate the SEF, we stimulated along the dorsomedial edge of the convexity cortex, starting at approximately the same anteroposterior level as the FEF and mapping rostrally and caudally, as well as medially and laterally. We tried to identify the rostral part of the supplementary motor area (SMA) by monitoring upper body and head movements in response to the cortical microstimulation. Because eye movements were monitored visually, and also because ketamine may disrupt the oculomotor neural integrator (in cats, Godaux et al., 1990), the SEF and the FEF defined here are probably biased toward regions from which relatively large saccades can be elicited.

Tracer injections: In all but one experiment (M7), tracers were introduced into the cortex through glass micropipettes at sites determined during the mapping session and identified by reference to the photographic print on which stimulation sites were marked. The micropipettes were attached to a pressure-injection system (Picopump, World Precision Instruments) capable of delivering tracer in aliquots as small as 1-2 nl. In case M7, tracer injections were made with a Hamilton syringe that was held in the same well used for chronic microelectrode recording studies performed on that animal (Tehovnik and Lee, 1990). Injection sizes were varied between ca. 15 - 200 nl of WGA-HRP or [³⁵S]methionine at each of the sites within each cortical area (Table 2.1).

Tissue preparation and histology: Following ca. 48-hour survival times, the monkeys were deeply anesthetized with ketamine (average - 16 mg/kg), followed by Nembutal (average - 20 mg/kg) and were perfused transcardially with 4% paraformaldehyde in 0.1 M PO₄ buffer containing 0.9% saline. Brains were photographed and blocked in the transverse or midsagittal plane, and the blocks, after being soaked in buffer containing 20-30% sucrose or glycerol, were cut on a freezing microtome at 40 μm in coronal or sagittal sections. Sections were processed in serially adjacent sets for autoradiography, WGA-HRP histochemistry and enkephalin immunohistochemistry.

For autoradiography, sections were mounted on chrome-alum subbed slides, dried, defatted, dipped in Kodak NTB-2 emulsion, dried again, and stored in light-tight boxes at -20°C for 1-8 weeks. The exact exposure times were estimated by trials, and typically, series of sections were prepared at different exposure times for each case. Sections were developed in Kodak D19 developer and counterstained through the emulsion. WGA-HRP histochemistry was carried out

by Mesulam's tetramethyl benzidine (TMB) method (Mesulam, 1978) with the modification that the incubation solutions were changed every 3 minutes to decrease accumulation of artifact (Illing and Graybiel, 1985). Immunohistochemistry with a polyclonal met-enkephalin antiserum (kind donation of Dr. R.P. Elde) was carried out to demonstrate striosomes (Graybiel and Chesselet, 1984). Either the avidin-biotin (ABC) or the peroxidase-antiperoxidase (PAP) method was followed after treatment of the sections with 10% methanol and 3% H₂O₂ to eliminate cross-reaction with WGA-HRP and to inhibit endogenous peroxidases.

Data analysis: Sites of microstimulation and sites of tracer injections were mapped onto reconstructions of the frontal cortex made with the aid of the photographs taken at the time of mapping and after perfusion. Borders of effective injection sites, including central zones and surrounding regions of weaker labeling, were determined by eye according to the intensity of tracer visible. Sections were viewed with darkfield and lightfield optics, and, for WGA-HRP, with cross-polarized darkfield illumination (Illing and Wassle, 1979). Patterns of transported anterograde tracer labeling were charted with the aid of a drawing tube in serial sets of sections processed for autoradiography and for WGA-HRP, and striosomes in adjoining sets of sections stained for enkephalin-like immunoreactivity were also charted. Charts of adjacent sections were aligned according to local vascular landmarks, and the distributions of the anterograde tracers were plotted with respect to each other and to the location of striosomes visible as zones of reduced perikaryal enkephalin-immunostaining relative to the surrounding matrix. Charts were also made of transcortical connections. Because the TMB reaction was susceptible to artifact from tissue damage along the pipette tracks, it was often impossible to chart reliably the anterograde WGA-HRP labeling in and near the [³⁵S]methionine injection sites. Judgements of interconnectivity, therefore, typically were made on the basis of one corticocortical direction, i.e., in the anterograde direction from the [³⁵S]methionine injection; and all illustrations of cortical connectivity are shown for this direction only. Mention of intracortical transport of WGA-HRP is made in the text where possible.

RESULTS

Repeated microstimulation at any one site in the cortex anterior to the arcuate sulcus elicited contraversive saccadic eye movements that appeared qualitatively similar to one another, and longer stimulus trains elicited "staircase saccades". No other obvious movements accompanied these saccades. As documented in previous studies of this area (Robinson and Fuchs, 1969; Bruce and Goldberg, 1985), a progression of larger to smaller saccades was found as the stimulating electrode was moved from medial (anterior) to more lateral (posterior) sites along the anterior bank of the arcuate sulcus. We identified as the FEF a discrete region, usually found immediately anterior to the arcuate genu, from which this pattern of saccades could be elicited with microstimulation currents under 50 μ A. Microstimulation of prearcuate cortex along the upper limb of the arcuate sulcus, rostral to the FEF so defined, also elicited saccades (Robinson and Fuchs, 1969). However, these saccades had larger thresholds and were often accompanied by ear or neck movements. It has recently been reported that a region at the fundus of the arcuate cortex is involved in the control of smooth pursuit eye movements (MacAvoy et al., 1991). We did not identify such an area, but it is possible that the deepest FEF tracer injections encroached on this territory.

Microstimulation of the cortex along the dorsomedial part of the frontal convexity cortex, in the expected region of the SEF, elicited eye movements less reliably than microstimulation of the arcuate cortex. Considerable mapping, over as much as 10-15 mm anteroposteriorly and 5 mm or more mediolaterally, was often required to identify a discrete eye movement field. The lowest currents used for microstimulation were 50 μ A. In 6 monkeys (M1, M2, M3, M5, M8, M9), we identified relatively circumscribed medial convexity cortex within which microstimulation elicited contraversive saccades. The saccadic response often habituated with repeated stimulation, and it typically was accompanied by movements of the ear and facial muscles, even at sites with very low movement-evoking thresholds. In most of the monkeys, the medial eye field so identified seemed to correspond to the SEF as originally described by Schlag and Schlag-Rey in the macaque (1987): it lay just anterior to cortex in which upper body and head movements could be triggered by microstimulation; and it was several millimeters medial

but only slightly anterior to the FEF. We considered this region to be the SEF. In one monkey (M3), the region from which we elicited saccades lay farther anterior, as documented below.

In the course of our experiments, we injected (a) the FEF and the SEF, as defined by low-threshold microstimulation; (b) the dorsal limb of the arcuate sulcus (from which saccades could also be elicited at stimulation thresholds exceeding 50 μ A); and (c) adjoining territories of the dorsomedial frontal cortex and of the periarculate cortex.

Characteristic properties of corticostriatal projections from the FEF and from cortex in and adjacent to SEF.

Injections both in the FEF and in the medial cortex labeled corticostriatal fibers in a considerable part of the caudate nucleus (Fig. 2.1), but the fiber projections traced to the striatum from the SEF and adjacent cortex were larger than the projection traced from the FEF, even for medial injection sites smaller than the corresponding FEF injection sites. Injections in SEF and adjacent cortex labeled a strongly bilateral projection to the caudate nucleus and to localized, mainly adjoining, parts of the putamen. The projection field extended from approximately the level of the anterior pole of the putamen (ca. A24 in the cynomolgus macaque (Szabo and Cowan, 1984)) to the level of the posterior body of the the caudate nucleus (ca. A9). By contrast, the corticostriatal projection traced from the FEF began at about the anteroposterior level of the anterior commissure (ca. A19). The FEF projection fields were restricted to the caudate nucleus, striatal cell bridges, and a discrete dorsomedial zone in the putamen and invariably were much stronger on the ipsilateral than on the contralateral side. Contralateral labeling was present only in regions of the caudate nucleus corresponding to those most heavily labeled on the side ipsilateral to the FEF injection. The parasagittal section illustrated in Fig. 2.1, taken through the medial caudate nucleus, illustrates the full anteroposterior length of a typical FEF projection field. The SEF projection field illustrated, although much larger, actually underrepresents the projection because at more caudal levels, the SEF projection was centered quite laterally in the caudate nucleus.

In all cases, the corticostriatal projections were broken up into densely labeled focal zones less than a millimeter in diameter. These appeared in transverse as well as sagittal sections as patches of tracer labeling in a surrounding field of much weaker labeling. Serial-section

reconstructions of the distributions of individual tracers was not possible, because we stained sequential sections for the two tracers and for enkephalin to permit accurate three-way comparisons. Nevertheless, the broken series suggested that many of the input zones that appeared as patches in single sections eventually joined together to form complex three-dimensional aggregates.

Overlapping corticostriatal projection fields are labeled from physiologically guided tracer injections in the SEF and the FEF.

In case M1 (Figs. 2.2A, 2.3, 2.4), we made more than 60 penetrations in order to map out the two cortical eye fields. Microstimulation of cortex at the genu of the arcuate sulcus clearly defined a discrete FEF from which only contraversive saccades could be elicited with currents under 50 μ A. The dorsomedial eye field identified as SEF was clearly delimited by unresponsive cortex and, especially caudally and medially, by cortex in which arm and neck movements could be elicited at low threshold without concomitant eye movements (Fig. 2.3A). This oculomotor field was centered approximately 5 mm lateral to the medial edge of the hemisphere and was slightly anterior to the FEF. A single injection of [³⁵S]methionine was made in the SEF and 2 closely spaced deposits of WGA-HRP were made into the FEF (Table 2.1). Both injection sites (SEF - 4 mm diameter, FEF - 3 mm diameter) were continuously labeled and spanned all cortical layers (Fig. 2.3B). Dense anterograde labeling from the SEF injection site was present bilaterally in the anterior bank of the arcuate sulcus, including the FEF injection site on the ipsilateral side and the corresponding region of arcuate cortex in the contralateral hemisphere (Figs. 2.4A, 2.9A).

The corticostriatal projections labeled in this case systematically overlapped one another. As illustrated in Figs. 2.2A and 2.3C, almost every one of the FEF input patches seen in individual sections fell within the bounds of a zone innervated by the SEF. However, the FEF and SEF projections were by no means identical. The FEF input patches were smaller than the SEF patches and the center of gravity of the FEF projection zone in the caudate nucleus was shifted slightly medially with respect to that of the SEF. Thus, there was often a small patch of FEF-derived label medial to the zone of overlap. In keeping with the patterns of corticostriatal projection observed in other cases of SEF and FEF injections, the SEF projection labeled had a

larger anteroposterior field of innervation, and it was strongly bilateral. The smaller FEF injection labeled a projection that was almost entirely confined to the ipsilateral striatum and that extended as far caudally as the SEF projection, but that began 4 - 5 mm posterior to the rostral appearance of the SEF projection field. The FEF injection labeled a few closely spaced patches in cross sections throughout the body of the caudate nucleus, and was restricted in the putamen to a dorsomedial region, except at the posterior end, where a pattern of strong crisp patches appeared throughout the putamen's dorsoventral length. Nearly all of these FEF input patches overlapped with SEF input zones, but the larger extent of the labeled SEF projection left large parts of that projection unmatched.

The input patches labeled by the SEF injection site varied in size from anterior to posterior. Anteriorly (ca. A23 to A18 in this rhesus macaque (Snider and Lee, 1961)), they were very small (200-300 μm) both in the caudate nucleus and in the putamen. Farther posteriorly, in the caudate nucleus, cell bridges, and dorsal putamen, the patches seem at once to coalesce and to become more diffuse, so that the projection field appeared as an almost confluent set of heavily labeled patches running in a single diagonal band through the middle of the striatum. The smaller patches in the middle and ventral putamen persisted only as far caudally as ca. A16, the level at which the anterior commissure crosses the midline, and then the projection became limited to one patch in the ventrolateral caudate nucleus and one patch in the dorsomedial putamen. This pattern persisted into posterior levels of the putamen, where once again many discrete patches appeared. The SEF projection to the caudate nucleus faded caudally and ended in the posterior body of the caudate nucleus.

The fiber projections from the two eye fields to the thalamus and the superior colliculus were also charted. In the ipsilateral thalamus, the SEF projection field almost completely included the FEF projection field (Fig. 2.4B). Zones of overlap were most obvious in the mediodorsal nucleus and in nucleus X. In the ipsilateral superior colliculus, however, the SEF projection was much weaker and was, unlike the FEF input, accompanied by a faint contralateral projection. The zone of SEF projection was shifted medially with respect to that of the FEF so that the two only partially overlapped (Fig. 2.4B).

Adjacent corticostriatal projection fields are labeled from the pre-SMA and the FEF.

In case M2 (Fig. 2.5), we placed a deposit of [³⁵S]methionine medial to the eye movement territory identified as the SEF, and mapped (Fig. 2.5A) and injected an equal amount of WGA-HRP into the low-threshold arcuate FEF (Table 2.1). For this monkey, higher stimulation currents were needed to elicit movements from the dorsomedial cortex than for case M1, and the mapping was not as extensive as that for case M1. Nevertheless, we did observe a caudal-to-rostral progression in which arm movements followed by ear and eye movements were elicited by microstimulation. The tracer was injected medial to the eye movement territory, along the medial wall of the hemisphere in the superior frontal gyrus (Fig. 2.5B). This cortex appears to correspond to a rostral region of the supplementary motor cortex (the medial part of area 6a β of Vogt and Vogt or area F6 of Luppino et al., 1991), which does not share somatotopy with the more caudal SMA. The injection site will be referred to provisionally as being centered in the pre-SMA (Tanji et al. 1991, see Discussion).

This pre-SMA injection site ([³⁵S]methionine) confluent labeled cortex extending 3-4 mm along the shoulder and medial bank of the superior frontal gyrus, and included all cortical layers. The WGA-HRP injection in the FEF was centered in the rostral lip of the arcuate sulcus, spanned 5-6 mm along the anterior bank, and spread rostrally approximately 3-4 mm from the sulcus as well as into the underlying white matter. The pre-SMA injection was centered 1-2 mm anteriorly to the FEF injection site center. Anterograde autoradiographic labeling from the pre-SMA injection appeared in the postarcuate cortex and along the dorsal and ventral limbs of the arcuate sulcus, but very little labeling was detectable in the prearcuate cortex (Fig. 2.9D). Thus the two cortical sites injected were not transcortically connected, at least in this direction.

In the striatum, there was very little overlap of the corticostriatal projections traced from these FEF and pre-SMA injections. The projection from the FEF was still very similar to that of the previous case (Fig. 2.5C), despite the larger size of the FEF deposit. The pre-SMA projection to the rostral striatum appeared as tiny patches in the putamen and the ventrolateral caudate nucleus (much like the SEF projection field). However, by the level of the crossing of the anterior commissure (ca. A18), the clusters of labeled fibers in the putamen became very large and diffuse and the putamen became the main target for the projection along with the lateral caudate nucleus. Thus, the pre-SMA injection, centered medial to the field from which eye movements

were evoked, labeled much more of the putamen than the SEF injection site in the convexity cortex of case M1. Farther posteriorly, the fibers labeled from both injection sites terminated in patches in the caudate nucleus and adjoining dorsomedial putamen. There was a striking tendency for the two sets of patches to lie adjacent to one another where both appeared at the same level.

Tissue was not available for mapping projections to the posterior striatum, the thalamus, and the superior colliculus.

Non-convergent corticostriatal projections are labeled by tracer injections in rostral pre-SMA eye movement cortex and the FEF.

In an attempt to repeat the paired convexity SEF/FEF injections, we once again mapped out and injected the medial and arcuate eye movement territories in case M3, injecting WGA-HRP into the medial cortex and [³⁵S]methionine into the arcuate cortex (Table 2.1). Unexpectedly, we found practically no overlap of the labeled projection fields in the striatum (Fig. 2.6). However, a hallmark of the SEF is its cortical interconnectivity with the FEF, and in this case, there was no labeled fiber projection from the FEF injection site detectable at the site of injection in the dorsomedial cortex. Instead, anterograde label traced from the FEF deposit appeared in dorsomedial cortex several millimeters posterior to the injection site, at about the same transverse level as the FEF. Both anterograde and retrograde labeling from the medial injection site were present in the periarculate cortex, but the label was in columnar zones within the posterior bank of the arcuate sulcus and at the fundus of the sulcus, and did not appear in the anterior bank and lip of the sulcus, where the FEF injection site was located (Fig. 2.9E). We will use the term, pre-SMA eye movement cortex, to refer to the cortical zone injected because of its anterior location relative to the FEF and to FEF-innervated medial cortex.

The corticostriatal projection traced from this eye movement cortex appeared very far anteriorly in the caudate nucleus, and labeling was prominent on the contralateral as well as on the ipsilateral side. The projection field included more of the putamen than did the SEF projection in case M1, but less than did the pre-SMA projection in case M2. It began to fade at about the level where the striatum is completely split by the fibers of the internal capsule (ca.

A15), somewhat anterior to the level at which the SEF projection in case M1 dwindled. The FEF projection field had an anteroposterior distribution similar to that seen in case M1.

In the striatum (Fig. 2.6C), although the FEF input patches were often next to the pre-SMA input patches, and occasionally interdigitated with them, the two sets of patches rarely overlapped. The only convergence between them was in the striatal cell bridges splitting the internal capsule, and the amount of convergence was small.

Thus, although we are confident that we injected cortical territory from which we could elicit eye movements, both medially and laterally, there were neither interconnections between the two cortical sites injected nor (with rare exceptions) converging corticostriatal projections from them. There was no evidence for convergence of the outputs of these two cortical fields within the thalamus or superior colliculus, either. In the thalamus, most of the labeled FEF fibers were medial to the labeled pre-SMA fibers. We could find no transport of WGA-HRP to the superior colliculus from the pre-SMA eye movement cortex.

Overlapping corticostriatal projections are labeled from the SEF and the dorsal arcuate cortex.

The FEF injections in the cases just described were aimed at the cortex of the arcuate genu, which has very low microstimulation thresholds for evoking saccades (Bruce and Goldberg, 1985). However, eye movements also can be evoked from cortex adjacent to this low-threshold area (Mitz and Godschalk, 1989), and it has been shown that prearcuate cortex along the dorsal limb of the arcuate sulcus, the "large eye movement" territory (Robinson and Fuchs, 1969), projects more anteriorly in the striatum than does the low threshold FEF (Stanton et al., 1988). Because we had found in case M1 that the projection to the striatum from the SEF reached more anteriorly than that of the low-threshold FEF, we wondered whether there would be overlap of this more anterior part of the SEF projection field with corticostriatal inputs from the dorsal limb of the arcuate sulcus. We first tested, and confirmed, the arcuate dorsal limb topography by making paired tracer injections in the arcuate eye field of case M4, placing WGA-HRP at the genu of the arcuate sulcus and [³⁵S]methionine in the cortex of the dorsal limb of the sulcus (data not shown). Consistent with observations in single-tracer studies (Stanton et al., 1988), we found that the dorsal limb cortex projects to a larger, more anteriorly placed and more dorsal projection field in the caudate nucleus than does the genual cortex.

Therefore, in M5, we paired a small SEF injection (WGA-HRP, ca. 3 mm diameter) with a much larger injection ([³⁵S]methionine, ca. 3 mm X 8 mm) extending along a large part of the dorsal limb of the arcuate sulcus as well as the dorsal part of the genu of the sulcus (Fig. 2.7). The arcuate injection site encroached slightly into the post-arcuate cortex at the genu, and the SEF injection site spread to the upper part of the medial wall of the hemisphere (Fig. 2.7B).

Transcortical fibers labeled by the FEF injection projected to a wide zone of medial cortex that included the SEF injection site (Fig. 2.9B). WGA-HRP was retrogradely transported from the SEF injection site to periarculate cortex, but the label was concentrated primarily in the anterior and posterior banks of the genu. There was partial corticocortical connectivity of the two injected sites, with genual cortex apparently being the main area of the arcuate cortex that was connected with the SEF.

There was considerable overlap of the two projection fields in both the caudate nucleus and the putamen (Figs. 2.2B and 2.7). In the putamen, the overlap was patch for patch; but in the caudate nucleus, the arcuate input zone labeled was shifted medially and dorsally with respect to the labeled SEF input zone.

The dorsal arcuate cortex projected quite strongly throughout the length of the head and body of the caudate nucleus and the heaviest label appeared dorsally and centrally. In the putamen, tiny discretely labeled patches were present in both the most anterior and the most posterior sections (data not shown); but there was very little tracer visible elsewhere in the putamen, except at its dorsomedial edge. In spite of a very strongly labeled ipsilateral corticostriatal projection from this large injection site, there was less label in the contralateral striatum than would have been produced by a comparable medial cortex projection.

The SEF projection field labeled in this case was restricted to parts of the caudate nucleus and putamen that abutted the internal capsule, to the cell bridges within it, and to discrete patches in the very posterior putamen. The SEF labeling became visible a few millimeters farther posterior than in other cases (ca. A20), a few millimeters rostral to the crossing of the anterior commissure. The restricted size and pattern of the SEF projection suggests that the injection site did not include the entire SEF. Accordingly, in spite of the considerable overlap of the two projections in the lateral caudate nucleus and medial putamen and in the

striatal cell bridges, the amount of overlap between the SEF and the anterior arcuate may be underestimated in this case (compare Fig. 2.2A and Fig. 2.2B).

In keeping with the similarities between thalamic and striatal projections observed in other cases, the projection from the SEF and the FEF also showed considerable but incomplete overlap in the thalamus (data not shown). There was no label from the SEF injection in the superior colliculus.

Corticostriatal projections from the medial superior frontal gyrus and the periarculate cortex suggest their convergence in the putamen.

In order to follow up on our finding of massive labeling of the putamen following injection of the medial face of the superior frontal gyrus in case M2, and the increase in putamenal labeling we saw from the one FEF injection that included the post-arcuate cortex (in case M5), we paired a medial superior frontal gyrus injection with an injection in periarculate cortex that extended through the fundus of the arcuate sulcus onto the postarcuate convexity cortex (case M6, Fig. 2.8). We had already noted the presence of strong corticocortical connections between the medial superior frontal gyrus and the postarcuate part of area 6 in case M2 (Fig. 2.9C). Guided by these results, we injected WGA-HRP along an 8-9 mm extent of medial cortex in the vertical wall of the superior frontal gyrus and made a large injection of [³⁵S]methionine into pre- and post-arcuate cortex (Table 2.1). This site presumably corresponded to the SMA and perhaps also to the pre-SMA. The injection site placement was based on cortical topography alone; there were difficulties in maintaining appropriate levels of anesthesia during the experiment and, in fact, we were unable to identify reliably a discrete dorsomedial oculomotor field to which we could directly relate our injection into the medial cortex.

Transcortical autoradiographic labeling from the pre- and post- arcuate injection site clearly overlapped with the site injected in the medial wall of the hemisphere (Fig. 2.9C). In addition, anterograde WGA-HRP labeling from the medial injection site was found along the post-arcuate cortex of the genu and lower limb.

Along with a labeled fiber projection to the caudate nucleus that was reminiscent of that seen in other cases, we observed a discretely patchy projection from the large arcuate injection site to the main body of the putamen in this case -- a projection not labeled in the other cases

with FEF injections, in which the tracer deposit did not reach the arcuate fundus and postarcuate cortex. The putamen projection in M6 converged at many points with the more diffusely labeled projection from the medial cortex to the putamen (Fig. 2.8). This overlap makes it likely that the fundal/postarcuate cortex and the medial wall cortex send at least partly, and probably highly convergent projections to the putamen. By contrast, in the caudate nucleus, the patches respectively labeled from the two injection sites were largely non-convergent. In fact, the pattern of labeling in the caudate nucleus was quite similar to that of case M2, in which a large medial wall injection was paired with an injection confined to the prearcuate genual cortex.

The corticostriatal projections from dorsomedial cortex and arcuate cortex follow different topographic ordering.

Despite the fact that no simple topographic rule seemed to account for the pattern of dispersed and often farflung patches of corticostriatal input (see Discussion), we found that cortical topography was predictive of the relative distributions of projections to the striatum labeled from local territories in and around the FEF and SEF (Fig. 2.10). In the dorsomedial frontal cortex, we injected laterally placed sites in the dorsal convexity cortex (Fig. 2.9A and B) as well as more medial sites, including cortex along the medial bank (Fig. 2.9C and D). Comparing the labeled projections resulting from progressively more medial injection sites (Fig. 2.10A-C), we saw a corresponding shift of striatal projection fields from one that was centered dorsally in the caudate nucleus (Fig. 2.10A) to one that was centered ventrally in the putamen (Fig. 2.10C). There was a similar ventral shift of projection patterns within the striatum for arcuate injection sites placed at successively more posterior locations along the dorsal limb of the arcuate sulcus (Fig. 2.10D-E).

Corticostriatal projections from oculomotor and premotor areas of the frontal lobe terminate primarily in the extrastriosomal matrix.

In all monkeys, we compared the distribution of the corticostriatal projections labeled by each injection with the locations of striosomes identified in adjacent sections. In every instance, the projection fields were predominantly in the matrix. Heavily labeled input patches sometimes

abutted striosomes, but they were never coincident with them. There often were higher background levels of tracer in striosomes located within the labeled striatal districts than the background levels of labeling in the sections; but we never observed heightened input-labeling of striosomes relative to input-labeling of the nearby matrix. There was a tendency for the FEF-labeled projections to avoid striosomes more crisply than those labeled from SEF or from adjoining cortex of the medial wall of the hemisphere (Fig. 2.11). However, labeling from the largest arcuate cortex injections did not as crisply avoid striosomes (Fig. 2.2B). Moreover, even case in M7, in which we injected 3.5 μ l of WGA-HRP over a 10 mm length of dorsomedial cortex and produced massive labeling in the striatum, striosomes in the putamen were surprisingly devoid of label, and those in the caudate nucleus were poorly labeled relative to the surrounding matrix (Fig. 2.11B). We could not determine whether the weak labeling in the striosomes in some projection fields resulted from spread of tracer from the extremely intense labeling of adjoining matrix, or was actually attributable to a bona fide projection to the striosomes. It was clear, however, that matrix labeling predominated throughout the case material.

DISCUSSION

Our findings demonstrate three striking properties of the corticostriatal projections from the principle oculomotor fields of the primate frontal cortex. First, the frontal eye field (FEF) and the supplementary eye field (SEF), although separated from one another by many millimeters and although innervating a dispersed set of patchy zones in the striatum, have projections that overlap, often patch for patch in parts of their striatal termination fields. Second, cortical areas that lie adjacent to the FEF and the SEF project to patches of striatum that tend to lie adjacent to the oculomotor input patches. Third, the corticocortical connectivity of the oculomotor fields and the cortical areas adjoining them is predictive of their corticostriatal connectivity: interconnected cortical areas send projections to the striatum that are at least partly coincident, whereas nearby but unconnected cortical areas send projections to the striatum that are largely non-overlapping. We conclude that on a macroscopic anatomical level, there is major convergence within the oculomotor circuit of the basal ganglia. Hence, parallel processing is not the exclusive principle of organization of pathways from the forebrain through the basal ganglia. We further show that patterns of termination of corticostriatal fibers are subject to rules of intrinsic striatal organization. Ultimately, therefore, the distributions and degree of convergence of corticostriatal inputs are governed by multiple constraints at more than one level of organization.

Convergence of SEF and FEF projections within the oculomotor sector of the striatum.

We originally chose to focus our study on the FEF and the SEF because these cortical areas are functionally related -- and indeed are interconnected cortically -- but appear to represent different modes of oculomotor processing. The strict parallelist model of basal ganglia function would predict that these cortical areas, by sending separate inputs to the striatum, set up independent basal ganglia output pathways coding different oculomotor parameters. Our results clearly do not support this prediction. In the cases in which we injected discrete low-threshold saccade-related SEF and FEF regions, there was systematic overlap of the projections from the two eye fields. If the observed convergence persists at the level of individual neurons within the zones of overlap, this would mean that signals from the two eye fields, only one of which is

thought to be eye-position dependent, must combine in the striatum. Even if the convergence were not at the single-neuron level, the fact that fibers from the two eye fields project to the same local patches of striatum makes it highly likely that functional interactions between the two macroscopically convergent systems occur within the striatum.

We were unable to determine the full extent of convergence of FEF and SEF projections to the striatum not only because of limitations inherent in our technique of microstimulation in ketamine-anesthetized monkeys, but also because the definitions of these cortical areas are still undergoing refinement and are sensitive to which methods are used to probe them. On the basis of repeated experimentation, the arcuate eye field has been reduced from one including the entire prearcuate region posterior to the principle sulcus (Ferrier, 1875; Robinson and Fuchs, 1969; reviewed in Goldberg and Seagraves, 1989) to a low-threshold zone at the junction of cytoarchitectonic areas 8 and 45, at the genu of the arcuate sulcus along its rostral bank (Bruce and Goldberg, 1985; Stanton et al., 1989). However, saccades with large amplitudes can be elicited in the dorsal prearcuate cortex (Robinson and Fuchs, 1969), and smooth pursuit eye movements have been elicited by microstimulation at the fundus of the sulcus (MacAvoy et al., 1991). New recording and stimulation studies have also suggested that the originally identified SEF (Gould et al., 1986; Mitz and Wise, 1987; Schlag and Schlag-Rey, 1987; Huerta and Kaas, 1990; Schall, 1991b; in humans, Fox et al., 1985) may be part of a larger region identifiable in the alert monkey as being engaged in the control of saccadic eye movements and/or gaze fixation (Tehovnik and Lee, 1990). It is not yet clear how this larger area overlaps with the map of the body in the SMA (Woolsey et al., 1952; Mitz and Wise, 1987).

With these experimental findings in mind, we prepared cases with arcuate injection sites limited to the low-threshold genu FEF and other cases with larger arcuate injections extending rostrally into the dorsal prearcuate cortex and posteriorly into fundal and postarcuate cortex. With enlargements of the arcuate injection sites, we saw systematic increases in the striatal territory innervated, that included more anterior and dorsal caudate nucleus for the dorsal arcuate injections and more ventral caudate nucleus and putamenal regions for more caudal arcuate injections. To study the SEF, we injected the most discrete saccade-related territory we could identify, but noted that movements of the ear, neck or even shoulder often were elicited at nearby sites or at the same sites along with saccades. We also injected a very large medial territory in

one monkey in which the oculomotor field and associated forelimb movement region had been identified in the alert state (Tehovnik and Lee, 1990; Schall, 1991b). We did not see major differences in the projection mapped out in this animal and those from smaller injections of the medial cortex except that, not surprisingly, there was a much more massive projection labeled from the larger deposit.

Despite the fact that both stimulation and recording studies have demonstrated oculomotor-related properties in larger areas of the frontal lobe than exclusively the low-threshold FEF and the discrete SEF first identified in the macaque by Schlag and Schlag-Rey (Joseph and Barone, 1987; Funahashi et al., 1989; Mitz and Godschalk, 1989; Boch and Goldberg, 1989; Bon and Lucchetti, 1990; Tehovnik and Lee, 1990), we were, in general, unable to find precisely overlapping labeled projections when we paired injections of one discrete eye field with injections from cortex surrounding the other eye field. One case (M5) suggested that the anterior projection to the caudate nucleus from SEF may be matched by projections from the cortex of the dorsal limb of the arcuate sulcus; however, the dorsal arcuate cortex projected to dorsomedial territory in the anterior caudate nucleus, in which we never saw label from an SEF injection. More remarkably, in one other case (M3), we injected an eye field resembling the SEF and found almost no overlap of its projections to the striatum and those from the low-threshold FEF. On the basis of cortical interconnectivity, the medial area could not be confirmed as the SEF, and in fact is more likely to be an eye movement territory rostral to SEF. Rizzolatti and coworkers have also described a second medial eye field in the dorsomedial frontal cortex (Camarda et al., 1991). If this analysis is correct, "oculomotor processing" alone is not a sufficient criterion for directing cortical projections to the SEF/FEF input patches in the striatum.

Functional implications of convergence of oculomotor input to the striatum.

Neurons in the caudate nucleus have saccade-related profiles resembling those of some FEF and SEF neurons (Hikosaka et al., 1989a). The onset of their activity is usually presaccadic, related to intentional rather than spontaneous saccades, and often shows a preparatory phase. These task-related cells have been found in regions of the caudate nucleus, the striatal cell bridges, and the dorsal putamen that appear comparable to zones of FEF and SEF inputs documented here (cf. Fig. 2.1 with Fig. 2.6 of Hikosaka et al., 1989a). Units in the caudate

nucleus also show fixation-related activity similar to that seen in many forebrain regions including the SEF (Schlag and Schlag-Rey, 1987). No studies have yet addressed the question of what coordinate frame the striatal cells encode, but Hikosaka et al (1989) did observe some units with activity that was modulated by eye position. One possibility raised by our findings is that FEF saccade-related signals in retinotopic coordinates and SEF saccade-related signals in oculocentric coordinates are combined in the striatum. This hypothesis suggests not a parallel model for the two corresponding oculomotor paths to the striatum, but an integrative model in which striatal neurons form systematic combinatorial computations.

In addition to units with activity that correlates with the sensory and/or motor facets of saccade paradigms, the caudate nucleus also contains cells that seem to fire in expectation of target or reward (Hikosaka et al., 1989b). Hikosaka and coworkers found that these neurons were often located more anteriorly in the caudate nucleus, in regions which may correlate with the anterior projections we observed from the SEF (case M1) and from our large dorsal arcuate injection (case M5). Anticipatory activity of this kind has been found in the dorsolateral prefrontal cortex, but also has been recorded in the SMA (Kurata and Tanji, 1985). The SEF might play a stronger role in modulating the more straightforward saccade execution-related activity of the FEF with behavioural cues.

The doubly inhibitory path from the oculomotor district of the caudate nucleus to the superior colliculus by way of the substantia nigra is thought capable of facilitating orienting saccadic eye and/or head movements to actual or remembered targets (Hikosaka and Wurtz, 1983b; Chevalier and Deniau, 1990). The effects of Parkinson's disease on oculomotor abilities are of some interest in this context. There are not only deficits in saccadic latency, amplitude and peak velocity (as well as deficits for smooth pursuit, optokinetic nystagmus, and vestibuloocular reflex eye movements), but also an impairment of eye-head coordination for large gaze changes (White et al., 1983; White et al., 1988). Though it was once thought that the vestibuloocular reflex (VOR) could completely integrate the head and eye movement systems, it is now known that for large gaze saccades, the VOR is inoperative and that eye-head coordination must be accomplished farther centrally (Tomlinson and Bahra, 1986). The oculomotor striatum could be in a position to participate in this processing by combining cortical information to coordinate orienting movements.

Functional implications of differences between the FEF and the SEF projections to the striatum.

Although we found convergence of FEF and SEF outputs to the striatum (and to the thalamus), in at least three interesting respects the outputs of the FEF and SEF were notably different. First, there was a considerable expanse of the striatum, in the head of the caudate nucleus, in which the SEF input was not matched by FEF input. More anterior parts of the arcuate cortex did project to this more rostral striatal territory. Thus, there are rostrocaudal differences in the inputs to the oculomotor sector of the striatum. Interestingly, Hikosaka and coworkers (1989a,b) have found subtle differences in the rostrocaudal distributions of unit activity profiles in the caudate nucleus. These may relate to the differences in cortical input that we have observed.

Second, taken together, our cases suggest that the direct projection from the SEF to the superior colliculus is much weaker than that from the FEF. The fact that the SEF has a weak direct path may give special functional importance to its indirect cortico-striato-nigro-tectal projection. It could be involved more in setting conditions for release of saccades specified by other cortical and subcortical areas rather than in directing the eye movements itself.

A third difference between the descending projections from the two eye fields is that the SEF projections to the striatum (and, in part, to the superior colliculus) are bilateral whereas the FEF projection is predominantly ipsilateral. Given that the task-related neurons in the caudate nucleus are mostly related to contraversive eye movements, the strong contralateral SEF projection may not relate to sensorimotor parameters per se but to other functions of saccadic organization. Patients with cortical lesions involving the SMA but sparing the FEF are reported to have bilateral impairments in performing remembered sequences of saccades, while maintaining normal reflexive and memory-guided saccades (Gaymard et al., 1990). By contrast, deficits occurring after lesions of the FEF are reported to be unilateral (affecting the visual field contralateral to the cortical lesion) (Guitton et al., 1985). In monkeys, lesions of the SMA also disrupt bilateral (bimanual) tasks (Brinkman, 1984), and neurons in the primate SMA that code for arm movement sequences have been reported (Mushiaki et al., 1990). The SMA, including its rostral oculomotor representation - the SEF, may be specialized for such sequential ordering of bilateral movements, the metrics of which are programmed elsewhere. In contrast, the FEF

appears to code for the next contraversive saccade (Goldberg and Bruce, 1990). These differences in function of the two cortical areas may be reflected in the degree of bilaterality of their striatal projections.

Corticostriatal projections from other premotor areas.

A clearcut finding in our experiments was that the mediolateral position of the medial injections is a major determinant of the distribution of the resulting label in the striatum. When we injected midline cortex of the superior frontal gyrus, medial to the saccade-related zones we mapped out, we found much more transport of tracer to the putamen than when we injected convexity cortex on the dorsal surface of the hemisphere, from which we could elicit saccades on microstimulation. Our results suggest that these shifts in striatal labeling reflect a systematic topography of the corticostriatal projections of the SEF/periSEF and arcuate/periaucate cortex. The topography of the medial cortical areas appears to correspond to that in the maps of Rizzolatti and colleagues (Luppino et al., 1991), who place a cortical area related to projective body movements in medial area 6a β , medial to the cortex from which they were able to evoke saccades. This medial area may correspond to the pre-SMA of Tanji and coworkers (1991).

Our evidence also suggests that there are converging corticostriatal inputs to the putamen from the postarcuate cortex (area 6), including the arcuate premotor area and the SMA or pre-SMA. Neurons in the postarcuate cortex have been reported to have combined visual and tactile receptive fields (Rizzolatti et al., 1981), and the part of the putamen to which the postarcuate cortex projects appears to contain neurons that are similarly responsive (Gross and Graziano, 1990). We did not have sufficient case material to study these inputs in detail, but we did note that when an injection involving one of these cortical areas was paired with an injection in one of the eye fields, the projections did not overlap extensively even though some sets of patches from the two injected areas were physically adjacent in the caudate nucleus and medial putamen. This evidence suggests that the premotor and eye field projections are handled as parallel systems; but the frequent adjacency of the different input patches raises the possibility that the inputs are being brought into proximity in the striatum for cross-patch interactions. Such a functional view would strongly favor the idea that the striatal matrix is organized in patches in part to bring into

proximity different cortical signals so that they can be recombined in novel ways (Malach and Graybiel, 1986).

Principles of corticostriatal connectivity.

It is well known that corticostriatal projections from most areas of the cortex form dispersed terminal fields within the striatum (Kunzle, 1975; Kunzle, 1977; Goldman and Nauta, 1977; Jones et al., 1977; Yeterian and Van Hoesen, 1978; Ragsdale and Graybiel, 1981; Selemon and Goldman-Rakic, 1985; Flaherty and Graybiel, 1991a). What is novel about our findings in this context is the demonstration that dispersed sets of projection patches from distant cortical sites can converge systematically or, as just discussed, can be adjacent. This evidence suggests that shared mapping rules govern both the widespread dispersion of the patchy inputs from a pair of cortical areas and the local convergence of their two sets of inputs in the striatum.

Our experiments clearly show this patchy, distributed but convergent organization for FEF and SEF projections to the striatum. In addition, our results suggest similar patterns of overlapping striatal inputs from the medial wall cortex (area 6a β) and postarcuate cortex. As discussed above, both pairs of cortical areas with converging projections are cortically interconnected. Furthermore, cortically unconnected or weakly connected pairs of areas, including one eye field and cortex adjacent to the other (for example, the low-threshold FEF and the medial wall cortex) can have corticostriatal projections directed to adjacent sets of striatal sites. Thus, for the cortical regions studied, it appears that cortical connectivity predicts overlap and cortical adjacency predicts adjacency of fiber projections to the striatum.

Several previous attempts have been made to analyze the relationships among different corticostriatal pathways. Experiments with fiber degeneration methods indicated that there was a relatively simple topography of these input pathways governed by the relative physical locations of the cortical areas, with rostral cortical areas projecting rostrally within the striatum and caudal areas projecting more caudally (Kemp and Powell, 1970). Once the more sensitive autoradiographic axon transport methods were developed, it was found that the corticostriatal connections are much more extensive in the anteroposterior dimension than the topographic model suggested (Goldman and Nauta, 1977; but see Saint-Cyr et al., 1990), and the proposal was made that distant but cortically connected areas projected to overlapping regions of the

striatum (Yeterian and Van Hoesen, 1978). The first dual-tracer study addressing this issue produced evidence for interdigitation rather than overlap of the projections from cortically interconnected areas (Selemon and Goldman-Rakic, 1985). However, experiments on physiologically identified corresponding sites in different areas of the primate somatic sensory and motor cortex showed that such sites can send convergent projections to the striatum (Flaherty and Graybiel, 1991b) even when they are not heavily interconnected at the cortical level (Jones et al., 1978).

The apparent contradiction in these findings would be resolved if the amount of convergence in the striatum reflects the output organization of the striatum, not just its input organization. The appeal of this proposal is that functionally related inputs would converge, with the degree of functional-relatedness being determined by the striatal target. This would allow for activity-dependent sculpting of the convergence patterns. For example, if the signal sent to the superior colliculus via a striato-nigro-tectal connection coded for saccades without respect to body movements, it would be reasonable to have converging inputs from cortical eye field zones to the striatal origin of the pathway, but not inputs from the nearby medial and lateral premotor areas encoding non-oculomotor body movements. By contrast, targeting to output channels consolidating somesthetic signals might call for convergence of cortical inputs, for example deep and cutaneous inputs from areas 3a and 3b respectively, whether the cortical areas are interconnected or not. The fact that the output cells of the striatum, by far the predominant cell type in the striatum, are themselves organized into clusters (Desban et al., 1989; Jiménez-Castellanos and Graybiel, 1989; Giménez-Amaya and Graybiel, 1990; Selemon and Goldman-Rakic, 1990) suggests that not just the divergence or convergence of different corticostriatal inputs, but also their patchiness, could reflect the functional output architecture of the striatum.

Several observations from our experiments support the view that the intrinsic architecture of the striatum may influence its afferents. First, we found well matched dispersion of input patches of fibers originating in pairs of physically separated cortical areas. This suggests that cortical inputs follow striatal cues in terminating in one set of patches in the striatum rather than another. Second, we found that the oculomotor and adjoining premotor regions of the frontal lobe, even when projecting densely to a given striatal zone, nevertheless projected only very

weakly to the striosomes in that zone, if at all. Third, even though local cortical topography was correlated with the total distributions of the inputs to the striatum (for example, more anterior and dorsal arcuate cortex projected more anteriorly and dorsally within the striatum than did more posterior arcuate cortex), the degree of overlap of the corticostriatal projections was not readily predicted by the topographic layout of the cortical areas of origin. Clusters of input fibers labeled from medially placed cortical areas overlapped fiber clusters labeled from lateral cortical areas. Taken together, these patterns suggest that cortical inputs to the striatum follow rule systems of at least two types, one relating the degree of input convergence to characteristics of the cortical areas, and another relating input architecture to the local macroscopic organization of the targeted striatal neurons.

Table 2.1. Summary of experimental protocols. Asterisks(*) indicate *Macaca mulatta*; all other monkeys were *Macaca fascicularis*. Abbreviations: d - dorsal, v - ventral, arc. - arcuate sulcus, SMA -supplementary motor area, SEF - supplementary eye field, FEF - genual frontal eye field (unless specified otherwise). See text and figures for further description of the cortical areas injected. met: [³⁵S]methionine, HRP: wheat germ agglutinin-conjugated horseradish peroxidase.

Case #	Cortical Area	Tracer	#injections	amt/inj
M1	SEF	met	1	40 nl
	genu FEF	HRP	2	40 nl
M2	SMA	met	1	200 nl
	genu FEF	HRP	1	200 nl
M3	rostral SMA	HRP	1	18.2 nl
	genu FEF	met	1	17.5 nl
M4	dorsal FEF	met	1	70 nl
	genu FEF	HRP	1	70 nl
M5	SEF	HRP	6	9-18 nl
	arcuate	met	18	12-63 nl
M6	SMA	HRP	7	150 nl
	arcuate	met	7	150 nl
M7	DMFC	HRP	20	200 nl
M8	SEF	met	1	15 nl
	FEF	HRP	3	7-14 nl

Figure 2.1. Darkfield photographs illustrating fiber projections traced to the striatum in case M8 from the SEF (A) and the FEF (B) in serially adjacent sagittal sections approximately 3.5 mm lateral to the midline. "v"s indicate corresponding blood vessels in the two sections. Locations of the two injection sites are shown on the drawing of the hemisphere (SEF site indicated by horizontal lines, FEF deposit by vertical lines). **A** shows the extensive anteroposterior distribution of the corticostriatal projection traced from a single [³⁵S]methionine injection site centered slightly medial to the center of the SEF as determined by microstimulation. **B** illustrates the sharply bordered clusters of fibers labeled from the WGA-HRP injection site in the FEF. AC - anterior commissure, CN - caudate nucleus, IC - internal capsule, Th - thalamus. Scale bar indicates 2 mm.

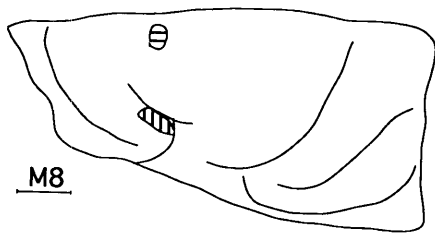
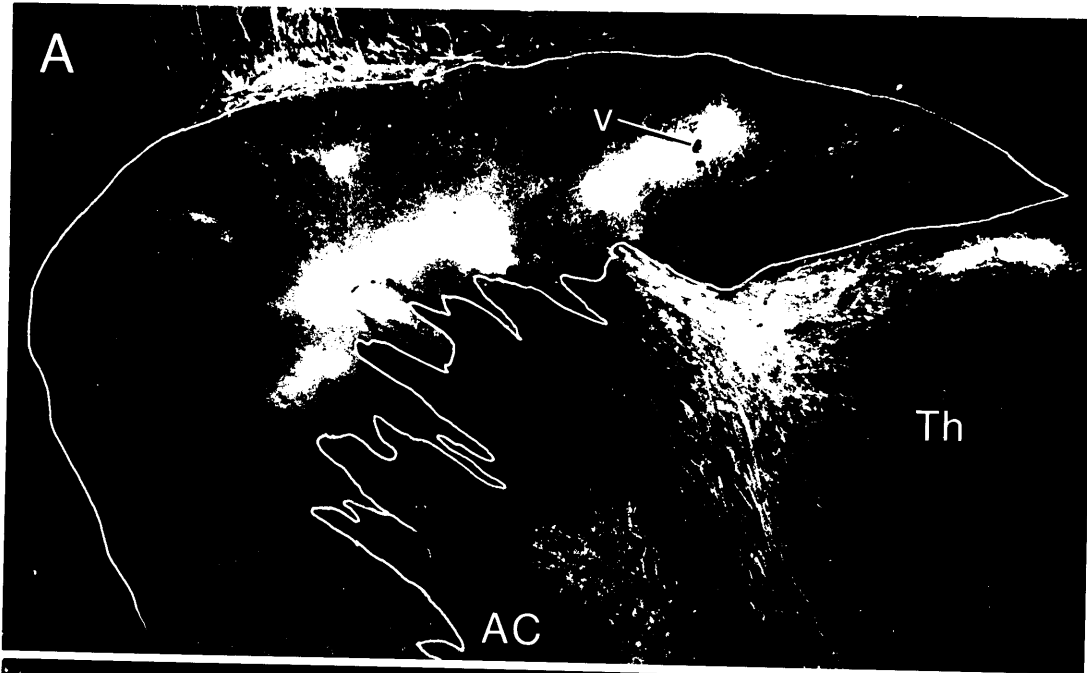


Figure 2.2. Comparisons of the corticostriatal projections of the supplementary eye field (SEF)/SMA cortex (left) and frontal eye field cortex (FEF)/arcuate cortex (right) labeled in pairs of serially adjacent tranverse sections through the striatum of cases M1 (A,A'), M5 (B,B'), and M3 (C,C'). All sections were photographed under darkfield illumination. **A,A'**: Sections at approximately A14 (*Macaca mulatta*), showing that the WGA-HRP labeled FEF projection field (A') is almost completely contained within the SEF projection field (A, labeled with [³⁵S]methionine). The microstimulation map for this case is shown in Fig. 2.3. **B,B'**: Sections at approximately A17.5 showing overlap of projections from the SEF, labeled with WGA-HRP (B), and projections from the cortex of the dorsal bank of the arcuate sulcus and the genual arcuate cortex (FEF+), labeled with [³⁵S]methionine (B'). The projection from the SEF is almost completely contained within the projection field of the arcuate cortex (B'). Note the similarity between the arcuate projection field in this case (B') and the SEF projection field in case M1, shown in A'. **C,C'**: Interdigitation rather than overlap of corticostriatal projections traced from the pre-SMA cortex, labeled with WGA-HRP (C), and from the FEF, labeled with [³⁵S]methionine (C'). The sections are at approximately A18. The microstimulation map for this case is shown in Fig. 2.7. CN -caudate nucleus, GPe - globus pallidus external segment, IC -internal capsule, LV - lateral ventricle, P - putamen, v - blood vessel. Scale bar indicates 2 mm.

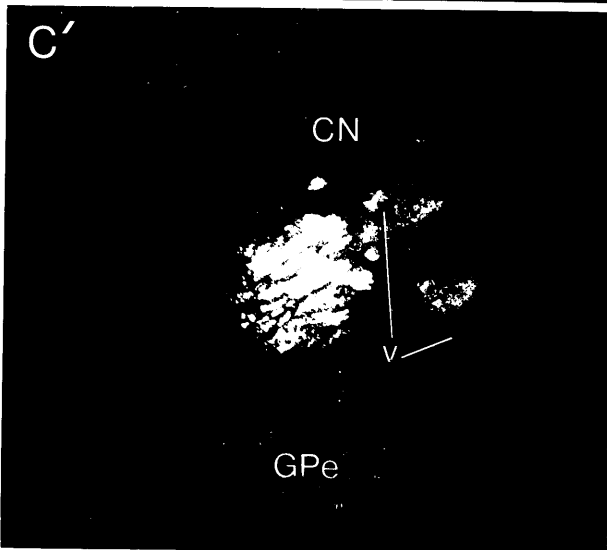
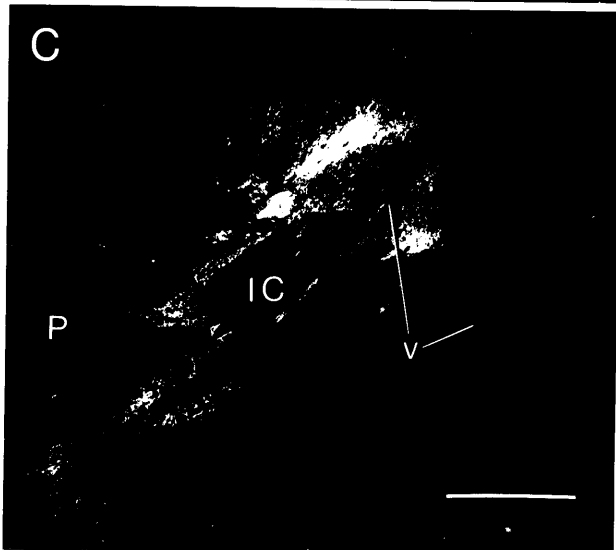
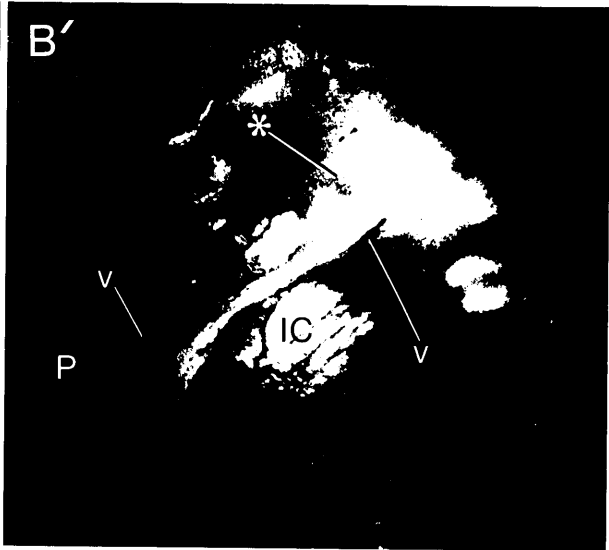
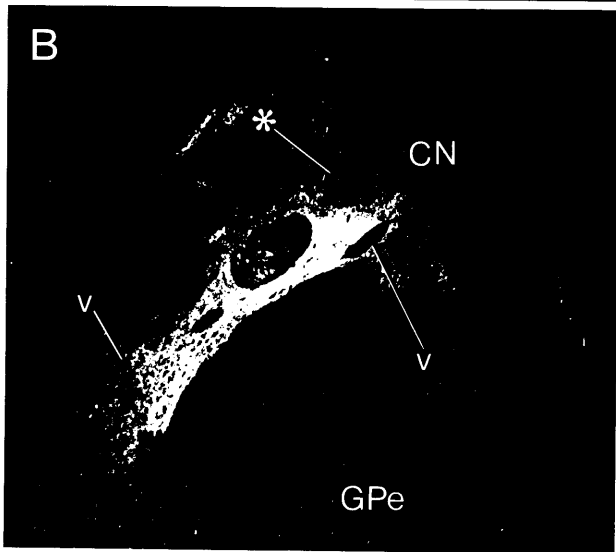
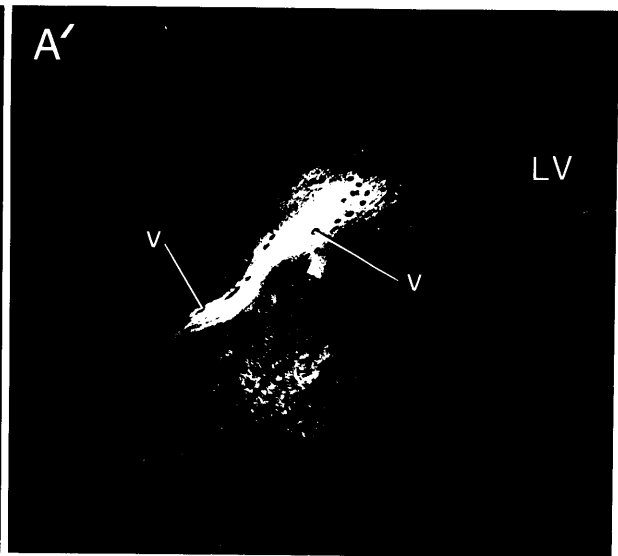
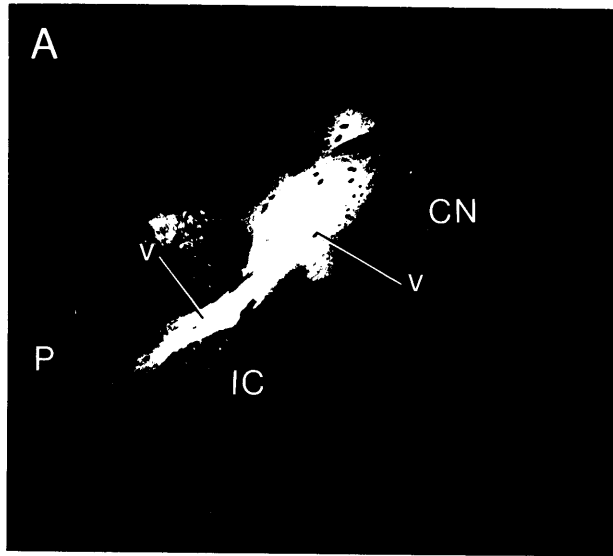
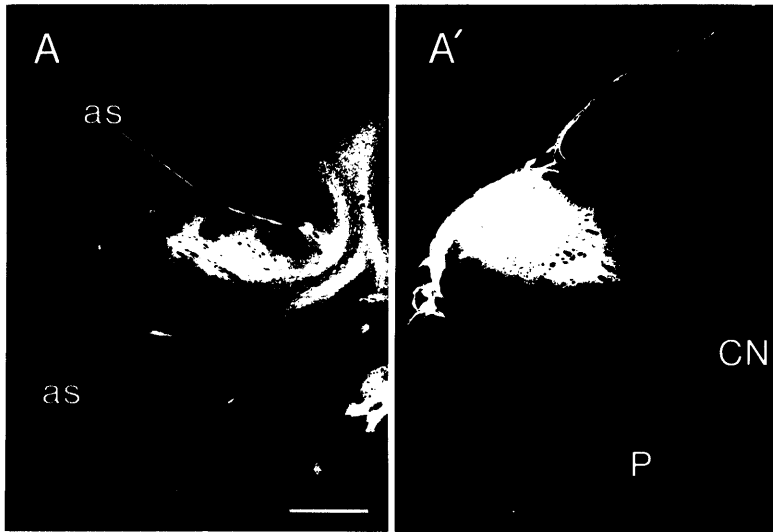


Figure 2.3. Monkey M1. **A:** Microstimulation map of frontal cortex, showing sites at which stimulation elicited movements of arm (A), body (B), digit (D), eye (E), hand (H), jaw (J), neck (N), ear (R), shoulder (S), and sites at which no response was evoked (X). Thresholds are indicated by the use of circled capitals for currents $<50 \mu\text{A}$ and uncircled capitals for currents of $50\text{-}100 \mu\text{A}$. Lowercase symbols indicate that threshold at the site was not defined. Solid triangles mark injection sites. **B:** Schematic drawings of the dorsal view of the hemisphere and of cross sections through the SEF injection site ($[^{35}\text{S}]$ methionine, horizontal stripes) and the FEF injection site (WGA-HRP, vertical stripes). (See also Fig. 2.4). Less intensely labeled marginal zones of the injection sites are indicated by dotted lines. **C:** Schematic drawings of cross sections through the striatum (CN - caudate nucleus, IC - internal capsule, P - putamen) ipsilateral to the injection sites. Labeled projection fields are indicated by the same symbols used to code the injection sites in B. Dotted outlines enclose regions that were weakly labeled compared to the rest of the projection field. Indicated zones of weak overlap are regions of coincident projections from the paired cortical injections in which one or both projection fields was weakly labeled. Asterisks after AP coordinates indicate values for *Macaca mulatta* (Snider and Lee 1961). Scale bars for A-C all indicate 5 mm.

Figure 2.4. Monkey M1. **A:** Photomicrographs illustrating the projection of [³⁵S]methionine labeled fibers from the SEF (left) to the FEF injection site (WGA-HRP, right). CN - caudate nucleus, P - putamen, as - arcuate sulcus. Scale bar indicates 3 mm. **B:** Schematic drawings of inputs to the thalamus and superior colliculus from the SEF and the FEF. Symbols are the same as those in Fig. 2.3C. Scale bar indicates 5 mm. MD - mediodorsal nucleus, VL - ventrolateral nucleus, SC - superior colliculus, Teg - tegmentum. Asterisks after AP coordinates indicate values for *Macaca mulatta*.



M1

B

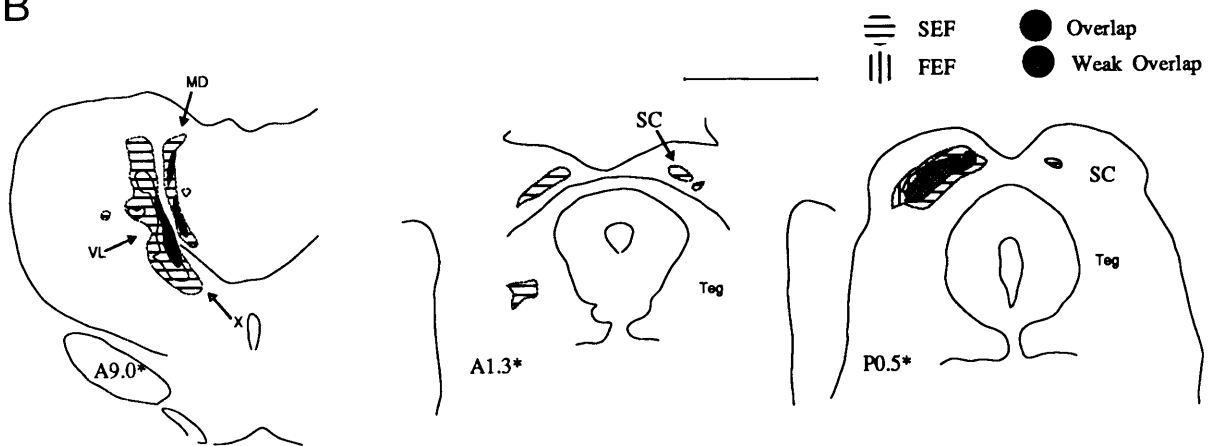


Figure 2.5. Monkey M2. Microstimulation map (A) and schematic drawings of the injection sites (B) and projection fields (C). Conventions are the same as for Fig. 2.3 except that in A, capital letters indicate thresholds of 100-500 μ A (thresholds were higher for this monkey than for M1), and in B, horizontal stripes represent the pre-SMA injection site ($[^{35}\text{S}]$ methionine) and vertical lines represent the FEF injection site (WGA-HRP). The microstimulation map (A) and drawing of the left hemisphere (B) were traced from photographs taken during the experiment. Dotted lines represent the border being traced if it was occluded or not present in these photographs.

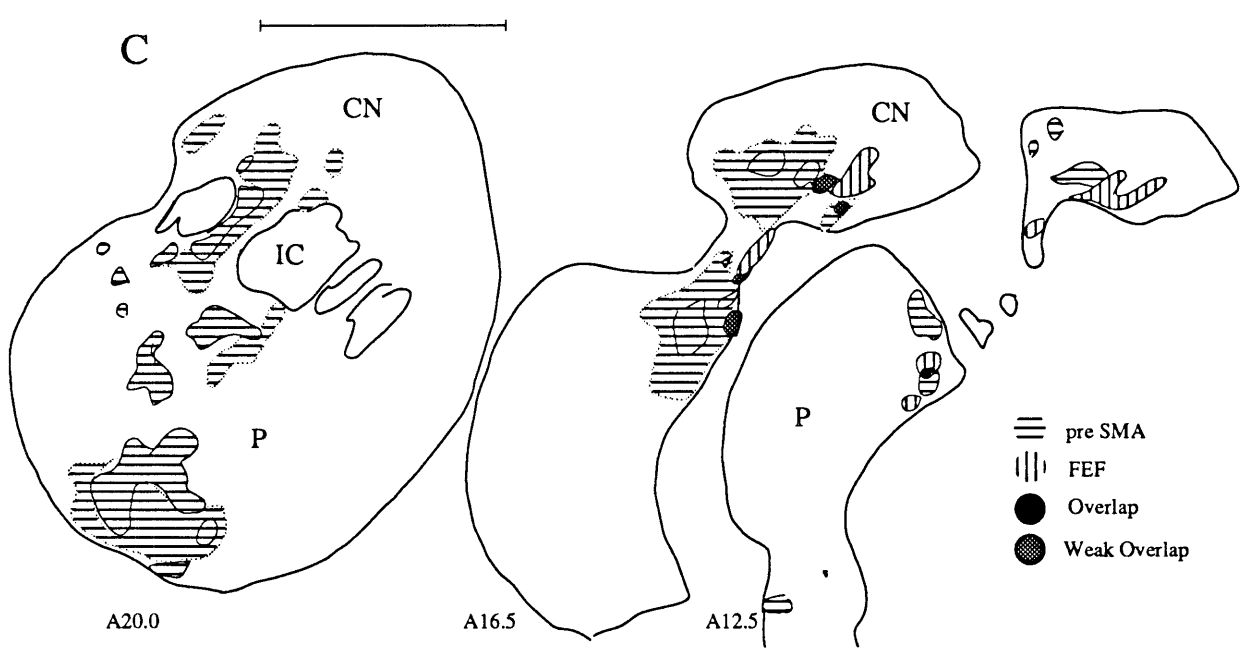
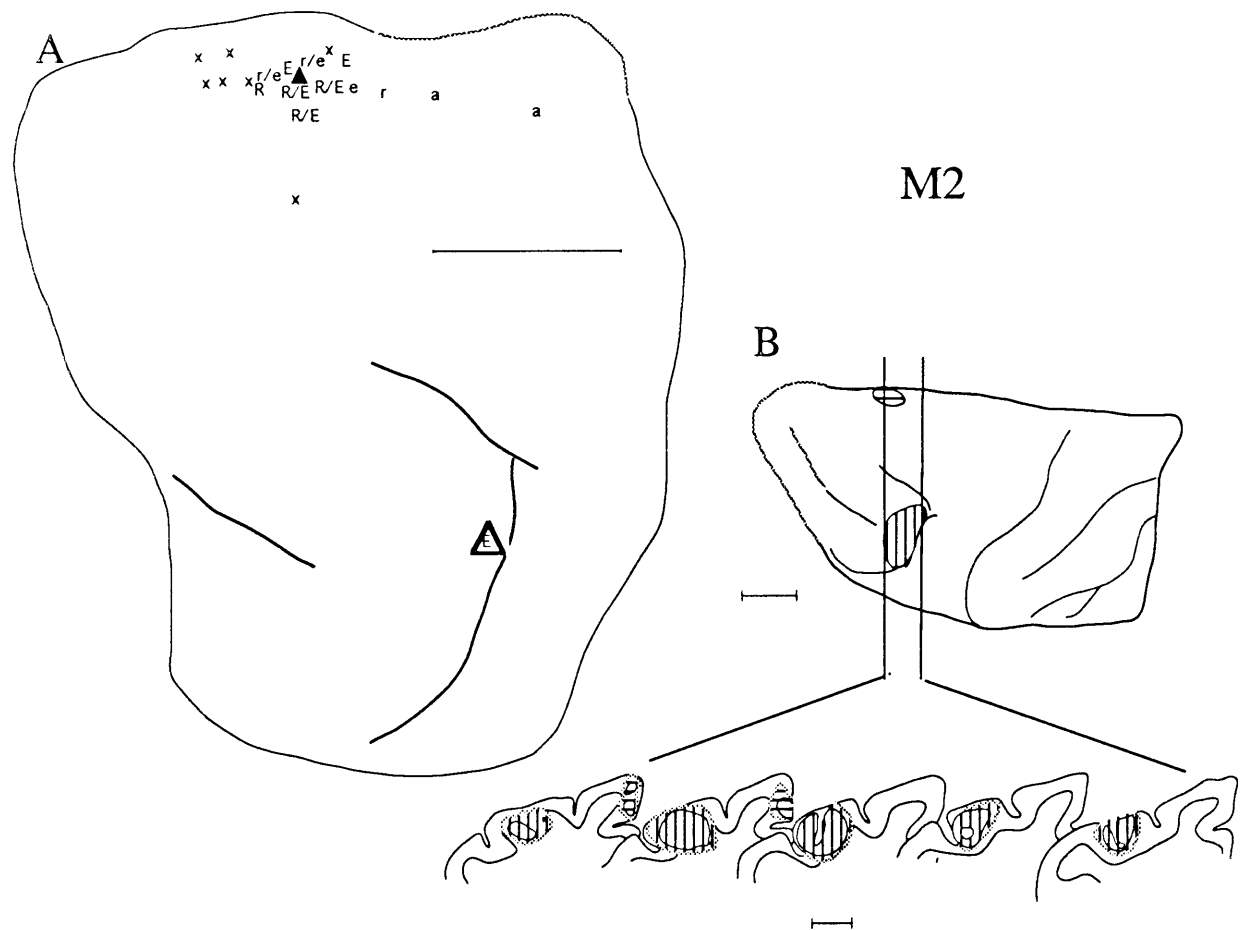


Figure 2.6. Monkey M3. Microstimulation map (A) and schematic drawings of the injections sites (B) and projection fields (C). Conventions as in Fig. 2.3 except that in A, circled capital letters indicate thresholds of 50-100 μ A, capital letters indicate currents of 100-500 μ A and in B, horizontal stripes represent the pre-SMA injection site (WGA-HRP) and vertical stripes indicate the FEF injection site ($[^{35}\text{S}]$ methionine).

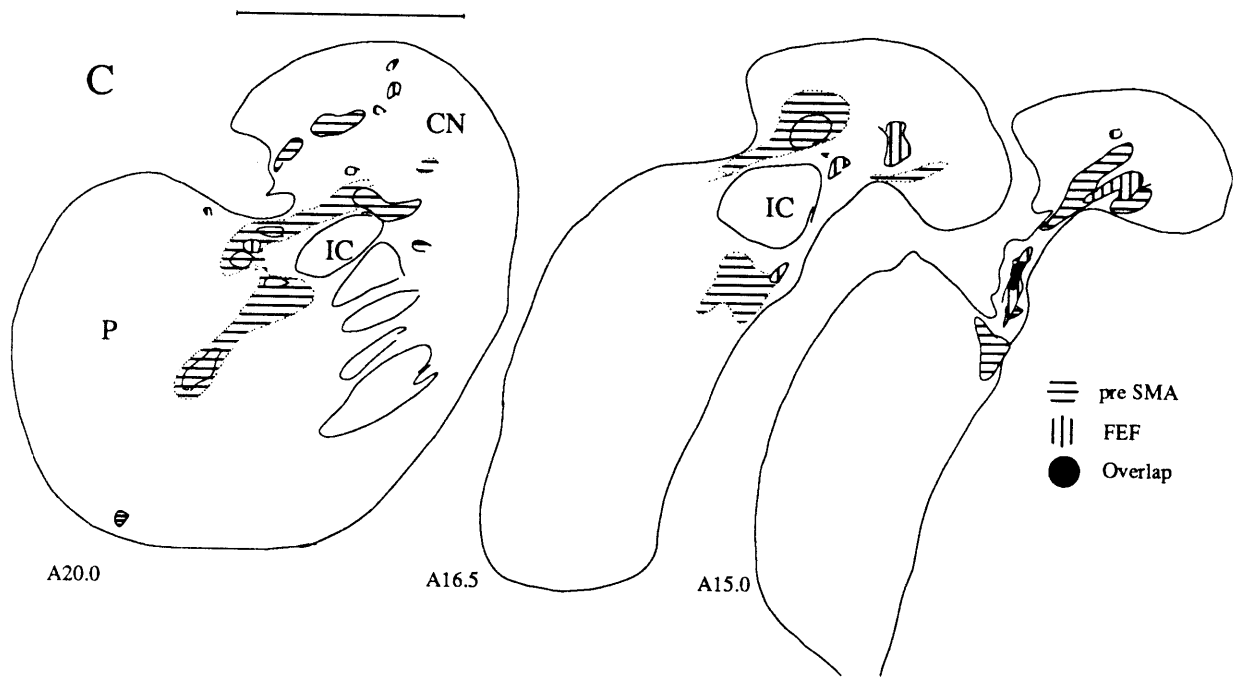
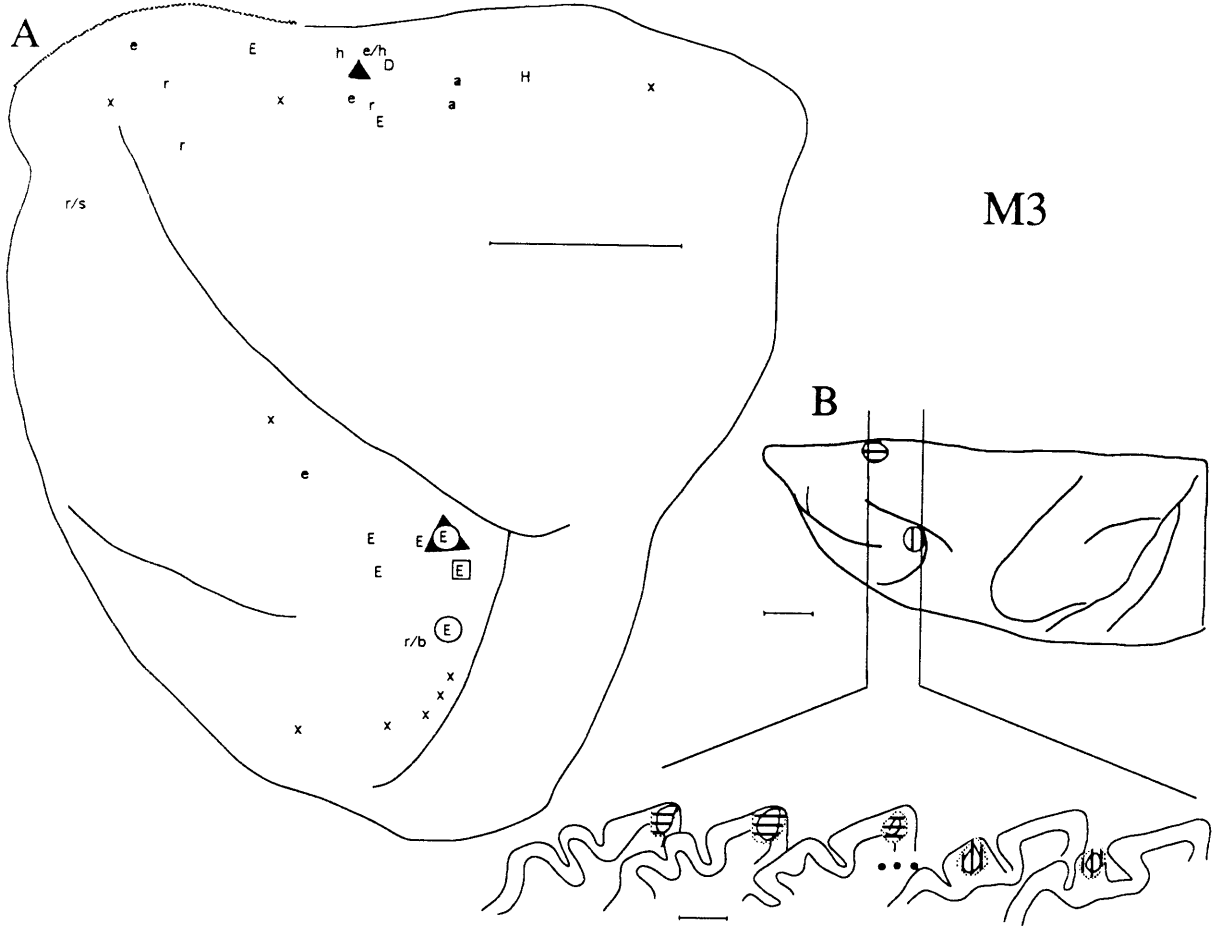


Figure 2.7. Monkey M5. Microstimulation map (A) and schematic drawings of the injection sites (B) and projection fields (C). Conventions are the same as for Fig. 2.3 except that in **B**, horizontal stripes indicate the SEF injection (HRP-WGA) and vertical stripes represent the arcuate injection ($[^{35}\text{S}]$ methionine).

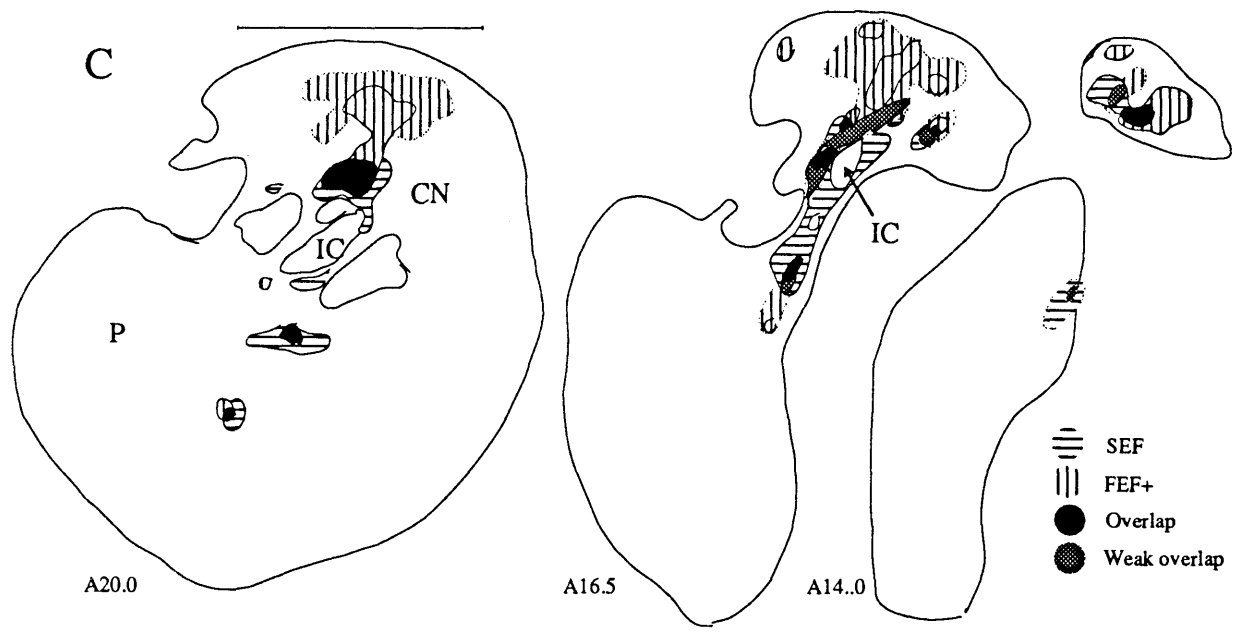
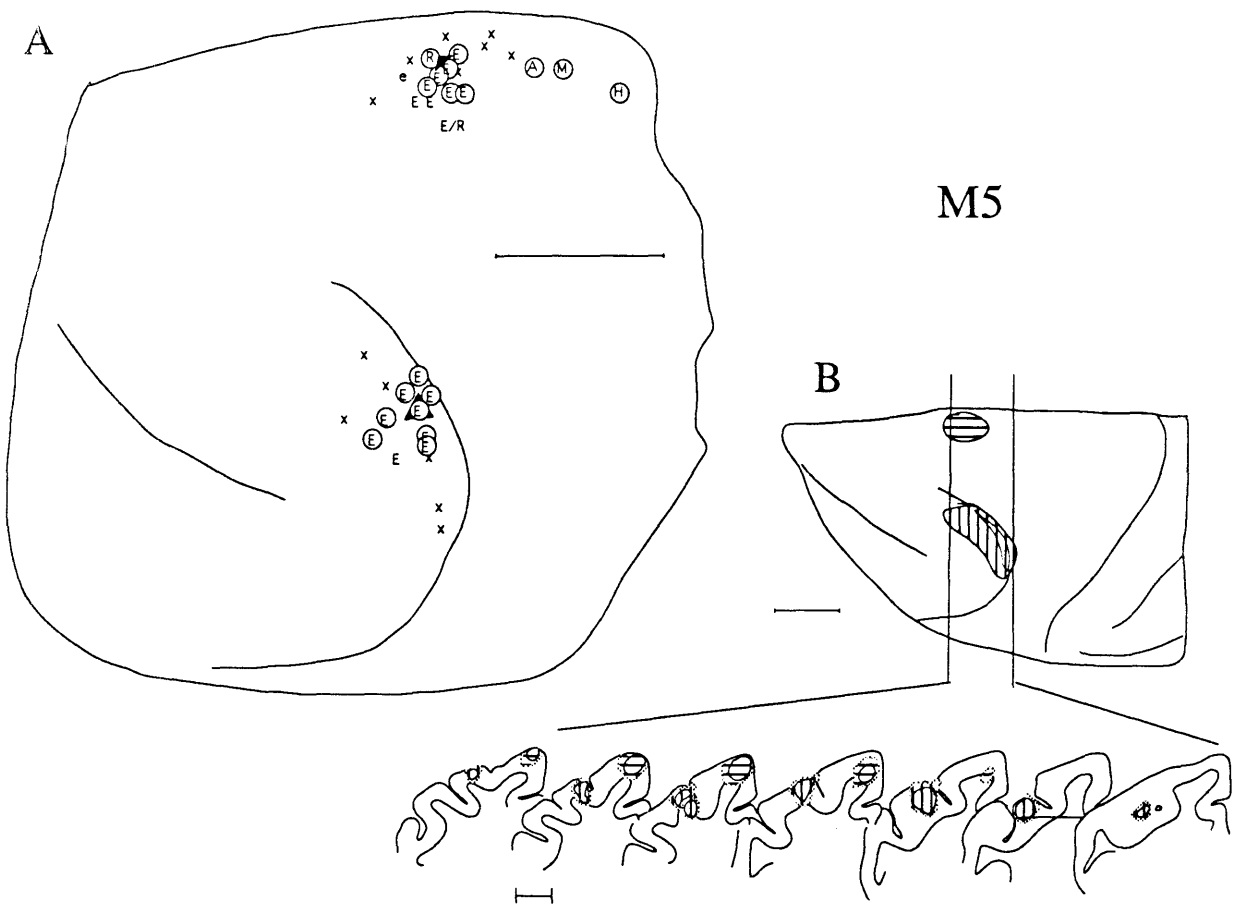


Figure 2.8. Darkfield photomicrographs of serial transverse sections at approximately A19 illustrating projections to the putamen in monkey M6 traced from the SMA (A, WGA-HRP) and from arcuate cortex (B, [³⁵S]methionine). Injection sites are labeled on the dorsal view of the hemisphere (SMA site is marked with horizontal lines, FEF injection site by vertical lines). Examples of overlap of labeled patches is indicated by arrows. IC - internal capsule, P -putamen. Scale bar indicates 2 mm.

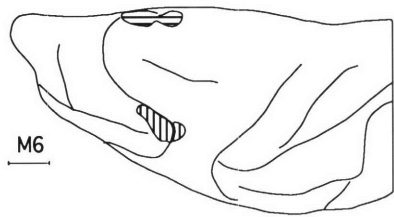
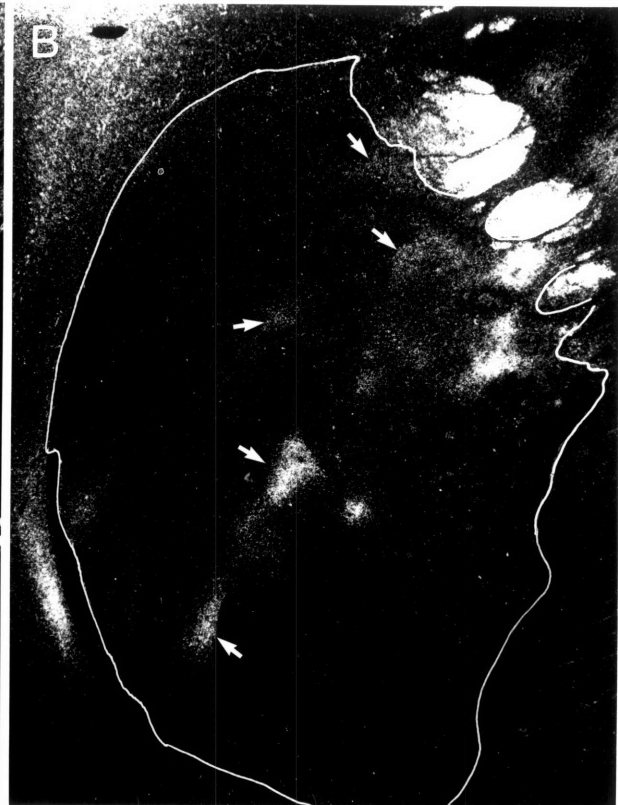
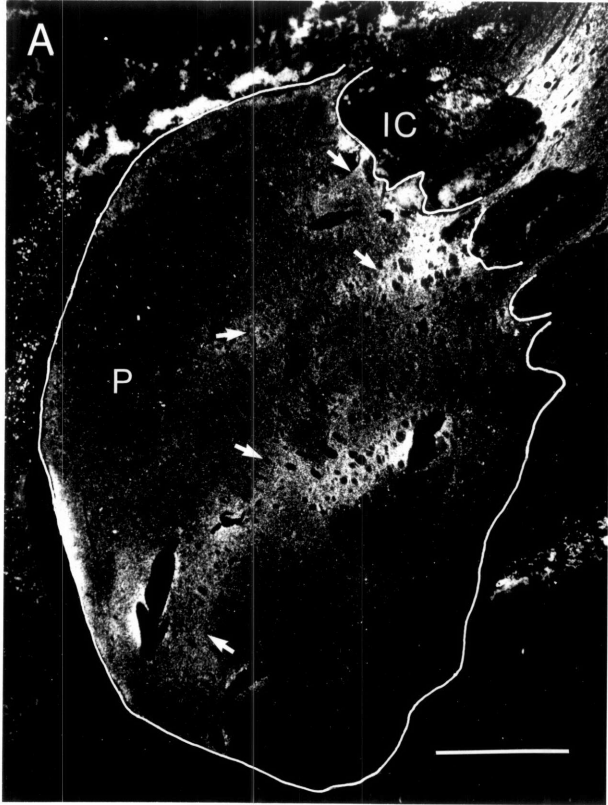


Figure 2.9. Diagrams summarizing patterns of connectivity between cortical sites injected in five experiments. Transverse sections through the WGA-HRP injection sites (injection site and its halo are outlined); projections from the [³⁵S]methionine injection sites are indicated by light shading. Darker shading shows the part of the [³⁵S]methionine injection site visible at the level illustrated. Corresponding dorsal views of the brains are shown on the right. The WGA-HRP injection is outlined. The [³⁵S]methionine injection site is indicated in black, and projections traced from it are charted between the vertical lines at approximately one millimeter intervals. Dots indicate labeling of convexity cortex. Arrows indicate labeled cortex buried within a sulcus. In monkey M1 (A) the SEF projects to cortex at the FEF injection site and in monkey M5 (B) arcuate cortex projects to cortex at the SEF injection site. C illustrates the connectivity between arcuate cortex and the SMA injection site in monkey M6. No interconnectivity of the injected cortical sites was seen in case M2 (D), indicating that rostral SMA cortex does not project to the FEF. Nor were corticocortical connections found in monkey M3 (E) between the pre-SMA oculomotor area and the FEF. Scale bars (under case names) indicate 5 mm and apply to the cross sections only.

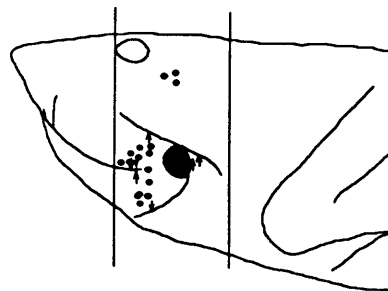
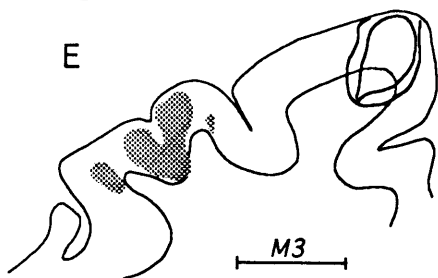
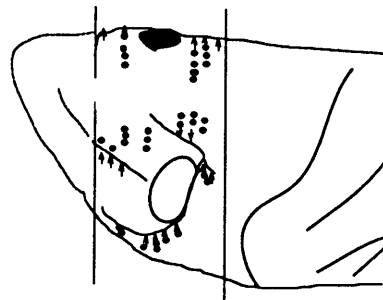
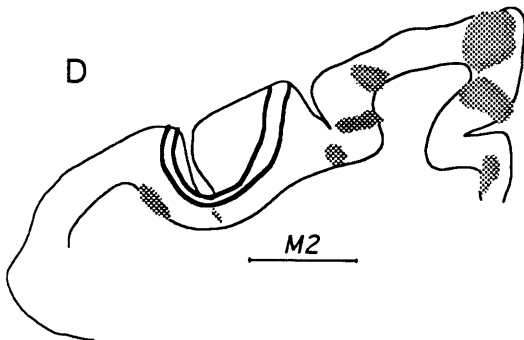
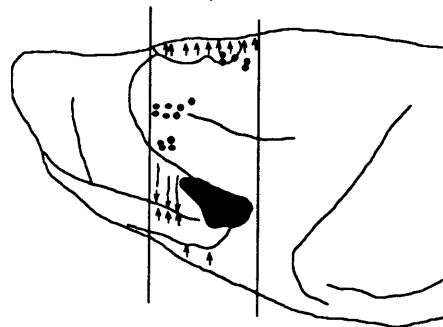
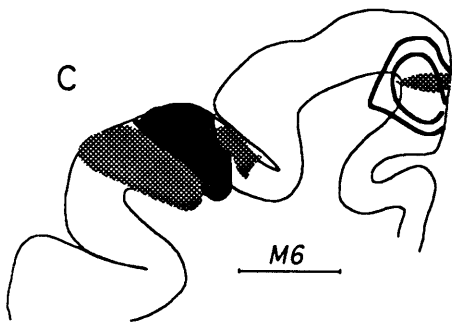
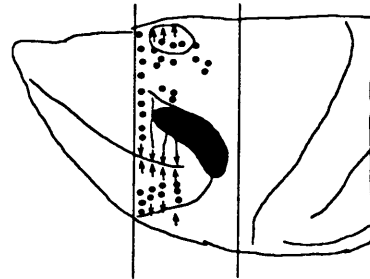
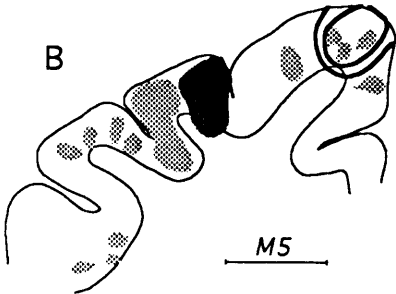
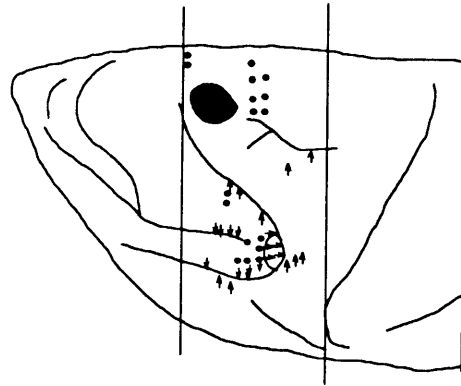
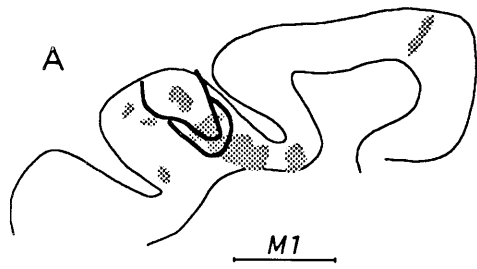


Figure 2.10. Topographic order of corticostriatal projections from the periarculate cortex and from the SMA/periSMA cortex shown in schematic drawings from six representative cases. Strongly labeled projections are shown in black, lighter shading represents qualitatively more weakly labeled projections. In the SMA region, more lateral cortex projects dorsomedially in the striatum (A) and progressively more medial cortex in the SMA region (B, then C) projects to striatal districts centered progressively farther ventrolaterally in the striatum. A similar pattern was found for anterior to posterior arcuate cortex (D-F). Scale bars denote 5 mm.

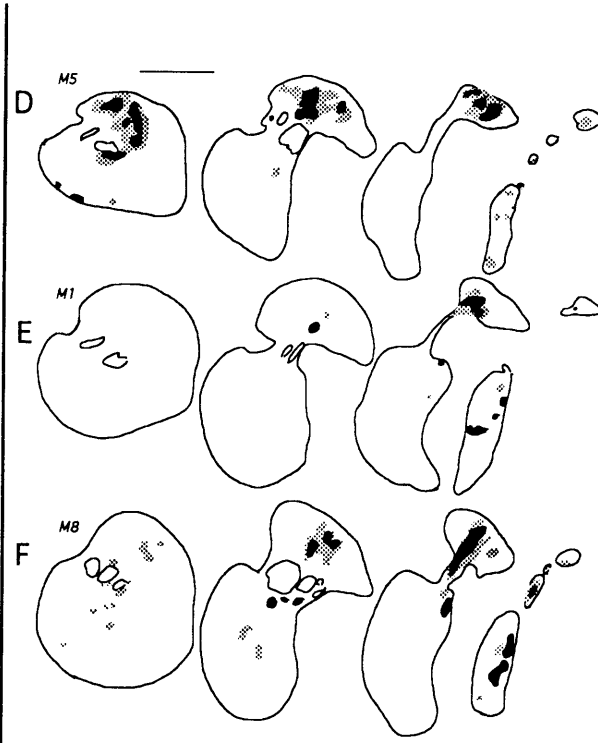
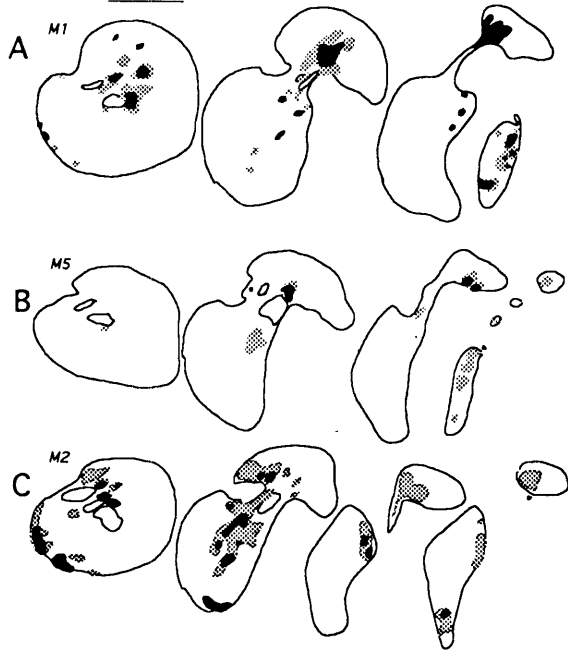
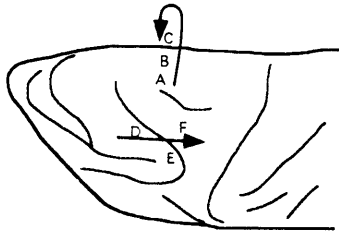
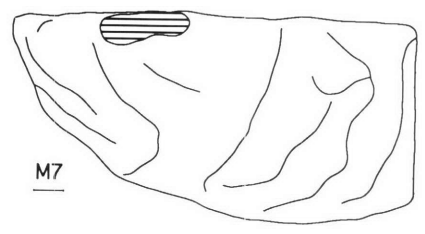
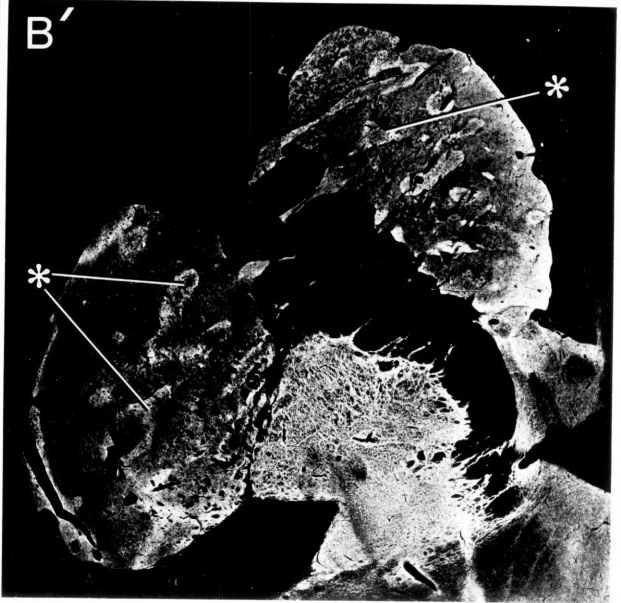
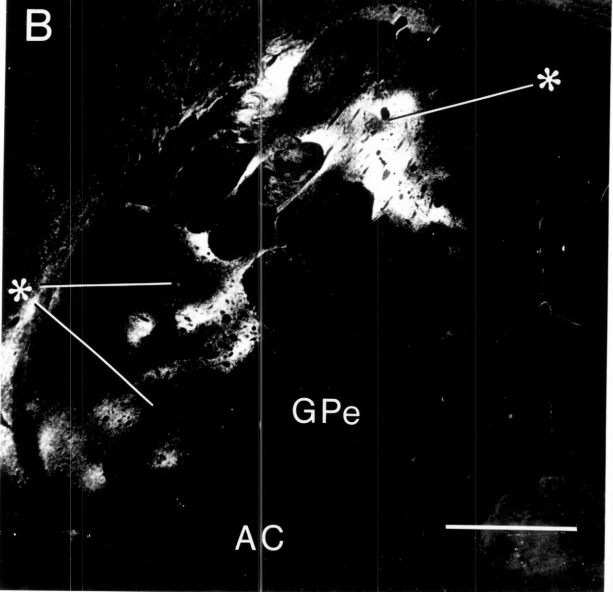
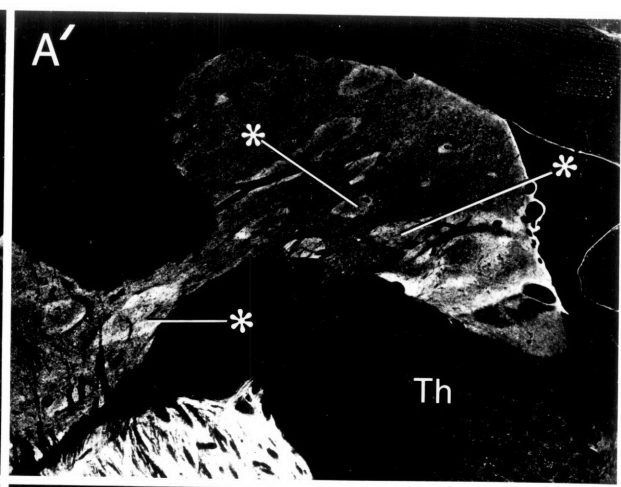
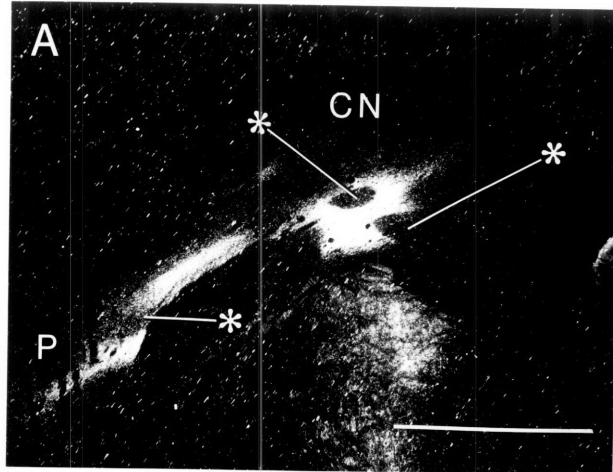


Figure 2.11. Photographs of serially adjacent sections processed for corticostriatal labeling (darkfield photographs, A,B) and for enkephalin-like immunoreactivity (reverse contrast photographs, A',B') demonstrating the relationship between corticostriatal projection fibers and striosomes. In monkey M2 (A,A'), sections at approximately A16 show that projection fibers labeled by an injection of WGA-HRP in the FEF crisply avoid striosomes (see Fig. 2.5 for injection site). In monkey M7 (B,B'), sections at approximately A15.0 (*Macaca mulatta*) show that the SMA fibers (WGA-HRP) crisply avoid striosomes in the putamen; where striatal labeling is heaviest in the caudate nucleus, striosomal avoids are less obvious (injection site indicated on the brain hemisphere shown here). Asterisks indicate the locations of corresponding striosomes on the pairs of sections. AC - anterior commissure, CN - caudate nucleus, GPe - external segment of the globus pallidus, P - putamen, Th - Thalamus. Scale bars denote 3 mm.



CHAPTER 3. Functional Terminations Of Cortical Afferents On Neuronal Subpopulations In Multiple Striatal Zones: cortically-driven immediate early gene expression in the squirrel monkey putamen.

ABSTRACT

Numerous anterograde tract tracing studies have shown that corticostriatal fibers form densely labeled, widely distributed patches in the striatum usually surrounded by less densely labeled striatal fields. We show here that electrical stimulation of sites chosen within somatosensory cortex induces the immediate early genes (IEGs), Fos and Jun B, in localized patches in the putamen which correspond with striking precision to the densely labeled fiber patches (matrisomes) anterogradely traced from those sites. Furthermore, using the recently-developed anterograde tracer, biotinylated dextran amine (BDA), we were able to visualize presumptive terminal varicosities of the cortical axons. Stimulation of the motor cortex induces IEGs within striatal regions circumscribed by the terminals labeled from the corresponding representations in somatosensory cortex.

IEGs are not induced in every neuron. We used double-label immunohistochemistry to characterize the neurons expressing Fos after cortical stimulation. Perhaps because of the variability engendered by using an anesthetized preparation, similar parameters of electrical stimulation induced a pattern of IEGs in the striatum that had similar distributions but varied markedly in the density of induction. Interestingly, when the density of induction within a matrisome was sparse, almost every neuron expressing Fos was a parvalbumin-containing (GABAergic) interneuron. Furthermore, almost every parvalbumin-containing neuron within the matrisomes were found to strongly express Fos.

Only when cortical stimulation resulted in more intense Fos induction, were other types of neurons activated. In the areas of densest induction, 75% of the Fos-positive nuclei were found in enkephalinergic neurons. This expression pattern would argue for a

differential influence of the somatomotor cortex on enkephalinergic as opposed to substance P/dynorphin-containing neurons, although technical limitations prevented us from assaying this directly. Fos was also found in a subset NADPH-diaphorase containing and calretinin-containing interneurons. In contrast, cholinergic neurons were never found to express Fos in response to cortical stimulation.

In conclusion, the spatial pattern of IEG expression and the distribution of terminal varicosities after injections of BDA support the notion that patches densely labeled by anterograde tracers correspond to areas of dense functional synaptic input onto striatal neurons. Sparser label does not seem to represent terminals which as effectively induce IEG expression. We speculate that cortical input may first target parvalbumin-containing interneurons, which depress the remaining neuronal activity within a matrix in a feed-forward manner, until stronger input can overcome the inhibition to selectively influence the enkephalinergic projection neurons.

INTRODUCTION

From experiments detailed in the previous chapter, and from the work of others, it is now well-established that even small regions of the cerebral cortex send fiber projections to the primate striatum that are distributed in patches and that span an extensive longitudinal domain (Künzle, 1975; Künzle, 1977; Yeterian and Van Hoesen, 1978; Selemon and Goldman-Rakic, 1985; Flaherty and Graybiel, 1991; Parthasarathy et al, 1992; Eblen and Graybiel, 1995). Depending on the relationship between the cortical areas studied, afferent patches have been found to overlap or interdigitate within the striatum. On the basis of such evidence, the argument has been made that cortical afferents may delimit modules within the striatum (matrisomes; Graybiel et al., 1993) that, by analogy to neurochemically-defined striosomes, provide a substrate within which neuronal interactions may be restricted (Walker et al., 1993) or across which they may be combined (Kawaguchi, 1992).

The aforementioned studies of corticostriatal projections have mainly employed anterograde tracers such as radioactive amino acids or wheat-germ agglutinin-conjugated horseradish peroxidase (WGA-HRP) to provide a low resolution image of the cortical fibers within the striatum. On the basis of electron microscopic evidence which has shown that cortical fibers exhibit en passant terminals as they traverse the striatum (Fox et al., 1971; Wilson et al., 1990), it is assumed that these patches represent functional cortical terminations. Fibers thus revealed are often found as patches in the striatal matrix that are intensely stained, but surrounded by much more lightly stained striatal territory. The question arises as to whether this pattern represents a gradual thinning out of the cortical terminations from a given area, or an artifact of the methodology, and how this relates to the functional efficacy of the cortical input.

In order to examine a measure of the overall spatial pattern of striatal activity in response to cortical input, we chose to assay the expression of immediate early gene proteins after electrical stimulation of the cerebral cortex. In the past several years, many laboratories have used, with varying degrees of success, the induction of immediate early gene (IEG) mRNAs and their protein products as a kind of trans-synaptic tracer, or

marker of activation within a given neural system (Morgan and Curran, 1991; Sheng and Greenberg, 1990). The most commonly used of these is the transcription factor-component c-Fos, which is generally expressed at very low levels in the nervous system, but which can be induced transiently by appropriate stimuli. The Fos-family (e.g. c-Fos, Fos B, Fra-1, and Fra-2) of proteins dimerize with Jun-family proteins (e.g. c-Jun, Jun B, Jun D) in various combinations to interact with AP-1 and related sites which are found in the promoter regions of many genes, including those for neuropeptides such as enkephalin and dynorphin (Sonnenberg et al. 1989; Naranjo et al. 1991). Extensive studies in rats have demonstrated that various neurotransmitter agonists and antagonists induce IEGs in the striatum, in a manner consistent with what is known about the pharmacological properties of the agents used with respect to the receptors present on striatal neurons (reviewed in Hughes and Dragunow, 1995).

An important goal for these experiments was to establish electrical stimulation of the cortex to induce immediate early gene protein expression as a viable method with which to study the spatial extent of functional efficacy of the corticostriatal projection. In the rodent, specialized parameters for stimulating the motor cortex (MI) are necessary to induce immediate early gene protein expression in topographically correct regions of the caudoputamen (Fu and Beckstead, 1992; Wan et al., 1992; Besson et al., 1993; Parthasarathy et al., 1994). It was by no means obvious that the same parameters would be equally effective in the primate.

Because the motor cortex not only projects into the basal ganglia, but receives strong projections from the basal ganglia-associated regions of the thalamus (Holsapple et al., 1991; Nambu et al., 1991), it was not clear whether recurring activity through this loop contributed to the observed IEG induction after sustained electrical stimulation of the motor cortex. If this were the case, afferent input alone might not be sufficient to activate IEGs. We therefore tested sites in the somatosensory cortex (SI), which is less directly linked to the outputs of the basal ganglia, for effective induction of IEGs in the striatum. In each case, we compared the distribution of two IEGs, Fos and Jun B, to the distribution of fibers labeled by anterograde tracer injections in SI. In an additional set of experiments, we compared the distribution of fibers labeled from SI, with immediate

early gene expression resulting from stimulation of MI. Thus, we were assured that damage from the injection site would not influence subsequent stimulation, and we were able to evaluate our results in the context of a set of projections whose relationship has been previously studied (Flaherty and Graybiel, 1993).

Because of the rapidity with which it traces anterograde pathways, the tracer we used in the majority of our experiments was [³⁵S]methionine. In two cases, however, we combined the stimulation-induced expression of IEGs with injections of the slower anterograde tracer biotinylated dextran amine (BDA), which allows visualization of individual fibers (Brandt and Apkarian, 1992; Veenman et al., 1992; Rajakumar et al., 1993; Reiner et al., 1993). By charting the distributions of corticostriatal terminal varicosities labeled in this manner, we were able to achieve a higher resolution of the borders of the corticostriatal fields.

Finally, we used double-label immunohistochemistry to characterize the neurons which expressed Fos in response to cortical stimulation. We assayed neurochemical antigens which define the major interneuron types of the striatum and in addition, we studied the expression of Fos in enkephalinergic projection neurons.

METHODS

Six squirrel monkeys (*Saimiri sciureus* and *Saimiri sciureus macrodon*) were used in these experiments.

Experiments were typically conducted in three-stage surgeries.

Prior to the first two surgical procedures, the animal was tranquilized with ketamine (12 mg/kg) and anesthetized with xylazine (0.7 mg/kg). In addition, atropine (0.04 mg/kg), dexamethasone (0.1 mg/kg) and DiTrim (30 mg/kg) were administered. Anesthesia was maintained by ketamine (in doses of 5 mg/kg) and supplemented, before surgical procedures, by buprenorphine (0.01 mg/kg). Lactated Ringer's solution (2.3 ml/kg/hr, i.v.) was given throughout the experiment, although it was sometimes discontinued to prevent cortical edema. Between surgeries, the animal was given Tribissen (30 mg/kg, b.i.d., p.o.).

During the first surgery, the cortical area of interest was exposed under sterile surgical conditions by removal of a bone flap. The dura mater was removed and a thin layer of viscasil was placed over the exposed neocortex. Motor areas were located by monitoring movements visually during intracortical microstimulation. Stimulus trains (cathodal or biphasic, 0.2 msec pulse width, 250 Hz) were delivered for 50-100 msec through a low-impedance platinum-iridium electrode. Somatosensory areas were located by monitoring neural activity recorded during tactile stimulation. Sites of electrode penetrations were marked on an enlarged photograph of the exposed cortex. Because of the multiple shortly-spaced survival surgeries entailed in this experiment, just enough time was taken to ensure localization within the cortical area of interest based on extensive experience in this laboratory of mapping the somatosensory and motor areas of the squirrel monkey. After sufficient mapping, biotinylated dextran amine (BDA, 10% in saline, Molecular Probes) was introduced into the cortex through a glass micropipette at the site chosen during the mapping session and identified by reference to the photographic print on which electrode penetrations were marked. The micropipettes were attached to a pressure-injection system (Picopump, World Precision Instruments) capable of delivering tracer in aliquots as small as 1-2 nl. The surgical field was thoroughly

lavaged with sterile saline, 2 drops of neomycin-sulfate/dexamethasone ophthalmic solution were applied to the cortex, and gelfoam was used to cover the opening before the skin flap was resutured.

During the second surgery, 10 days later, the original surgical field was reexposed and the cortical area was further mapped. [³⁵S]methionine (200 microCi/microl; New England Nuclear) or wheat germ agglutinin-horseradish peroxidase (WGA-HRP; 15% in saline; Sigma) were pressure-injected via glass micropipettes in the electrophysiologically-determined locations.

Finally, two days later, before termination, the animal was anesthetized with Nembutal (20 mg/kg induction) and microstimulation was used to induce immediate early gene expression. Parallel bipolar platinum-iridium (MicroProbe) or tungsten wire (A-M systems) electrodes, approximately 2 mm apart, were used to stimulate the cortex for 1-2 hrs. (40 msec trains, 4 trains/sec, 250 pps, 0.2 msec p.w., biphasic). For the experiments in which sites in motor cortex were stimulated, stimulus intensity was adjusted so that a visible, well-localized movement was maintained throughout most of the stimulation period. Two hours after the onset of stimulation, the animal was perfused.

Tissue preparation and histology. The monkeys were deeply anesthetized with Nembutal (average, 50 mg/kg) and perfused transcardially with 4% paraformaldehyde in 0.1 M phosphate buffer containing 0.9% saline or 4% paraformaldehyde in 0.1M sodium cacodylate buffer. Brains were blocked transversely or in the midsagittal plane, and the blocks, after being soaked in buffer containing 20-30% sucrose or glycerol, were cut on a freezing microtome at 40 and 20 microns in coronal or sagittal sections. Sections were processed in serially adjacent sets for WGA-HRP histochemistry, autoradiography, BDA histochemistry, or immunohistochemistry.

For autoradiography, sections were mounted on chrome-alum-subbed slides, dried, defatted, dipped in Kodak NTB-2 emulsion, dried again, and stored in light-tight boxes at -20°C for 1-8 weeks. Sections were developed in Kodak D19 developer and counterstained through the emulsion. WGA-HRP histochemistry was carried out by a modified TMB method (Mesulam, 1978). BDA histochemistry was identical to the avidin-biotin incubation for immunohistochemistry. Immunohistochemistry was carried

out with commercially-bought antibodies against c-Fos (Oncogene Science Ab-2, 1:200 and 1:500), ChAT (Incstar, 1:2000), parvalbumin (Sigma, 1:1000), met-enkephalin (Incstar, 1:1000), and Jun B antiserum (1:3000 lot#725-5 and 1:10,000 lot#725/3) from Dr. R. Bravo. Sections were treated with 10% methanol and 3% hydrogen peroxide to inhibit endogenous peroxidases and to eliminate cross-reaction with WGA-HRP, then incubated with 5% normal secondary serum, followed by overnight incubation at 4°C in primary antibody in phosphate-buffered saline with 0.2% triton X-100. After a 1-2 hour incubation with biotinylated secondary antibody, sections were processed with avidin-biotin kits (Vector) and visualized with nickel-enhanced diaminobenzidine (DAB). Double-labeling immunohistochemistry was performed serially, with overnight washing in phosphate buffered saline with 0.2% Triton X-100 (PBS-Tx) followed by blocking steps in hydrogen peroxide, avidin, and biotin between the two procedures. BSA was substituted throughout for normal secondary serum. The first antigen was detected with nickel-enhanced DAB (black reaction product), the second with cacodylate-buffered DAB (brown reaction product). For double-labeling of Fos and enkephalin antigens only, the Fos was visualized using gold-conjugated secondary (1:50) followed by silver intensification with Intense-M kit as necessary. Histochemistry for NADPH-diaphorase followed the immunohistochemistry (DAB) reaction for Fos or Jun B.

Data Analysis. Sections were charted using camera lucida, either by hand or on the Eutectics computerized image system. Fos-and Jun B-positive nuclei were charted at 20x. Unless otherwise specified, IEG plots are representative of the observed distributions (i.e., within the densest fields of induction, not every nucleus was counted), and were not used for quantitative comparisons.

For comparison of [³⁵S]methionine distributions to IEG distributions, serial sections were used unless otherwise indicated. The outline of the section processed for IEG immunohistochemistry was first traced on the Eutectics and printed. Blood vessels were then traced onto the printed image by hand, using a Wild microscope with drawing-tube attachment. The adjacent section processed for autoradiography was aligned according to the blood vessel pattern and the outlines of the corticostriatal fiber projection were drawn. This final composite drawing was retraced on a Summagraphics tablet into

the Eutectics system computer and saved as a Hewlett Packard Graphics Language (HPGL) file. Plots of IEG-positive nuclei, also within the boundaries of the same outline of the putamen, were also saved as an HPGL file and the two images were converted and aligned using an automatic function of Corel-Draw 3.0 (Corel Corporation).

Double-labeled neurons were charted at either 40x or 63x. Sections processed for double-immunohistochemistry were spaced approximately 1 mm apart. For each section, a border around the area of induction was drawn at low power, just sufficient to enclose all Fos-positive nuclei. For interneurons, all single and double labeled neurons within this area were counted and expressed as percentages of interneurons containing Fos. For enkephalinergic neurons, microscope fields were chosen randomly within the area of dense induction and all Fos-positive nuclei (colocalized or not with enkephalin) were plotted within these field and expressed as percentages of Fos-positive nuclei within enkephalinergic neurons.

Terminal varicosities labeled by injections of biotinylated dextran amine (BDA) were counted at 63x. Because sections were typically 40 microns thick, a plane of focus was chosen such that the observed density seemed maximal and all varicosities were charted within this plane. These charts were converted to HPGL files, and then to Corel-Draw files. BDA and IEGs were detected on the same section.

All plots accurately reflect the number of points charted, however, each point on the image is necessarily larger than the relative size of a nucleus (or varicosity) with respect to the size of the putamen.

Approximate density of Fos induction was calculated by counting the nuclei on three cross-sections and dividing the total counts by the volume in which they were found (area of the induction x 40 μm).

RESULTS

In eight hemispheres of six monkeys, we electrically stimulated sites in either somatosensory or motor cortex to induce the expression of immediate early gene proteins in the primate striatum (Table 3.1). Based on more extensive experiments in rats (see appendix), in these cases, we chose to stimulate through parallel bipolar electrodes, spaced 1.5 to 2 mm apart with trains of high frequency pulses for one hour. For stimulation of the motor cortex, stimulus intensities were adjusted to maintain a non-habituating, visible well-localized movement. For somatosensory cortex, stimulus intensities were chosen comparable to those used for the motor cortex.

In all cases for which we followed these parameters, Fos-like-immunoreactivity (Fos) was induced in striatal patches which ranged in cross-sectional area from 0.3 to 1.5 mm². In two unstimulated hemispheres, no Fos was observed in the striatum. In two cases, one using a single concentric bipolar electrode (SMRC48L), and one using electrodes spaced much more closely (SMRC48R), little or no Fos induction was observed.

Jun B-like-immunoreactivity (Jun B) was also induced in striatal patches corresponding to the distribution of Fos. However, within these patches, Jun B was more densely expressed and was present over a variable background of scattered nuclei throughout the striatum. This background was also observed in untreated control hemispheres.

Somatosensory Cortex. In three cases, we combined electrical stimulation in the somatosensory cortex (SI) with injections of anterograde tracers in SI and compared the subsequent expression of Fos and Jun B with the distributions of labeled corticostriatal fibers.

SMRC46. In one hemisphere, we mapped the foot region of area SI and injected [³⁵S]methionine into the digit representation of area 3b. In squirrel monkeys, the cutaneous receptors of the foot are represented in areas 3b and 1 as mirror images, such that the anteroposterior order of representation is: area 3b digits, area 3b pads, area 1

pads, area 1 digits (Sur et al., 1982). Our laboratory has previously shown that the corticostriatal fiber projections from different sites within the SI foot representation are largely convergent (Flaherty and Graybiel, 1993). Therefore, we matched our injection site by electrically stimulating across the cutaneous digit representation in SI, placing one electrode at the site of tracer injection in area 3b, and the second electrode in the foot region of area 1.

As expected, autoradiographically labeled fibers were found in an extended rostrocaudal distribution in the dorsolateral putamen, in a pattern which was observed as multiple patches in a given coronal section (Fig. 3.1). For longer exposure times, these patches were seen as intensely labeled “hot spots” surrounded by more weakly stained “halos”. Fos and Jun B were strongly induced in dense striatal patches (density of Fos > 16000 nuclei/mm³). Comparing the distribution of these afferent patches with that of the induced IEG expression, a striking precision was observed between the distribution of labeled nuclei and that of the methionine-labeled hot spots (Fig. 3.1 and Fig. 3.2).

SMRC48. In a second experiment, we again mapped and injected the foot representation of area 3b. We stimulated across the D2-5 digit representations, after having injected [³⁵S]methionine into the D1 and dorsal foot representation, found more laterally in the cortex. Stimulation in this case resulted in a somewhat sparser distribution of Jun B, and a much more sparse distribution of Fos (density of Fos < 4000 nuclei/mm³). In this case, the correspondence of IEG induction with anterogradely labeled corticostriatal fibers was still quite good, although the sparsely distributed Fos nuclei covered more of the halo of the corticostriatal fiber field as compared to the previous case. Part of this mismatch may be explained by the nonadjacency of sections processed for Fos and autoradiography (they are separated by an intervening 40 micron section). The same sections processed for Jun B were also processed by autoradiography. These sections demonstrated a sharper correspondence between the dense patches of Jun B and the intense patches of corticostriatal fibers (Fig. 3.3).

SMRC49. Previous work has established that fibers from a large part of the cutaneous foot representation in somatosensory cortex project to overlapping patches in the striatal matrix (Flaherty and Graybiel, 1991). Therefore, in the first two cases, we

attained a striking degree of correspondence between the distribution of immediate early genes and of afferent fibers even though the stimulating electrodes and the injection sites were not perfectly aligned. Indeed, there are technical difficulties in aligning parallel bipolar stimulation and a single injection site. Exactly straddling the injection site with the stimulating electrodes would not be ideal, because the current density would be highest at the two poles.

In order to examine the correspondence between afferent innervation and stimulated IEG expression more closely, we invoked two additional anterograde tracers, biotinylated dextran amine (BDA) and wheat germ agglutinin-conjugated horseradish peroxidase (WGA-HRP). BDA has the significant advantage of having a much higher resolution than the other tracers used in our experiments, such that individual fibers and varicosities can be easily observed at high magnification (Fig. 3.8B).

With three tracers, we were able to place each electrode at the center of an injection site and compare the IEG induction with the distribution of fibers from each injection as well as from a neighboring, non-stimulated injection site. We mapped the hand/forearm representation of area SI, placed BDA in the digit representation of area 1, [³⁵S]methionine in the digit representation of area 3b, and a third tracer, WGA-HRP into the forearm region of area 3b and 1. The electrodes were placed in the cortical sites corresponding to the methionine and BDA injection sites.

In this case, the BDA injection was less than 1 mm in diameter (Fig 3.4). Dense terminal varicosities from the BDA injection were found in ventrolateral patches separated by long sparsely-branching fibers. The diameter of the methionine injection site was twice the size of the BDA injection, and the fiber projection within the striatum extended more dorsomedially. The WGA-HRP injection was several millimeters in diameter, such that it encroached on the methionine injection site. The main innervation field in the putamen from this last injection site was found in sagittal sections considerably medial to the sections containing label from the BDA injection (data not shown).

Induction of Fos was sparse (< 4000 nuclei/mm³), but was found within the center of the distribution of terminal varicosities from the BDA injection in lateral sagittal

sections through the putamen. This distribution also matched the hot spots of autoradiographically detected methionine label. The most medial expression of IEGs was found on the edges of the BDA terminal field, but still centered within the methionine-labeled fiber projection. As expected, the expression of Fos was not found to overlap with the WGA-HRP-labeled fiber projection.

Motor Cortex. In four cases, we electrically stimulated regions of the motor cortex to induce IEG expression in the striatum. In all cases, we chose an intensity of stimulation sufficient to reliably obtain discrete movements throughout the stimulation period. Fos was induced in localized regions of the striatum in a pattern conforming to the known somatotopic organization of the putamen (Fig. 3.5). As found for stimulation of the somatosensory cortex, the intensity and density of subsequent IEG induction in the striatum varied considerably among the cases. Jun B was also induced in patterns closely corresponding to that of Fos, except that Jun B was generally more densely and strongly expressed and was present over a background of scattered expression throughout the striatum (Fig 3.6).

In one case, SMRC46R, in which the electrodes were placed less than 1 mm apart and Fos was found in only a few nuclei in the ventrolateral putamen, Jun B was found throughout the ipsilateral striatum (data not shown). While, with Nembutal anesthesia, microstimulation through parallel bipolar electrodes generated movements that were quite consistent throughout, or that waxed and waned somewhat in strength, in case SMRC46R, the stimulation seemed to potentiate in a manner reflecting a “Jacksonian march” (Jackson 1884), such that facial muscles were invoked in addition to forearm before the current intensity was lowered sufficiently. From data obtained in rats (see Appendix), we have concluded that while Fos is relatively insensitive to brief general seizure activity, widespread Jun B induction in the striatum can be observed even after brief cortical seizures.

Motor cortex and somatosensory cortex. It is known that afferent fibers from somatotopically corresponding regions of SI and MI overlap in the striatum (Flaherty and

Graybiel, 1992). There are many methodological constraints in understanding the precision with which this overlap is achieved. In two cases, we compared the distribution of cortical afferents from somatosensory cortex with IEG induction after stimulation of the motor cortex. Our aims were to (1) study somatomotor patches in the striatum without any possible damage resulting from tracer injection affecting subsequent stimulation (2) begin to assess the integrity of the borders of matrixes.

SMRC43. In this case, we electrically stimulated the foot representation of motor cortex. The distribution of Fos in the dorsolateral putamen was sparse (<4000 nuclei/mm³, Fig. 3.7) but quite similar to that induced by stimulation of the foot representation of SI. Injection of [³⁵S]methionine in the shoulder representation of somatosensory area 3b anterogradely labeled corticostriatal fiber projections ventral to the distribution of Fos and Jun B (Fig. 3.7). In rostral sections, the two distributions were well separated. In caudal sections, the two distributions were abutting, but did not appreciably overlap.

SMRC44. In a second case, we compared the distribution of BDA-labeled varicosities after injection of the hand/forearm representation of area SI with IEG induction after electrical stimulation of the motor cortex to induce flexions of the forearm. The Fos induced by this stimulation was strong and dense (>12,000 nuclei/mm³) In this case, the IEG induction pattern followed quite closely the distribution of terminals labeled from SI, although there were small areas of the putamen in which dense BDA-labeled terminals were found where there was no induction of IEGs (Fig. 3.8a and b).

Induction in other basal ganglia structures: In one animal (SMRC46), we processed almost every section for immunohistochemistry for Fos or Jun B. Stimulation of the somatosensory cortex in this case produced strong induction of both IEGs in multiple patches in the putamen. In addition, induction of Fos and Jun B was found in other direct targets of the somatosensory cortex: in a discrete area of LPL, in a dorsolateral quadrant of the subthalamic nucleus, and in a crescent of the reticular nucleus of the

thalamus. Thalamic and subthalamic IEG induction was found to closely correspond with the anterograde labeling from the corresponding cortical injection (Fig 3.9).

IEG induction was also observed in neurons distributed in a crescent in the external segment of the globus pallidus (Fig. 3.9), a structure which does not receive direct afferent input from the cerebral cortex. Notably, no induction was observed in the internal segment of the globus pallidus or the substantia nigra.

Phenotypic identification of striatal neurons expressing Fos.

In four cases, we used double-label immunohistochemistry to phenotypically characterized the neurons expressing Fos in response to cortical stimulation. We chose Fos rather than Jun B because of its almost complete lack of detectable constitutive expression in the primate putamen. Furthermore, because of the apparent response of Jun B to more general seizure activity, we felt that it may less accurately reflect a physiological efficacy of corticostriatal terminals.

Fos induction in parvalbumin-containing GABAergic interneurons is especially sensitive to cortical stimulation.

In four cases, we used double-label immunohistochemistry to phenotypically characterize the neurons expressing immediate early genes in response to cortical stimulation. One of the most striking results was the exquisite sensitivity of stimulation-induced Fos expression in parvalbumin-containing GABAergic interneurons. In cases where stimulation resulted in very sparse induction, almost all of the Fos-containing nuclei were found in these interneurons. In SMRC46R, stimulation of the hand representation of motor cortex, induced expression of Fos ventrolaterally in the caudal putamen such that only five nuclei were strongly labeled in one section. All were colocalized with parvalbumin (Fig. 3.10a). In another case, SMRC51 (Fig. 3.11a), stimulation of the hand area of motor cortex resulted in more dense expression of Fos (density < 2000/mm³). Again, of the strongly labeled nuclei, 84% were found in parvalbumin-containing neurons (146/174. NB: however, when the much weaker nuclei were counted, the percentage dropped to 53%). Similarly, in case SMRC48 (Fig.

3.11b), for which stimulation of SI resulted in sparse Fos induction (density < 4000 nuclei/mm³), 74% (180/241) of the Fos-containing nuclei were found in parvalbumin-containing neurons.

In SMRC46, for which electrical stimulation induced very strong dense expression of Fos in the striatum (density > 16,000 nuclei/mm³), although they came to be a minority of those neurons expressing Fos (<< 20%), virtually every parvalbumin-containing neuron in the field of induction strongly expressed Fos (95% , 275/291; Fig. 3.10b). Like the previous cases, it was apparent that the distribution of the uncolocalized Fos was more restricted as compared to the distribution of the parvalbumin-containing neurons expressing Fos. As seen in Fig. 3.11c, the parvalbumin-containing neurons expressing Fos seemed to form a halo around dense cores of Fos, similar to the observed pattern after injection of [³⁵S]methionine. These patterns in fact were similar to the point that the Fos found within the halo of the autoradiographically-traced fiber projection from the same cortical site was invariably expressed by parvalbumin-containing interneurons (data not shown, but compare Fig. 3.1 with Fig. 3.10c).

Fos was induced to varying degrees in other striatal interneurons, but almost never in cholinergic interneurons.

In SMRC51, for which induction was quite sparse, there was no Fos colocalization observed in calretinin-containing or NADPH-diaphorase-containing neurons. However, in SMRC46, in which induction was quite strong and dense, 60% (30/50) of NADPH-diaphorase-containing neurons were found to express Fos (Fig. 3.12a). NADPH-diaphorase-containing neurons in the center of the field of induction almost always expressed Fos and then the likelihood of colocalization dropped at the periphery, so that this percentage is somewhat misleading. On the other hand, only 12% (18/153) of the calretinin-containing neurons were found to express Fos. These neurons were unambiguously double-labeled (Fig. 3.12b), but distributed randomly and not concentrated in the center of the field of induction.

Fos was never found expressed in cholinergic interneurons (Fig. 3.12c).

Projection neurons. Finally, in cases SMRC46 and SMRC44, we assessed the colocalization of Fos with enkephalin. In both cases, approximately 75% (SMRC46 267/355 and SMRC44 115/150) of the Fos-positive nuclei were found in enkephalinergic neurons. (Fig. 3.12d).

To complete our immunohistochemical survey of Fos induction in identified striatal neurons, we tried commercially available antibodies against dynorphin (Peninsula Antibodies) and an antibody donated by S. Watson. Although the donated antibody worked in rat (see appendix), neither antibody worked satisfactorily on primate tissue. However, the sum of the numbers of Fos-positive nuclei colocalized with parvalbumin, enkephalin, NADPH-diaphorase, and calretinin leaves very little Fos-positive nuclei that could be expressed in dynorphin-containing projection neurons.

DISCUSSION

We have used cortically-driven immediate early gene expression in the striatum to demonstrate functional terminations of cortical fibers in multiple zones of the primate putamen. Electrical stimulation of the primate somatosensory and motor cortex induces the expression of Fos and Jun B in patches of neurons in the striatum which correspond to dense innervation by methionine-labeled cortical afferent fibers and BDA-labeled corticostriatal terminal varicosities. However, not all neurons within afferent patches responded to cortical input. In fact, cortical afferents appear to selectively target Fos expression in parvalbumin-containing GABAergic interneurons, NADPH-diaphorase containing interneurons, and enkephalinergic projection neurons.

Stimulation conditions. We chose stimulation conditions as described in a preliminary report on this technique in rats (Besson et al., 1993), and which we ourselves tested in rats (see Appendix, Parthasarathy et al., 1994): 250 pps in 40 msec trains, 4 trains/sec for 1-2 hours through parallel bipolar electrodes spaced 1.5-2 mm apart. Stimulation intensities were comparable to those used in rats (350-500 μ Amps). Discrete visible movements of the body were elicited throughout the stimulation period. The strength of the movement waxed and waned somewhat over time, but, except in one case, SMRC46R, did not qualitatively change.

In one animal, we stimulated somatosensory cortex in one hemisphere (SMRC48R) with our standard parallel bipolar electrode configuration and the somatosensory cortex of the other hemisphere (SMRC48L) with a concentric bipolar electrode. Even though all other parameters were identical, no induction was seen in the hemisphere stimulated with the concentric bipolar electrode (not shown). Similarly, in another animal, we stimulated the somatosensory cortex in one hemisphere (SMRC46L) with our standard parallel bipolar electrode configuration and the motor cortex of the second hemisphere (SMRC46R) with electrodes spaced less than 1 mm apart. Robust induction was observed to coincide with anterogradely-labeled fibers in the first

hemisphere, whereas only a very few Fos nuclei were visible in the second hemisphere. This was in spite of the fact that stimulation of the second hemisphere evoked strong movements of the forearm throughout the stimulation period. In this case, it should be noted that the current seemed to spread through the motor cortex during a brief period of the stimulation, such that facial muscles were also activated. This spreading “seizure-like” activity seems to have been the cause of widespread non-specific induction of Jun B throughout the ipsilateral putamen, while the stimulus itself was virtually ineffective for inducing focal expression of Fos in the striatum

We conclude from these results and from studies in the rat (see appendix), that there is a minimum volume of the cortex which must be activated in order to elicit the expression of immediate early genes in the striatum. Retrograde studies from the striatum have shown that primate corticostriatal neurons are not densely distributed (Jones et al., 1977; Arikuni and Kubota, 1986; Saint-Cyr et al., 1990). In the rat, it has been shown that a single corticostriatal fiber makes multiple sparse arborizations in the striatum (Cowan and Wilson, 1994) and indeed, our own experiments in which small amounts of BDA were injected in the squirrel monkey cortex agree with this result (data not shown). Furthermore, electrophysiological evidence indicates that, in particular, medium spiny projection neurons receive tens of thousands of cortical inputs (Wilson, 1993). It is likely that the area of stimulation necessary to elicit IEG induction is related to the number of corticostriatal fibers necessary to activate a particular striatal neuron.

Even among cases for which stimulation patterns were relatively standardized, there was a wide variability in the density of IEG expression. We suspect that this variation resulted from different degrees of anesthesia as well as from differences in the exact placement of the electrodes with respect to elements in the cerebral cortex. Parallel bipolar stimulation results in a complex field of stimulation, following a path of least resistivity between the two electrodes. The complexity is compounded by the fact that while one electrode is a cathode, the other is an anode, and the two types of stimulation have different radii of effectiveness. Particularly, the relationship of the electrode configuration to the passing fibers, which are not homogeneously distributed within the

cortex, is likely to influence the effectiveness of stimulation (Stark et al., 1962; Ranck, 1975; Hoeltzell and Dykes, 1979; Asanuma, 1981; Yeomans, 1990).

Immediate Early Genes. The use of the word “activation” in the above discussion has been kept deliberately vague. In the context of immediate early gene protein expression, we are obviously not necessarily referring to the generation of action potentials. Instead, the expression of these proteins marks the induction within these cells of an intracellular second messenger cascade. Many signals appear to converge on the nucleus to cause increased expression of these genes. In vitro, it has been shown that activation of protein kinase C by phorbol esters or calcium, protein kinase A by cAMP, or tyrosine kinases which are part of growth factor receptors, will all result in increased expression of Fos- and Jun-family members (Sheng and Greenberg, 1990).

While it has become clear that these genes cannot be used simply as universal markers of sustained neural excitation, the details of the stimuli which induce these genes in a specific neural system can be revealing about the nature of the system. For instance, in the circadian system, light stimuli induce Fos expression in the suprachiasmatic nucleus, but only when that stimulus will disrupt the normal circadian cycle (Rusak et al., 1990). Visual stimuli will also induce Fos in visual cortex of kittens after 1 week of total darkness, but will not have nearly the same magnitude of effect on adult cats beyond the critical period of visual plasticity (Mower, 1994). In the hippocampal system, electrical stimulation induces IEG expression in the dentate granule cells only in the case of stimuli which will also induce LTP (Cole et al., 1989; but see Wisden et al., 1990).

In the rodent, systemic administration of many neurotransmitter-related substances has been found to affect the expression of immediate early genes in the striatum. Systemic administration of indirect dopamine agonists, e.g. cocaine or amphetamine, induces Fos in striatal neurons via D₁-like receptor activation (Dragunow et al., 1991; Graybiel et al., 1990; Snyder-Keller, 1991; Young et al., 1991; Cenci et al., 1992; Berretta et al., 1992). In this system, D₁-like receptors are probably stimulated to cause cAMP production and subsequent cascades leading to the induction of IEGs.

The most parsimonious explanation for the observed induction of Fos and Jun B in our experiments is that glutamate released from cortical terminals induces sufficient depolarization of the particular neuron to allow calcium entry through voltage-gated channels (or through NMDA receptors), and a cascade through calmodulin-dependent phosphorylation to the expression of Fos and Jun B (Greenberg et al., 1986; Morgan and Curran, 1986; Szekely et al., 1987; see also Appendix Fig. A.11). While undoubtedly other IEG proteins are induced by this paradigm (data not shown suggests that the expression of Fos and NGFI-A are also induced), we chose to study only Fos and Jun B because of their low constitutive expression in the striatum. In fact, Jun B had a variable background expression which may have related to the state of the animal or the different lots of antibody.

Organization of the striatum

In these experiments, we have begun to take advantage of a powerful combination of tools with which to study the organization of corticostriatal system at the level of neuronal ensembles. Coherent activation of neuronal populations in the primary somatosensory or primary motor cortex induced the expression of Fos and Jun B in striatal patches that corresponded with the distributions of dense afferent fibers labeled by corresponding anterograde tracer injections. Injection of biotinylated dextran amine gave a much higher resolution of these afferent fibers and it became apparent that the afferent patches in the striatum corresponded to dense terminal arborizations which became somewhat sparser at the edges but which were connected to one another and to the white matter by long thick axons with only a few putative boutons. These fibers probably in large part account for the often observed background of low intensity signal which often join densely labeled striatal zones in autoradiographic tracer experiments. The picture that emerges is one in which a given domain in the cortex sends multiple axons to the striatum that arborize into largely overlapping patches in the striatum. The degree of this overlap might depend on the degree to which the neurons from which they arise are themselves “related”, (e.g. the degree to which the neurons are coactive during

development). Activation of a particular medium spiny neuron would then depend on the simultaneous activity of converging afferent axons.

Almost every Fos-containing nucleus was found within the densest fiber patches labeled by corresponding tracer injections. The exceptions to this rule were exclusively parvalbumin-containing interneurons (see below), which were found within zones of less intense anterograde label (projection halos). However, induction of Jun B was usually found well within the halo of the anterograde fiber projection. Thus a single cortical area can have differential effects on gene expression depending on the strength of afferent innervation.

In two experiments, we reexamined the convergence of corticostriatal projections from somatosensory and motor cortex. In the case for which corresponding body parts were studied, we found sharply defined parts of the matrix borders demarcated by both Fos expression and corticostriatal terminal fields (sections 424 and 472 of Fig. 3.8a). These borders might represent abrupt changes in corticostriatal topography in the striatal matrix. We did not compare this distribution to that of striosomes, but it is unlikely that they can account for all of the borders so observed.

In the case for which noncorresponding body parts were studied, we found patches that were widely dispersed in rostral sections, but abutting one another in caudal sections (Fig. 3.7). This changing organization has been described previously (Flaherty and Graybiel, 1991; Brown and Feldman, 1993). While Figure 3.7 indicates that there may have been some overlap between the Jun B induced by stimulation of the foot representation of motor cortex and the halo of fibers traced from the shoulder representation of somatosensory cortex (the sections charted were separated by an intervening 40 micron section), there is less overlap between Fos expression and this fiber projection (not shown). Thus in this border region, it may be the case that a single cortical area provides weak input, but that a combination of inputs is necessary for induction of Fos.

The discussion so far of patches in the matrix has been limited to two dimensions. If these patches are confluent in three dimensions, it does not necessarily change the argument of potential recombinations within the striatum, because even as labyrinthine

structures, matrisomes would have complex surfaces (rather than borders) at which to interact.

Spatial distribution of striatal neuronal types which express Fos in response to cortical stimulation.

Projection neurons.

In cases in which electrical stimulation of the cortex induced Fos densely in striatal neurons, the majority of Fos-containing nuclei were found in enkephalinergic projection neurons. Neurons which project out of the striatum can be divided into two subpopulations - enkephalinergic and substance P/dynorphin-containing neurons - which occur in approximately equal proportions (Penny et al. 1986, Shivers et al. 1986). Enkephalinergic neurons in the primate are found to colocalize with retrograde label from the external segment of the globus pallidus (GPe) much more commonly than with label from the internal segment (GPi) (Flaherty and Graybiel 1993). In the rat, the substance P/dynorphin-containing neurons are thought to project predominantly to GPi and the substantia nigra pars reticulata (Gerfen et al. 1990).

Unfortunately, we were unable to successfully immunohistochemically label substance P/dynorphin containing neurons in the primate striatum. Because enkephalinergic neurons are generally smaller than interneurons and their dendrites are not easily visualized by immunohistochemistry, it was necessary to use a careful balance of immunogold visualization of Fos combined with DAB-visualization of enkephalin. Under these conditions, it was more difficult to identify non-colocalized Fos-positive nuclei, and thus the estimate of 75% colocalization, may be slightly overestimated. (It should be noted, however, that using this same method, our laboratory has shown that systemic administration of cocaine induces Fos predominantly in non-enkephalinergic neurons). Furthermore, since it has not been established that projection neurons containing one neuropeptide project exclusively to one striatal target structure, arguments based on these numbers become somewhat harder to manipulate convincingly. Obviously, to address this issue, one would like to see these experiments combined with

retrograde labeling from the target structures (although this method, too, is not without caveats).

Nonetheless, our data suggest that cortical input has a differential influence on the so-called “indirect pathway” from the striatum through the external segment of the globus pallidus. While this difference may not be manifested in direct electrophysiological effects, it could imply that the cortex selectively modulates this pathway over a longer time scale. Indeed, cortical activity seems necessary for maintaining levels of enkephalin itself in this subpopulation (Uhl et al., 1988), and this effect may partially be mediated by Fos (Sonnenberg et al., 1989; but see Konradi et al., 1993).

We have also found greater, if not exclusive, induction of Fos and Jun B in neurons of the external segment of the globus pallidus as compared to the internal segment and the substantia nigra. The pattern of IEG-positive nuclei was very similar to that observed by Strick and his colleagues after injection of anterograde transneuronal viruses into the motor cortex (Strick et al., 1995). While at first glance, this would support the hypothesis of differential cortical influence on this pathway, there is no evidence to indicate that GABA (released from striatopallidal terminals) can enhance immediate early gene expression.

Instead, the two most obvious remaining possibilities are that the expression of IEGs is induced by some other factor released by cortical terminals - perhaps enkephalin acting at opiate receptors (Chang et al., 1988) or a growth factor (Peng et al., 1993; Korsching, 1993) - or that the IEG expression is driven by the subthalamic nucleus (STN). The STN receives somatosensory and motor afferents and sends an excitatory projection to the globus pallidus (Robledo and Féger, 1990; Smith et al., 1990; Ryan and Clark, 1991; Hazrati and Parent, 1992; Kita, 1992; Smith et al., 1994).

Parvalbumin-containing interneurons

One of the most striking results of these experiments was the sensitivity of Fos induction in parvalbumin-containing interneurons to cortical stimulation. When stimulation was only weakly effective, almost every Fos-positive nucleus was found in these interneurons.

In the squirrel monkey, electron microscopy has demonstrated synaptic contacts between corticostriatal fibers from the motor cortex and parvalbumin-immunoreactive neurons. All were asymmetrical membrane specializations and the majority occurred on distal dendrites, but also on the perikarya and proximal dendrites (Lapper et al., 1992). Parvalbumin-containing interneurons in the striatum are fast spiking with very short duration action potentials (half-amplitude of <0.4 msec) and lower input resistances (<140 Mohms), as compared to other interneurons. Single shock (synaptic stimulation) results in a single excitatory postsynaptic potential which occurred with or without a single action potential. Constant current injection (to -40 or -30 mV) gives repetitive firing with constant frequency. Thus, the firing of these neurons appear quite sensitive to depolarizing input (Kawaguchi, 1993).

Parvalbumin-containing neurons rarely have dendritic spines. However, close membrane appositions have been observed between neighboring parvalbumin-dendrites. The appositions are seen either on the smooth dendritic shaft or on small protrusions. "It is possible that GABAergic interneurons connected through gap junctions are activated synchronously by their inputs and simultaneously inhibit a large number of their target neurons" (Kita et al. 1990). Parvalbumin-positive symmetrical synapses have been in turn found on somata or proximal dendrites of medium-sized neurons.

Putting these results into a more spatial context, we speculate that cortical input rapidly activates all the parvalbumin neurons within a given matrixome, and these neurons in turn, inhibit the remaining neurons until stronger input overcomes this inhibition. This might be a mechanism for filtering cortical inputs to allow only strong coherent signals to modulate striatal processing.




Table 3.1. Summary of experimental protocols. Abbreviations: AP - anteroposterior, BDA - biotinylated dextran amine, Conc - concentric bipolar, D - digit, Elec - electrode, min - minute, MI - primary motor cortex, ML - mediolateral, Pt-Ir - platinum/iridium, stim - stimulus, surv - total survival time (including stimulation), SI - primary somatosensory cortex, [³⁵S]met - [³⁵S]methionine, WGA-HRP - wheat germ agglutinin-conjugated horseradish peroxidase, μ A - microamperes.

Summary of Experimental Protocols

CASE	Elec 1 Location	Elec 2 Location	Distance Between Electrodes	Current Intensity	Elec Type	Duration stim/surv (min)		Tracer Type	Tracer Location
SMRC43	MI foot	MI foot	1.5 mm AP	500 μ A	Pt-Ir	60	120	[³⁵ S]met	SI 3b shoulder
SMRC44	MI forearm	MI forearm	1.5 mm ML	500 μ A	Pt-Ir	60	120	BDA	SI 3b/1 forearm
SMRC46L	SI 3b foot D5-D3	SI 1 foot	2.0 mm ML	500 μ A (10 min), then 350 μ A	Tungsten	115	120	[³⁵ S]met	SI 3b foot
SMRC46R	MI hand	MI hand	<<1.0 mm ML	500-200 μ A	Tungsten	115	135	none	
SMRC48L	SI lower leg			350 μ A	Conc	90	120	none	
SMRC48R	SI 3b foot	SI 3b foot	1.7 mm	350 μ A	Tungsten	90	120	[³⁵ S]met	SI 3b foot
SMRC49	SI 3b hand D5	SI 1 hand D4/D5	2.3 mm	350 μ A	Tungsten	90	120	[³⁵ S]met, BDA, WGA-HRP	SI 3b/1 hand, forearm
SMRC51	MI hand/wrist	MI hand	2.0 mm	350 μ A	Tungsten	90	120	none	

Figure 3.1. Case SMRC46L. Electrical stimulation of the cutaneous foot digit representation in area SI strongly induces Fos in multiple patches in the primate striatum which correspond sharply with the afferent patches labeled by injection of [³⁵S]methionine in the 3b foot digit representation. **Upper right:** Map of sites in cortical area SI identified by neuronal recording in SMRC46L. A-ankle, D - digit, F - foot, LL - lower leg, P -foot pad. Dotted lines indicate the approximate borders between areas 3a and 3b, and areas 3b and 1. Darker circle indicates the reconstructed injection site. The lighter concentric circle indicates the less intensely labeled marginal zone of the injection site. **Below:** 3 camera lucida charts of Fos-positive nuclei superimposed on charts of autoradiographic label drawn from serially adjacent sections through the ipsilateral putamen. Black dots represent the distribution of Fos induced in this case. Intensely labeled fiber patches are drawn surrounded by zones of weaker label. Coordinates under each section indicate the approximate AP values for *Saimiri sciureus* (Gegen and MacLean, 1962) and the actual section numbers.

SMRC46L

-  Electrical stimulation
-  [³⁵S]methionine
-  Fos

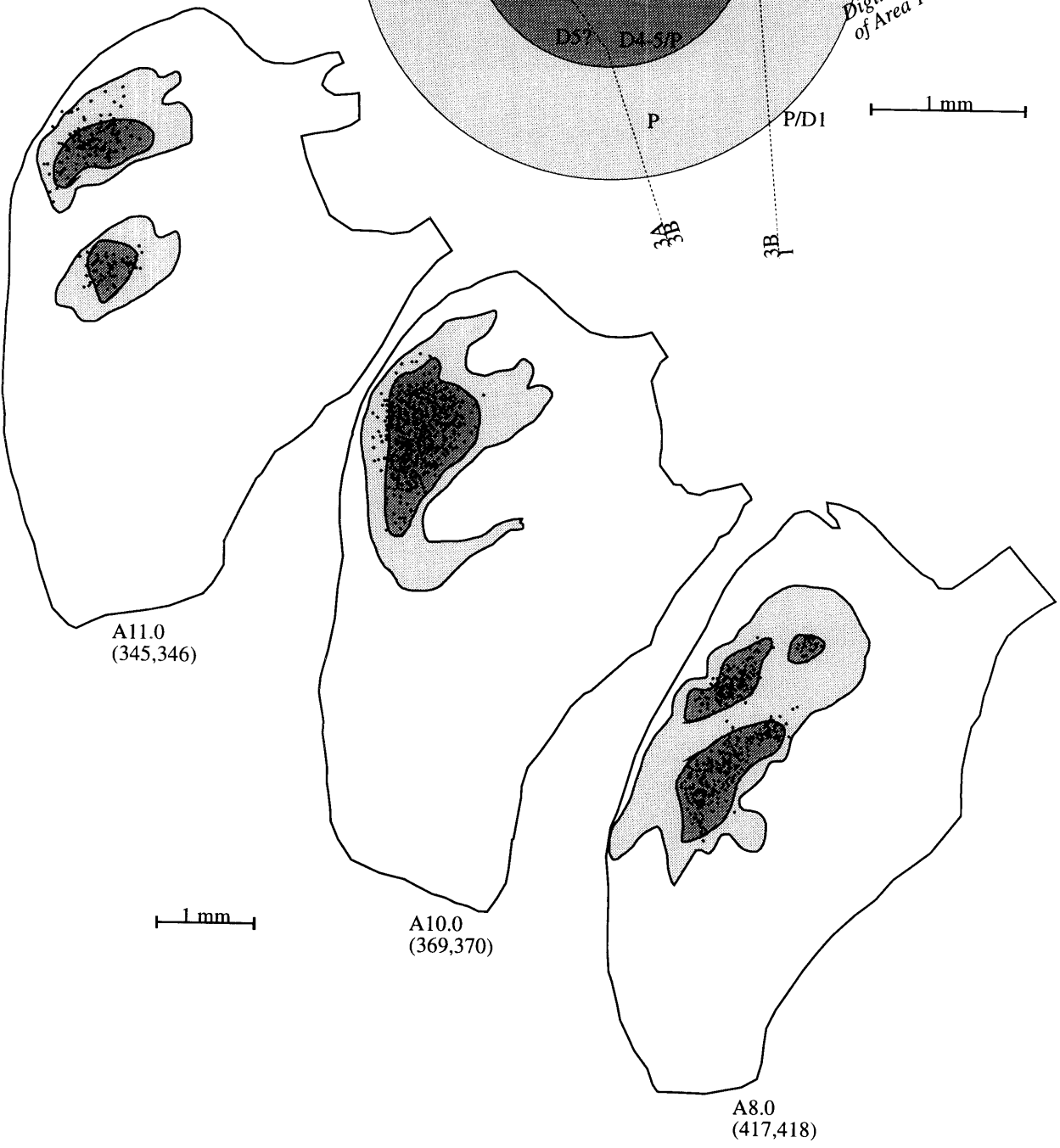
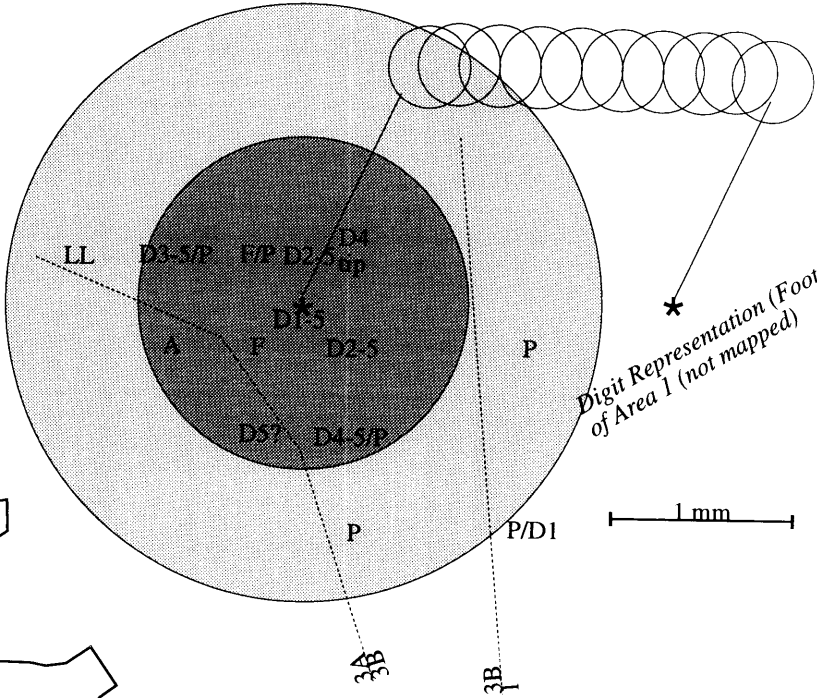


Figure 3.2. Overlap of labeled afferent fibers from the somatosensory cortex (SI) and immediate early gene expression induced by electrical stimulation of SI is shown in high power photomicrographs of serially adjacent transverse sections through the putamen. **A.** Patches of [³⁵S]methionine-labeled corticostriatal fibers viewed under dark field illumination. **B.** Patches of Fos-positive nuclei. **C.** Patches of Jun B-positive nuclei. **D.** The photographed fields are represented by a rectangle on a partial drawing of a transverse section. Sections containing labeled fibers and Fos-positive nuclei are the same as those charted in Figure 3.1 (417,418). V= blood vessel. Scale bar = 0.5 mm.

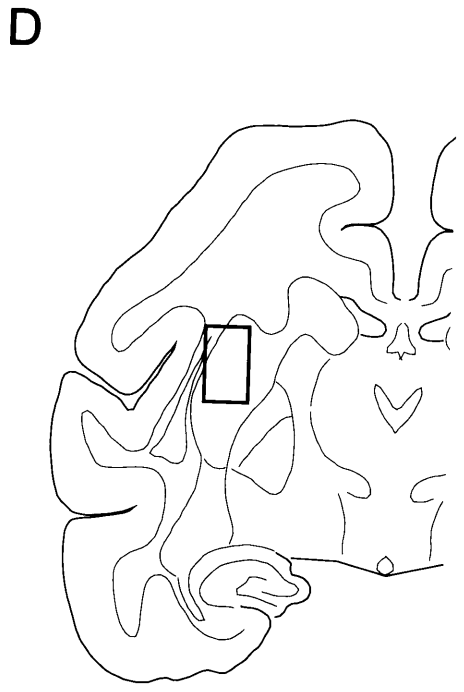
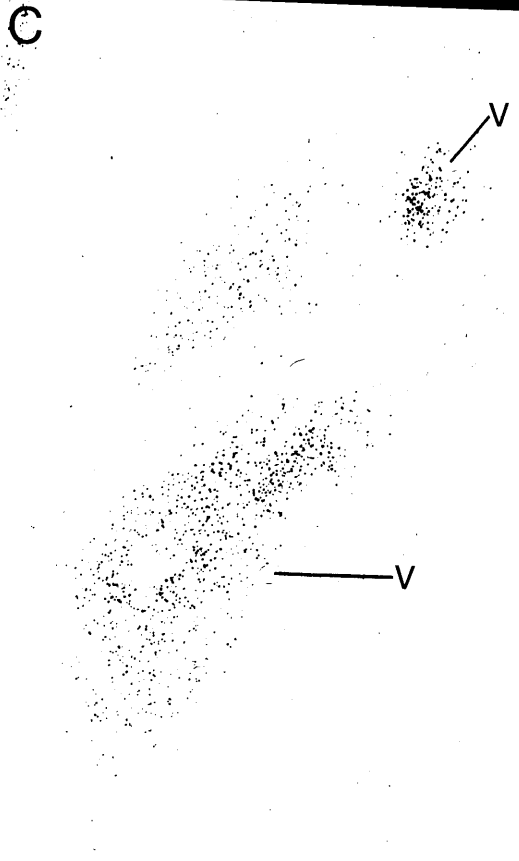
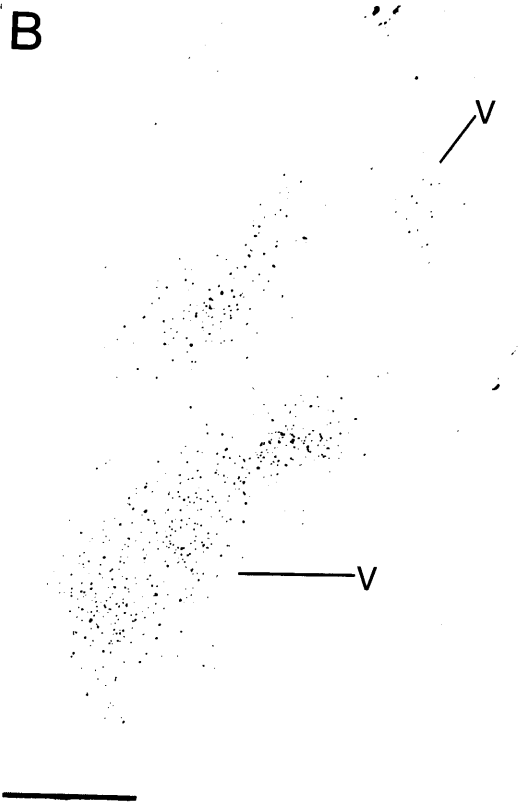

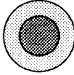



Figure 3.3. Case SMRC48R. Electrical stimulation of the cutaneous foot digit representation in area SI induces Fos and Jun B in multiple patches in the primate striatum which correspond sharply with the afferent patches labeled by injection of [³⁵S]methionine in the 3b foot digit representation. **Upper right:** Map of sites in cortical area SI identified by neuronal recording in SMRC48R. A - arm, D - digit, F - foot, LL - lower leg, Occ - occiput, P - foot pad, S - shoulder, T - trunk, X - no response. Dotted line indicates the approximate border between areas 3a and 3b. Dark circle indicates the reconstructed injection site. The lighter concentric circle indicates the less intensely labeled marginal zone of the injection site. **Below:** Left: Camera lucida chart of Jun B-positive nuclei and anterogradely labeled fibers visualized on the same transverse section through the putamen. Right: Superimposed camera lucida charts of Fos-positive nuclei and anterogradely labeled fibers from transverse sections separated by an intervening 40 micron section. The black dots represent the distribution of Fos or Jun B induced in this case. Intensely labeled fiber patches are drawn surrounded by zones of weaker label. Coordinates under each section indicate the approximate AP values for *Saimiri sciureus* (Gergen and MacLean, 1962) and the actual section numbers.

SMRC48R

-  Electrical stimulation
-  [³⁵S]methionine
-  IEG

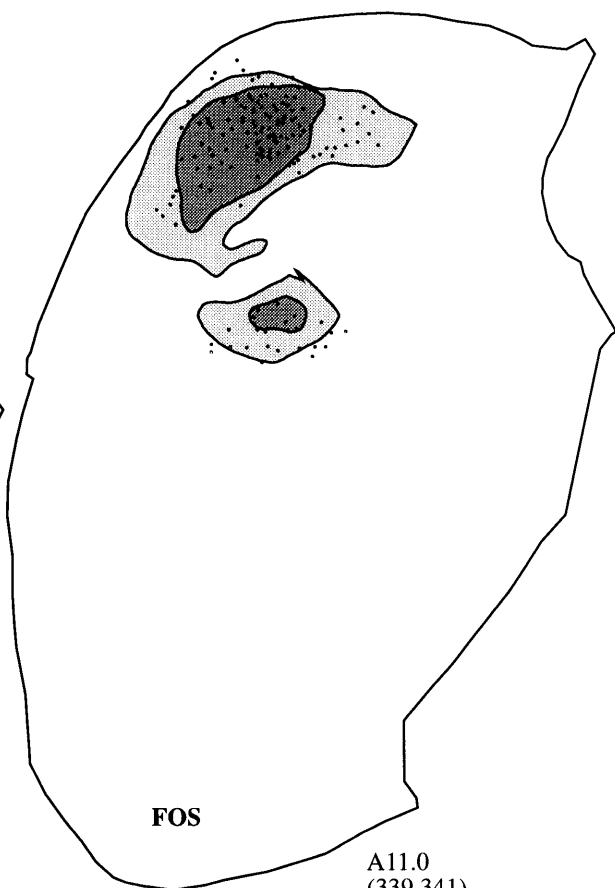
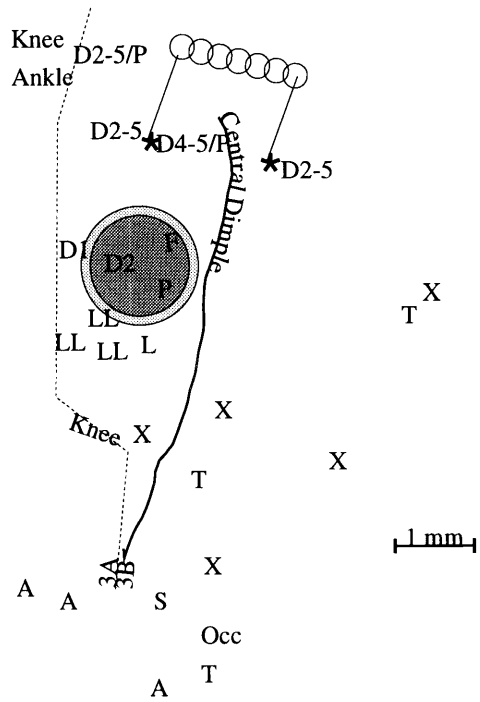
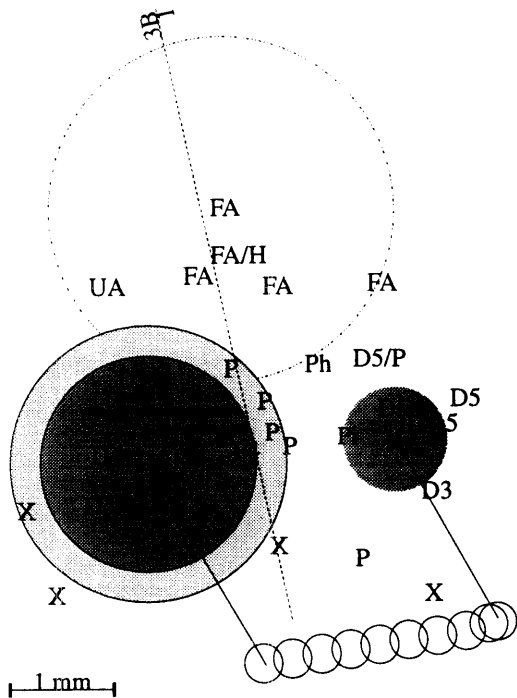





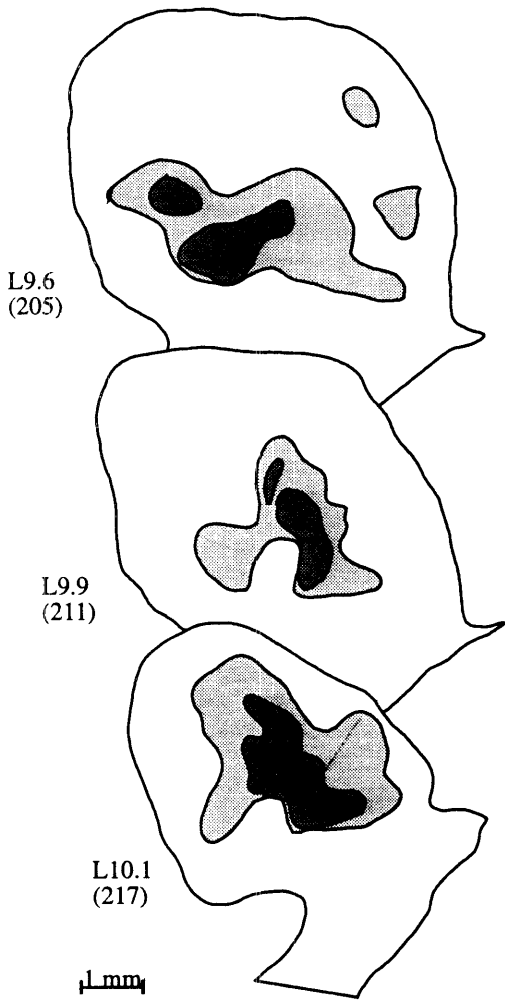


Figure 3.4. Case SMRC49. Parallel bipolar electrical microstimulation across the cutaneous hand digit representation in area SI induces Fos in the putamen in a pattern that corresponds with the convergence of corticostriatal fibers and terminal varicosities labeled from injections at each electrode. **Upper left:** Map of sites in cortical area SI identified by neuronal recording in SMRC49. D - digit, FA - forearm, H - hand, P - hand pad, X - no response. Dotted line indicates the approximate border between areas 3b and 1. Concentric circles indicate the [³⁵S]methionine injection site (intense and marginal zones). The single dark circle indicates the reconstructed biotinylated dextran amine (BDA) injection site. The dotted circle indicates the border of an injection of wheat germ agglutinin-conjugated horseradish peroxidase. **Below:** Left: Camera lucida charts of corticostriatal fiber projections in sagittal sections through the putamen, labeled by injection of [³⁵S]methionine. Right: Camera lucida charts of the distribution corticostriatal terminal varicosities labeled by injection of BDA (gray) and the distribution of Fos (black) visualized on the same section. There were no appreciable labeled fibers from the WGA-HRP injection in the planes of section represented here. Coordinates beside each section indicate the approximate AP values for *Saimiri sciureus* (Gergen and MacLean, 1962) and the actual section numbers.

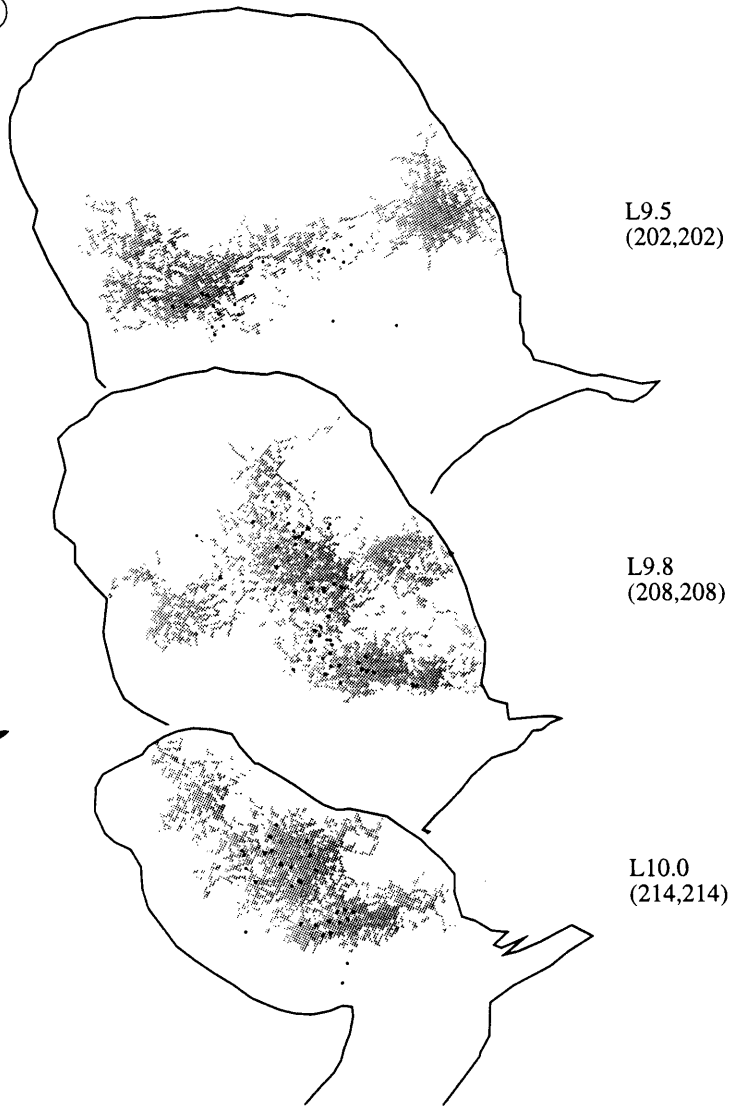
SMRC49



-  Electrical stimulation
-  WGA-HRP
-  [³⁵S]methionine
-  BDA
-  Fos

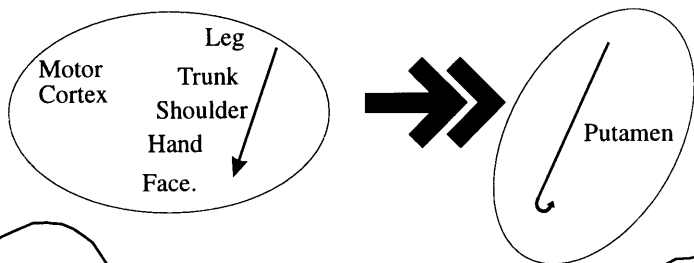


[³⁵S]methionine



BDA, Fos

Figure 3.5. Electrical stimulation of sites in the primary motor cortex (MI) induces Fos in patches in the primate putamen according to the known somatotopy of corticostriatal projections. Camera lucida charts of transverse sections through the putamen that are separated by approximately 1 mm. In SMRC43, stimulation of a medial site in MI to produce movements of the foot induced Fos in patches in the dorsolateral putamen. In SMRC44, stimulation of a more lateral site in MI to produce movements of the forearm induced Fos in patches located more ventrally in the putamen. Likewise, in SMRC51, stimulation of a yet more lateral site in MI to produce movements of the wrist induced Fos in patches located further ventrally in the putamen.



SMRC43
Foot



SMRC44
Forearm



SMRC51
Wrist

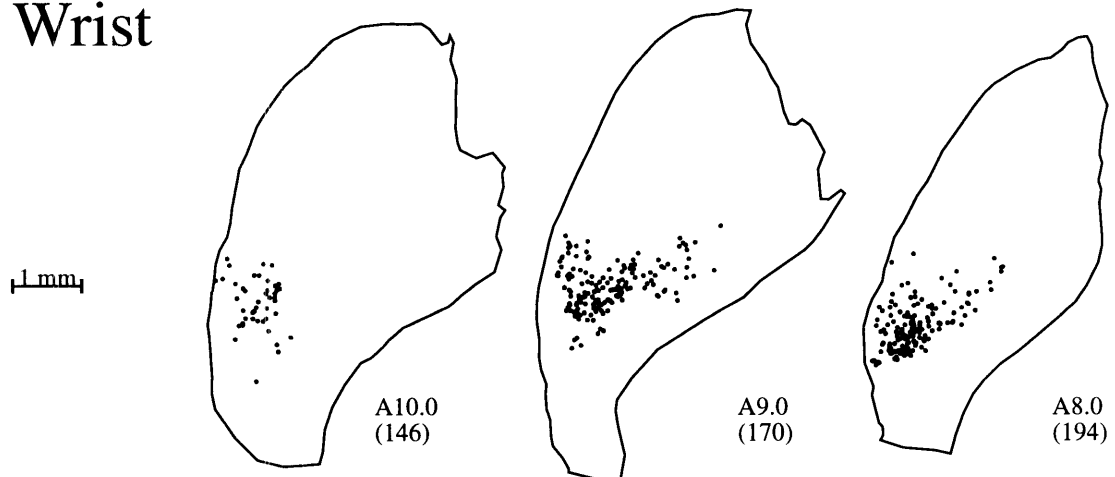
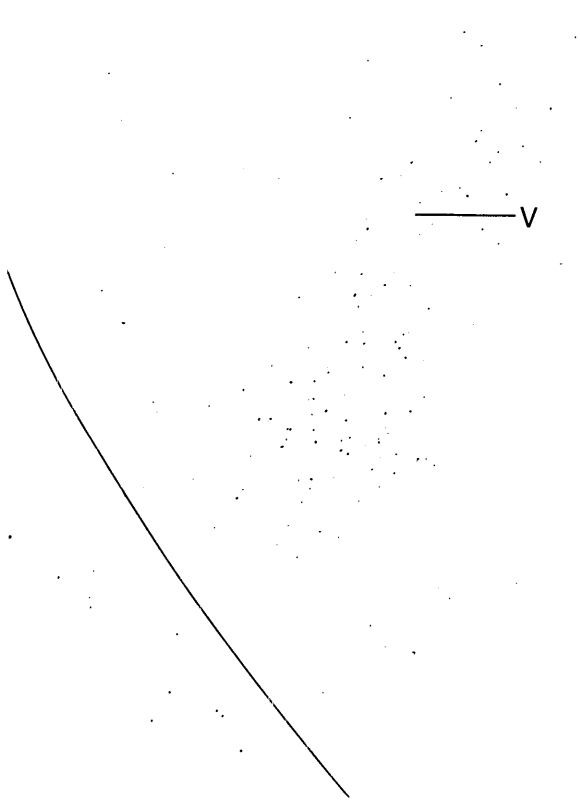


Figure 3.6. High power photomicrographs of transverse sections through the ventrolateral putamen demonstrate that Fos (A) and Jun B (B) are induced in the same pattern by electrical stimulation of the motor cortex. However, the distribution of Jun B is less restricted. V = blood vessel. Scale bare = 0.5 mm. The section immunohistochemically stained for Fos was charted in Fig.3.5 (SMRC51, #170).

A



B

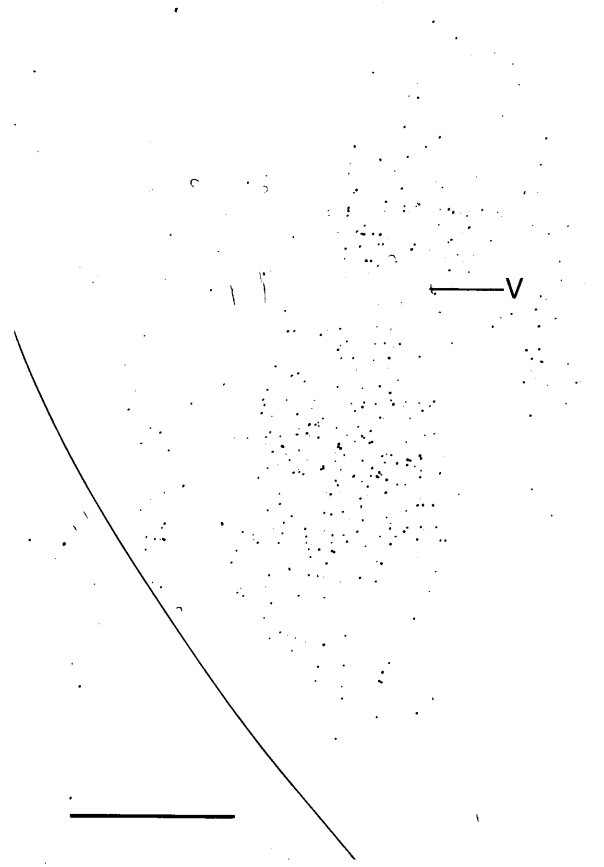

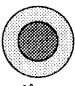



Figure 3.7. Case SMRC43. Electrical stimulation of the foot representation of the primary motor cortex induces Jun B in multiple patches in the primate striatum which do not overlap with the afferent patches labeled by injection of [³⁵S]methionine in the shoulder representation in area 3b. **Upper right:** Map of sites in cortical area SI identified by neuronal recording in SMRC43. D - digit, F - foot, FA - forearm, LL - lower leg, S - shoulder, T -trunk, UA - upper arm, UL - upper leg, X - no response. Dotted lines indicate the approximate borders between areas MI and 3a, 3a and 3b, 3b and 1. Dark circle indicates the reconstructed injection site. The lighter concentric circle indicates the less intensely labeled marginal zone of the injection site. **Below:** Superimposed camera lucida charts of Jun B-positive nuclei and anterogradely labeled fibers from transverse sections separated by an intervening 40 micron section. The black dots represent the distribution of Jun B induced in this case. Intensely labeled fiber patches are drawn surrounded by zones of weaker label. Coordinates under each section indicate the approximate AP values for *Saimiri sciureus* (Gergen and MacLean, 1962) and the actual section numbers.

SMRC43

-  Electrical stimulation
-  [³⁵S]methionine
-  Jun B

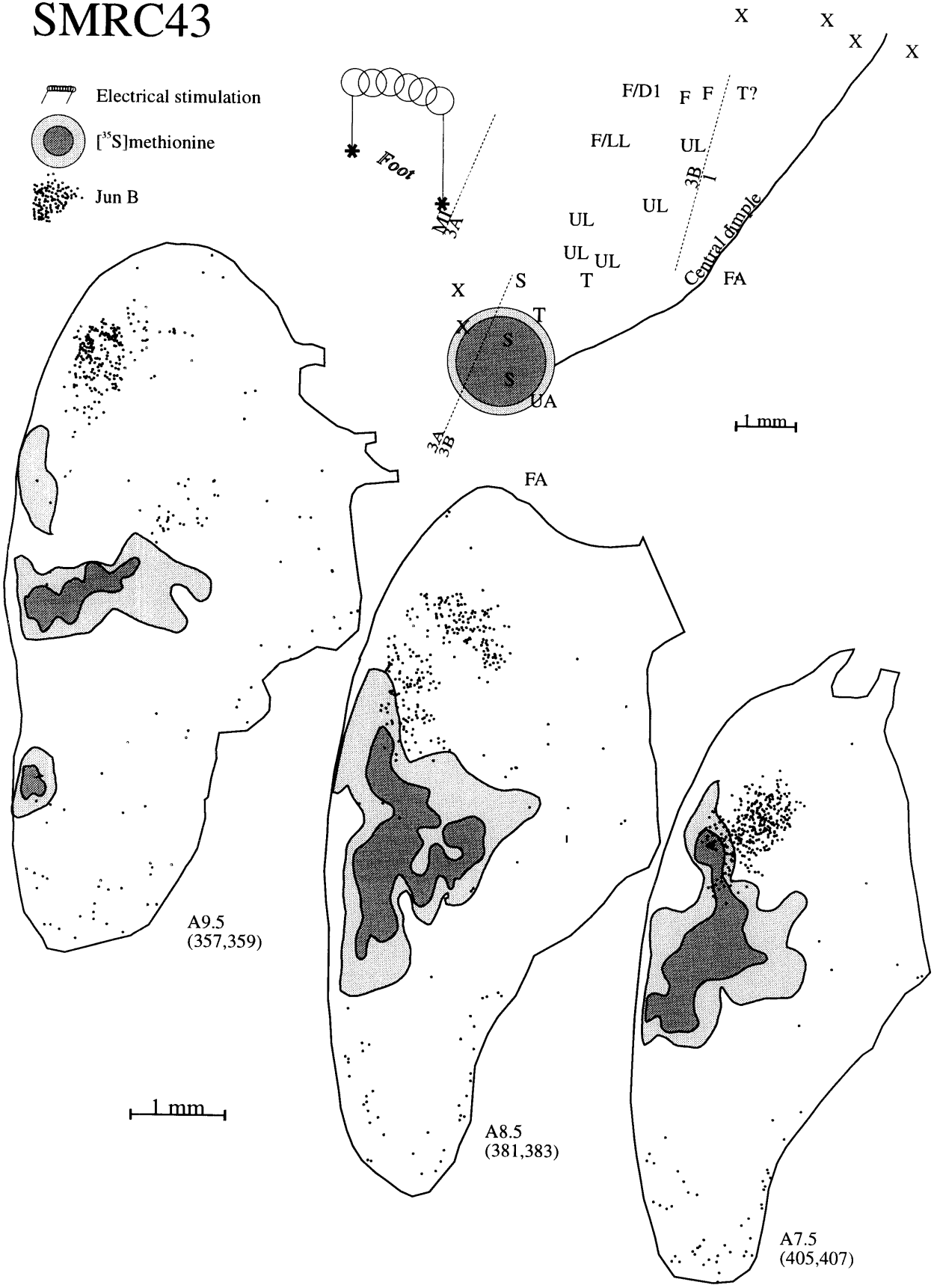

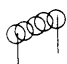
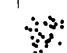


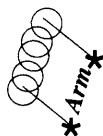
Figure 3.8a. SMRC44. Electrical stimulation of the arm representation of the primary motor cortex induces Fos in multiple patches in the primate striatum which correspond to the distributions of terminal varicosities labeled by injection of biotinylated dextran amine in the arm representation of the primary somatosensory cortex. . **Upper right:** Map of sites in cortical area SI identified by neuronal recording and in area MI identified by microstimulation in SMRC43. A - arm, D - digit, FA - forearm, H - hand, S - shoulder , T -trunk, UA - upper arm, X - no response. Dotted line indicates the approximate border between areas MI and 3a. The border between 3a and 3b is approximately along the central dimple. Dark circles indicate the reconstructed injection site. **Below:** Camera lucida charts of the distribution corticostriatal terminal varicosities labeled by injection of BDA (gray) and the distribution of Fos (black) visualized on the same section. Coordinates under each section indicate the approximate AP values for *Saimiri sciureus* (Gergen and MacLean, 1962) and the actual section numbers.

SMRC44

-  BDA
-  Electrical stimulation
-  Fos

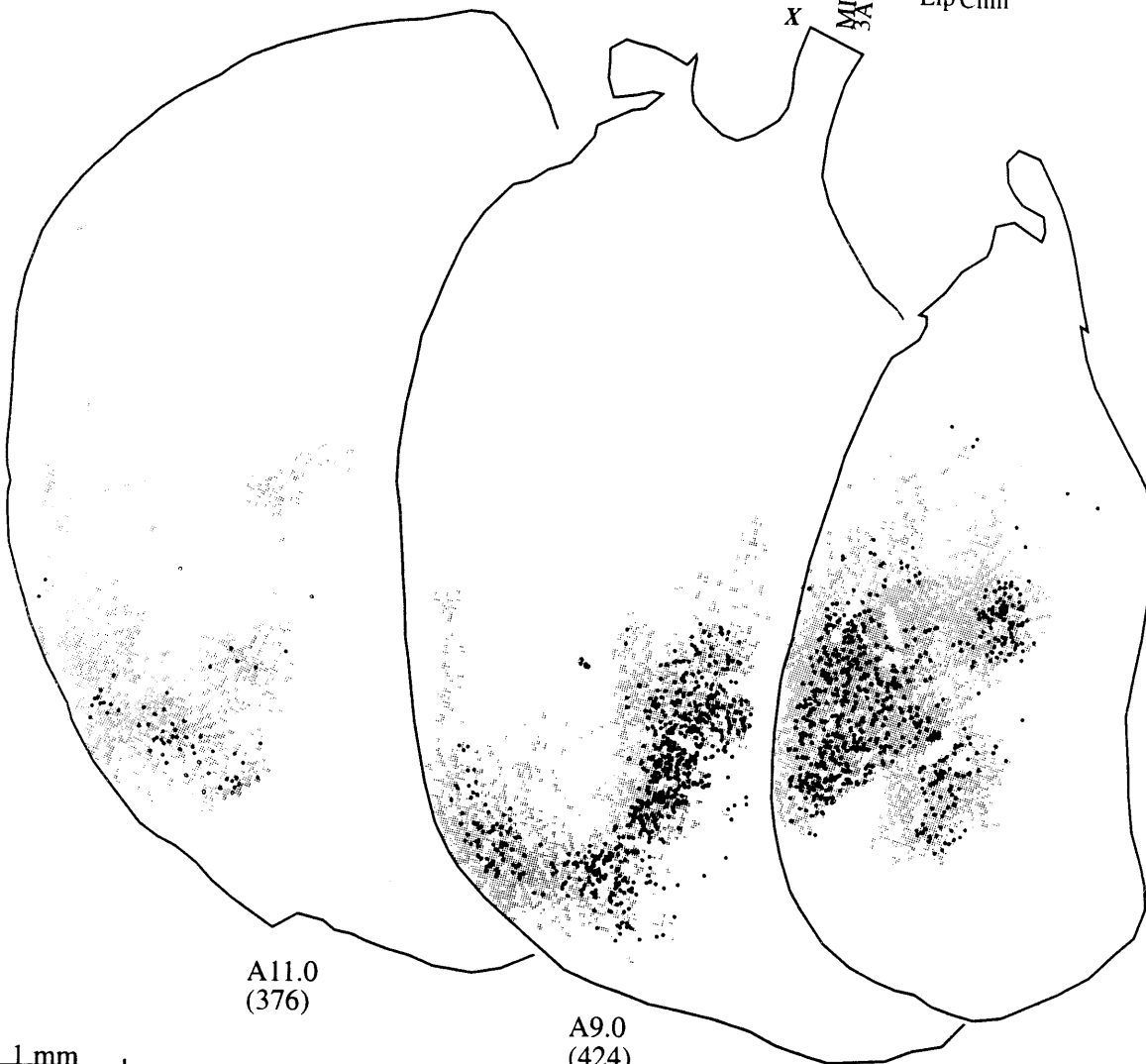
Trunk

1 mm



X Arm Arm D1-2
 X Chin X Wrist
 X Chin X

X T
 X T
 A T/UA X X
 S/UA UA
 A FA
 FA
 A X Central Dimple
 X FA PD1-5
 H D5/P
 D5/P
 P
 X D3-4
 X D3-4
 D2
 D1-2
 P
 P
 Lip Chin



A11.0
(376)

A9.0
(424)

A7.0
(472)

1 mm

Figure 3.8b. High power photomicrograph of corticostriatal fibers labeled by injection of biotinylated dextran amine and Fos-positive nuclei, taken from section 472 (charted in part A). Arrowhead points to a Fos-positive nucleus, thin arrows point to varicosities in corticostriatal fibers Scale bar = 20 microns.

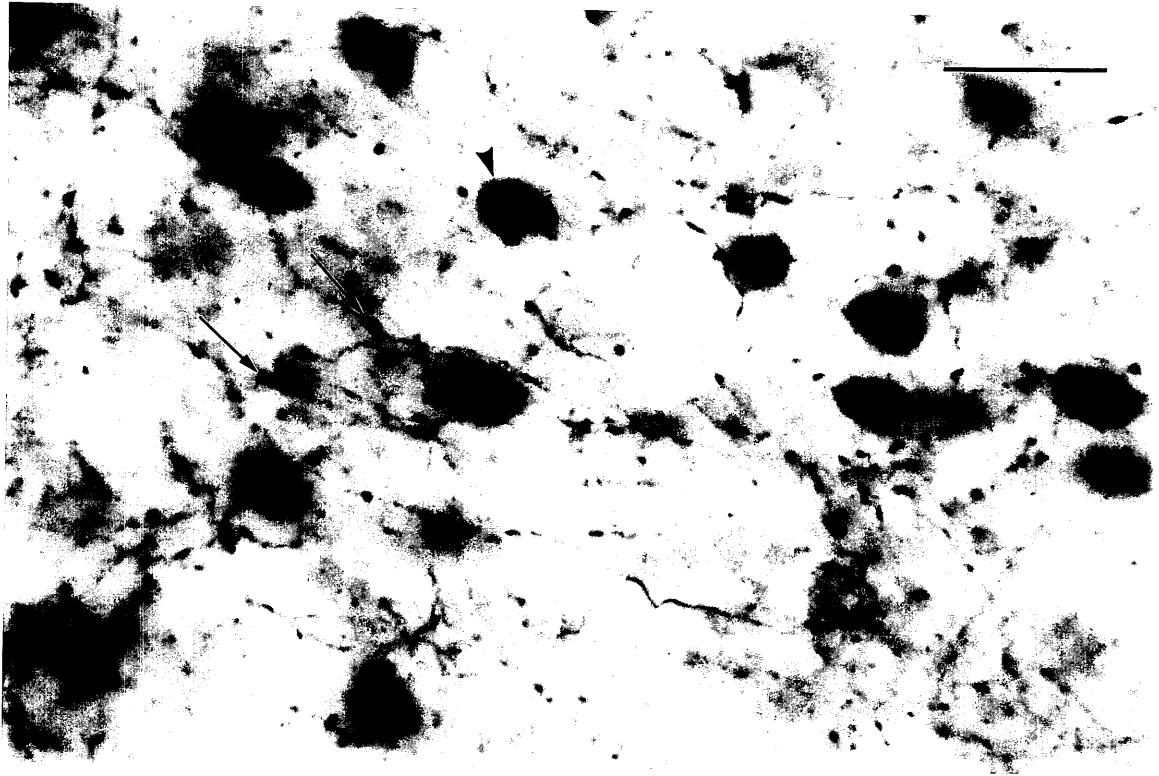


Figure 3.9. SMRC46L. Electrical stimulation of the foot representation of primary somatosensory area 3b induces Fos in the thalamus, subthalamic nucleus (STN), and external segment of the globus pallidus (GPe). Black dots represent the distribution of Fos in the subcortical structures. Shaded areas represent fibers labeled by injection of [³⁵S]methionine at the site of stimulation. NRT - reticular nucleus of the thalamus, VPL - ventral posterolateral nucleus of the thalamus.

SMRC46L



[³⁵S]methionine



Fos

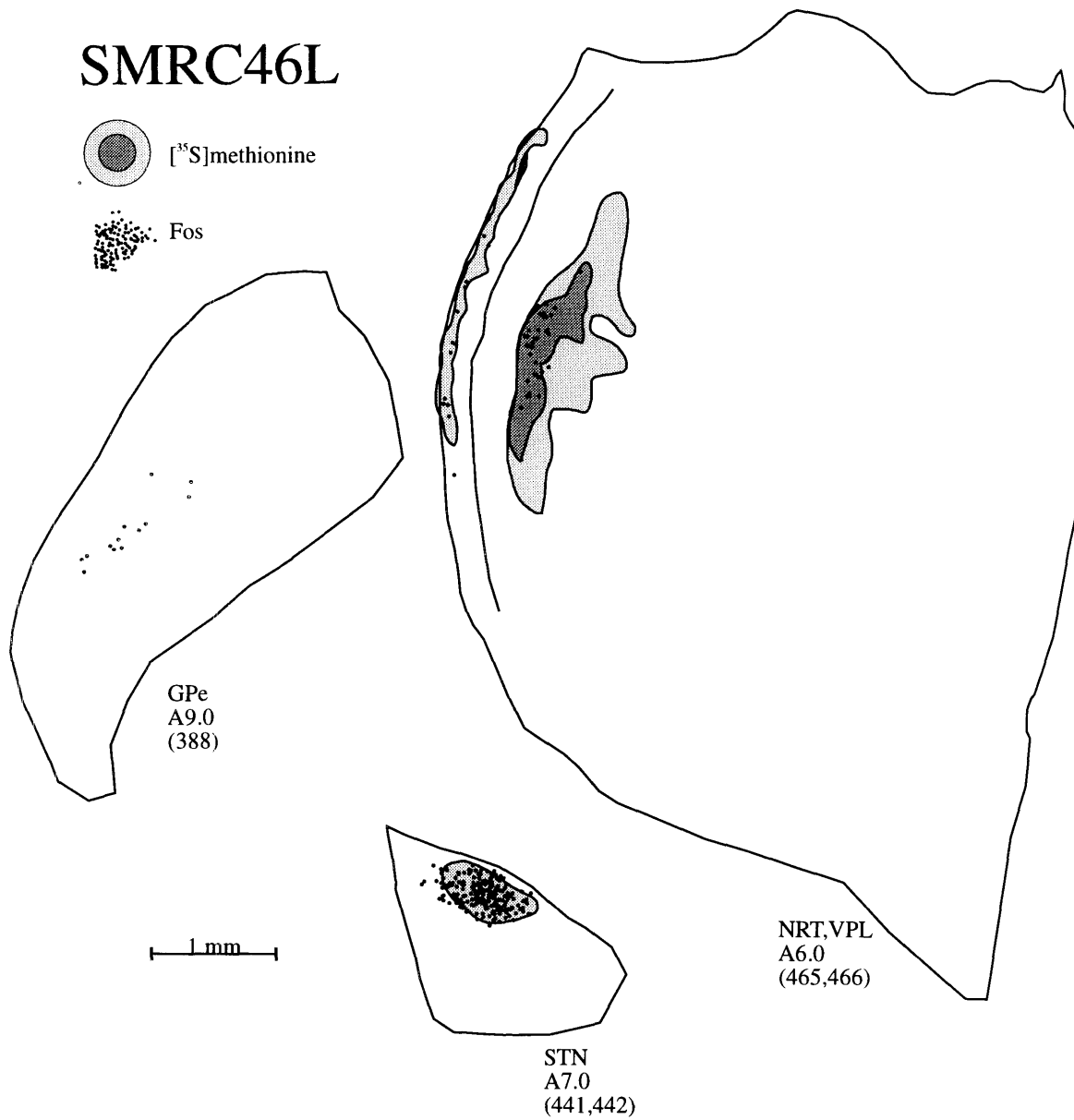


Figure 3.10. Electrical stimulation of the cortex induces Fos in the parvalbumin-containing interneurons of the primate striatum. Photomicrographs demonstrating colocalization of Fos and parvalbumin in (A) SMRC46R, for which Fos induction was only found in a few cells, and in (B) SMRC46L, for which Fos induction was very dense. Perikarya of parvalbumin-containing neurons are in brown, Fos-positive nuclei are black. Arrows point to parvalbumin-containing neurons expressing Fos, arrowheads point to Fos nuclei alone, and curved arrows point to parvalbumin-containing neurons not expressing Fos. Scale bar = 20 microns.

A



B



Figure 3.11a. Electrical stimulation of the cortex induces Fos in the parvalbumin-containing interneurons of the primate striatum. Red dots indicate Fos colocalized with parvalbumin in striatal neurons. Black dots indicate Fos not colocalized with parvalbumin. SMRC51. Stimulation of the hand representation of the motor cortex in this case induced Fos in a relatively sparse pattern. The majority of neurons strongly expressing Fos were found to contain parvalbumin. Coordinates under each section indicate the approximate AP values for *Saimiri sciureus* (Gergen and MacLean, 1962) and the actual section numbers.

SMRC51

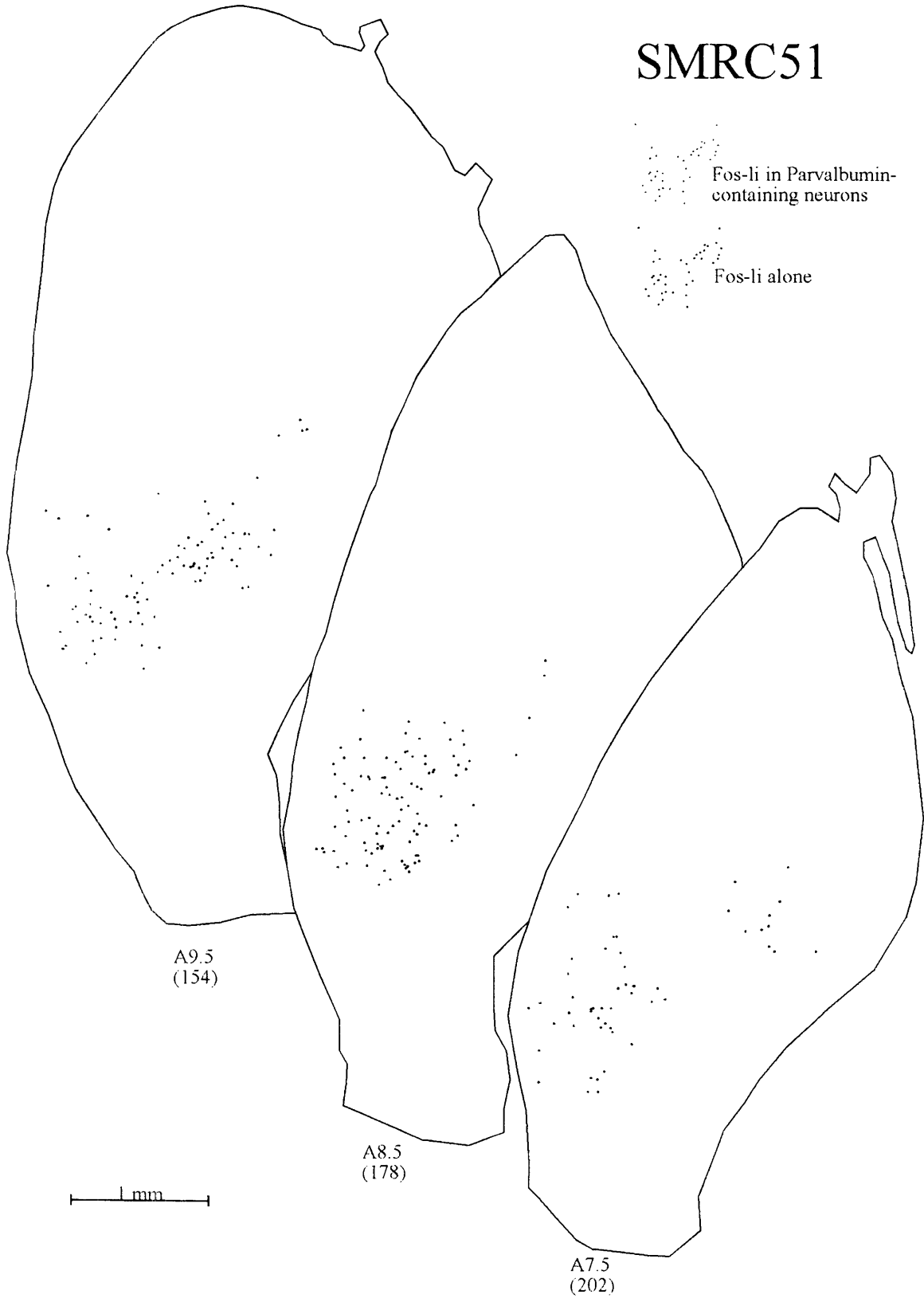


Figure 3.11b. Electrical stimulation of the cortex induces Fos in the parvalbumin-containing interneurons of the primate striatum. Red dots indicate Fos colocalized with parvalbumin in striatal neurons. Black dots indicate Fos not colocalized with parvalbumin. SMRC48R. Stimulation of the foot representation of somatosensory cortex also induced Fos in a relatively sparse pattern. Again, the majority of the neurons expressing Fos were found to contain parvalbumin. Coordinates under each section indicate the approximate AP values for *Saimiri sciureus* (Gergen and MacLean, 1962) and the actual section numbers.

SMRC48R

Fos-li in Parvalbumin-containing neurons
Fos-li alone

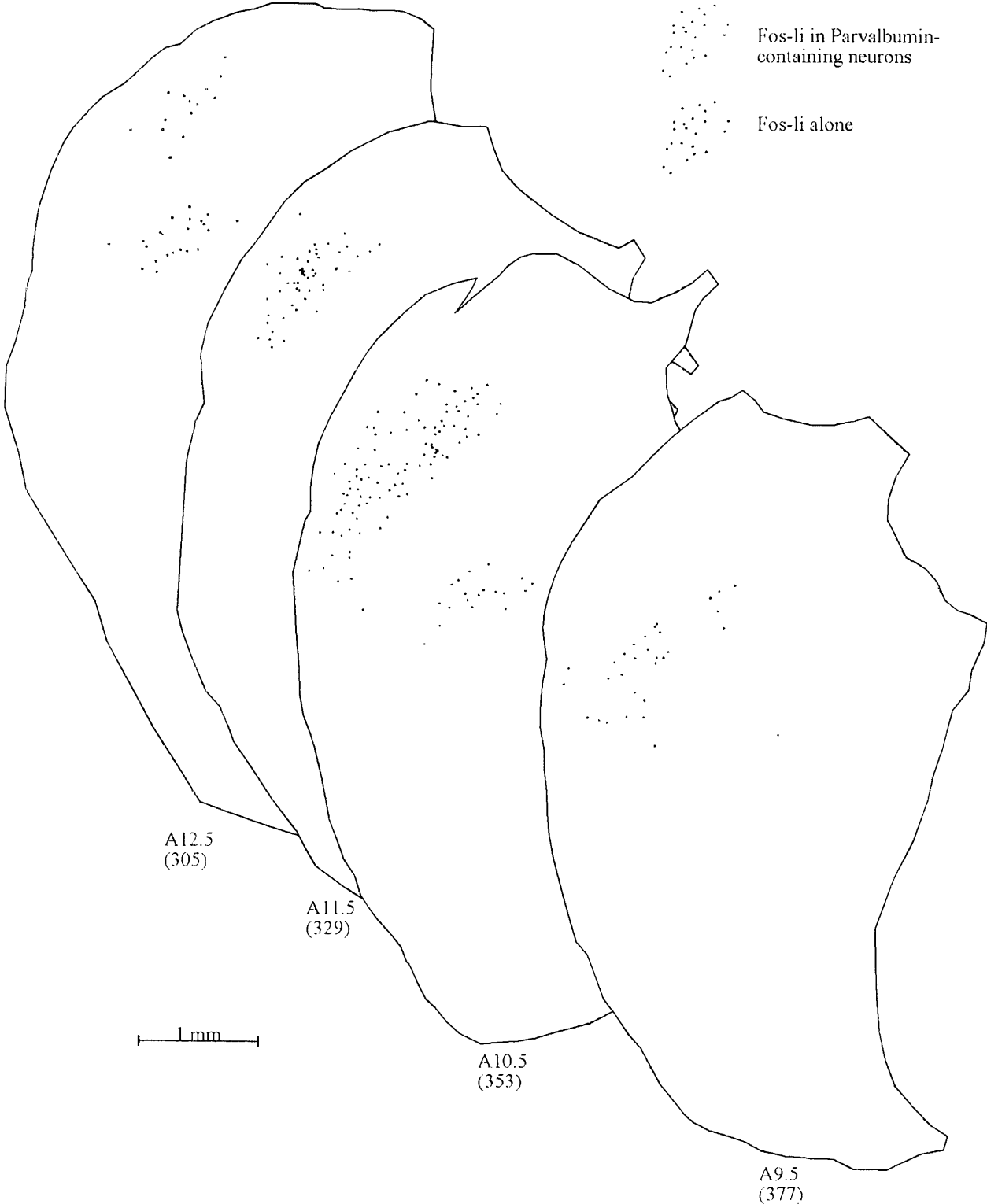


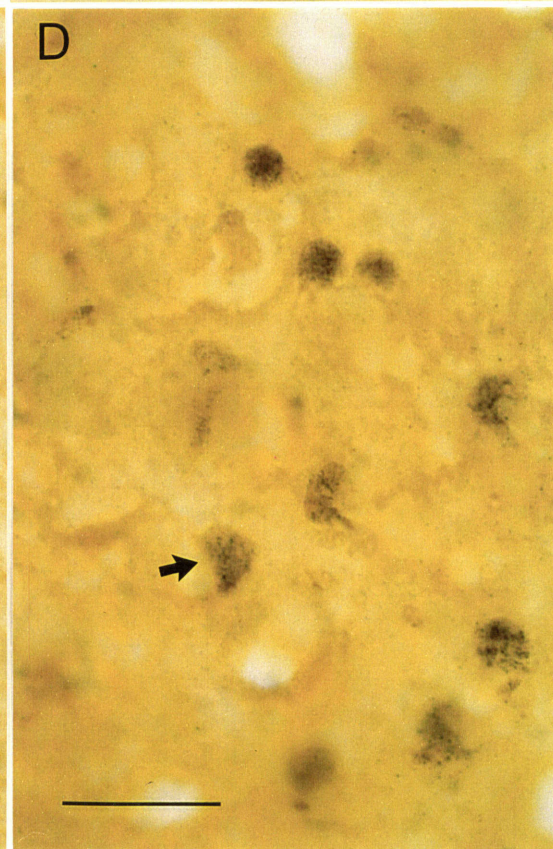
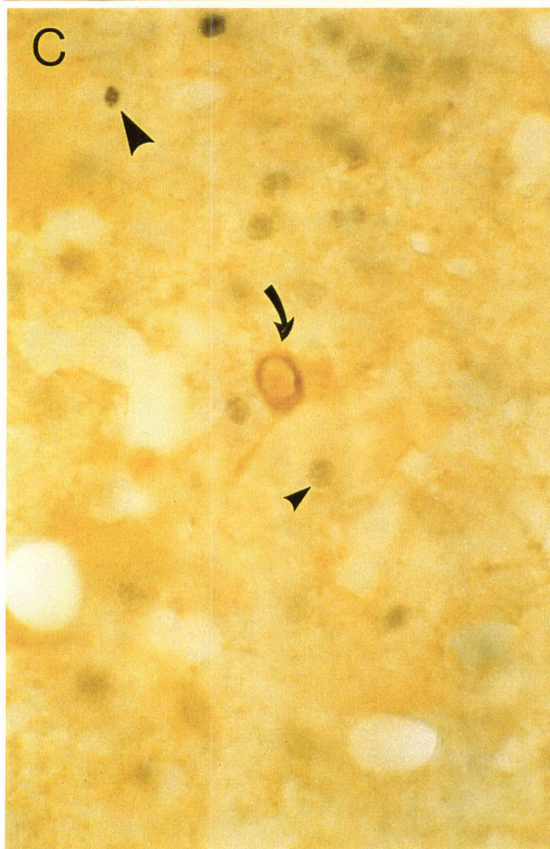
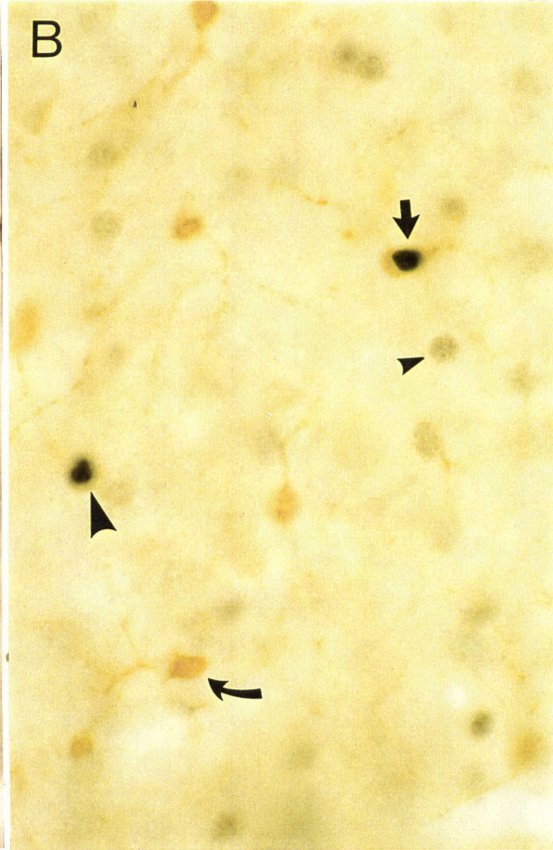
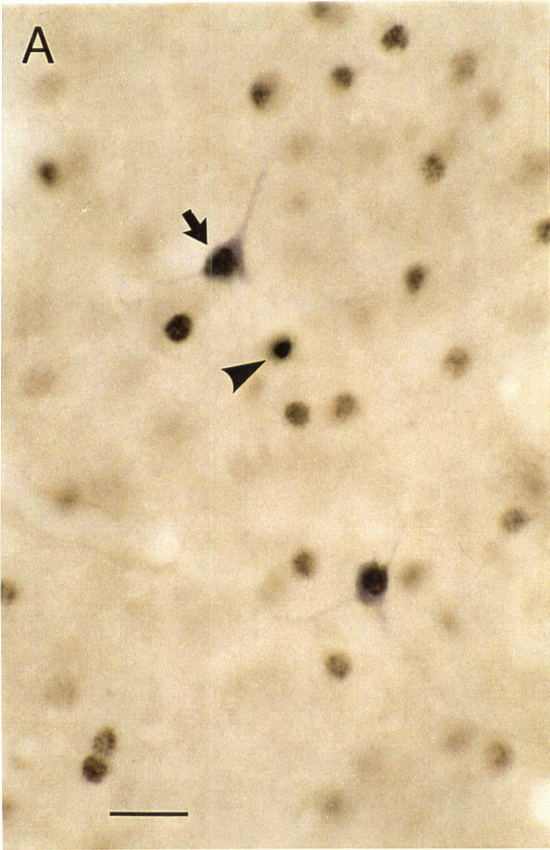
Figure 3.11c. Electrical stimulation of the cortex induces Fos in the parvalbumin-containing interneurons of the primate striatum. Red dots indicate Fos colocalized with parvalbumin in striatal neurons. Black dots indicate Fos not colocalized with parvalbumin. SMRC46L. Stimulation of the foot representation of somatosensory cortex induced Fos strongly and densely in the putamen. While they are only a minority, the parvalbumin-containing neurons which express Fos form a diffuse ring around the dense expression in neurons not double-labeled. Coordinates under each section indicate the approximate AP values for *Saimiri sciureus* (Gergen and MacLean, 1962) and the actual section numbers.

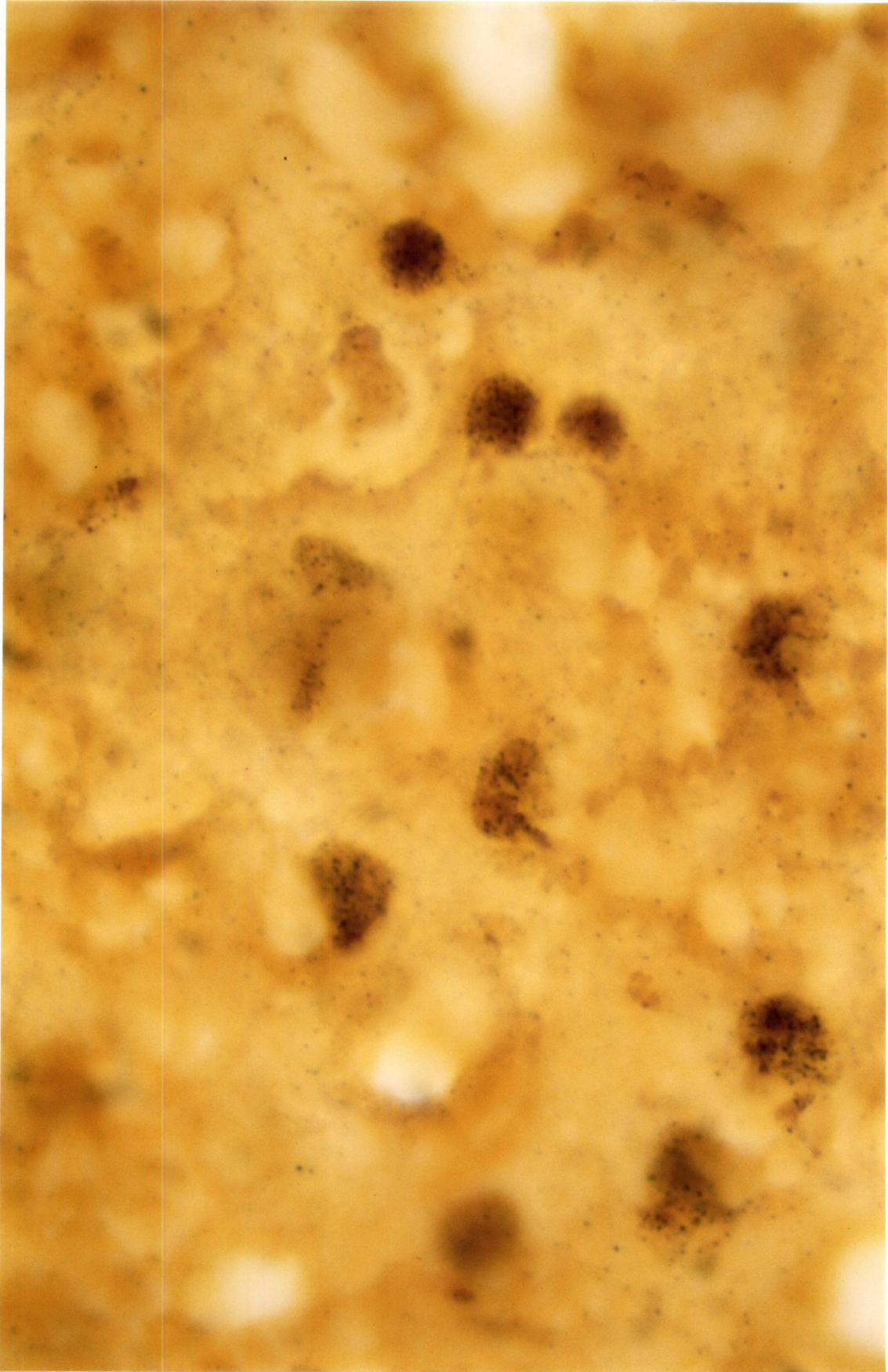
SMRC46L

Fos-li in Parvalbumin-containing neurons
Fos-li alone



Figure 3.12. Electrical stimulation of the somatosensory cortex induces the expression of Fos in (A) NADPH-diaphorase containing interneurons, (B) occasionally in calretinin-containing interneurons, (C) but never in cholinergic interneurons. (D) The majority of Fos-positive nuclei were found to be induced in enkephalinergic neurons. Scale bars are both 20 microns. Scale bar in A applies to B and C. Arrows indicate colocalization of Fos-positive nuclei in phenotypically-defined striatal neurons, arrowheads indicate Fos-positive nuclei alone, and curved arrows indicate striatal neurons in which Fos was not induced. (NB: See next page for original photograph of 3.12D).





CHAPTER 4. Conclusions.

Current hypotheses of basal ganglia function usually consider the basal ganglia as part of a cortico-basal ganglia-cortical loop. In this context, we have studied the first step in the neural system, i.e. the projections from the cortex to the striatum. One of the interesting emerging features of these projections is that there is modularity in the convergence of corticostriatal fibers in the striatum that seems to reflect functional relationships rather than spatial adjacency of cortical areas. This modularity has great potential for creating a base to understand how information is processed in the striatum, and thus how this processing would reflect on the entire basal ganglia circuitry. We have focused our experiments on the corticostriatal pathways from oculomotor, motor, and somatosensory cortex in the primate.

In the oculomotor system, widely separated cortical areas such as the frontal eye field and the supplementary eye field are involved in the generation of saccadic eye movements. We found that fiber projections from these areas to the striatum diverge into multiple patches in caudate nucleus and putamen. However, the fiber patches labeled from the frontal eye field were often coincident with those labeled from the supplementary eye field. Thus, at a macroscopic level of organization, there is convergence of corticostriatal fibers within the oculomotor system, that come from spatially distant but functionally related cortical areas.

In the somatosensory and motor cortex it has been previously shown that there is a similar convergence among afferent fibers in multiple striatal zones (matrisomes) labeled from corresponding representations in these cortical areas (Flaherty and Graybiel, 1993).

We have extended these results by demonstrating that these zones are actually comprised of dense corticostriatal fiber varicosities (presumptive terminals). Furthermore we have shown that activation of the cortex by electrical stimulation induces the expression of immediate early genes (IEGs) in subpopulations of neurons within these matrisomes. This last finding adds a new dimension to analysis of the corticostriatal system. We found that:

- a) there is a differential expression of the IEG, Fos, in different striatal neuron subclasses

- mainly enkephalinergic projection neurons and parvalbumin-positive interneurons express Fos in response to stimulation of the motor or somatosensory cortex; b) this differential induction reflects a well ordered arrangement - Fos-positive projection neurons are mainly found within the core of induction, while Fos-positive parvalbumin neurons are distributed throughout the core and in a halo which surrounds this core, in a manner more restricted but analogous to the distribution of corticostriatal fibers. In summary, the detection of immediate early gene induction adds a new degree of resolution to the characteristics of striatal modules as delineated by convergence of functionally related cortical afferents.

The further combination of these anterograde tracers and IEG expression could provide a valuable tool for the study of striatal architecture. Estimates of the number of terminal varicosities from a given region of the cortex to a particular volume of the striatum (which was not possible in our experiments because of the thickness of the tissue sections used) would be useful as a more quantitative approach to characterizing patterns of corticostriatal termination from individual areas (Strick et al. 1995).

Furthermore, at borders sharply defined by both the distribution of terminal varicosities (which could be quantified if thinner tissue sections were used) and IEG expression, it would be interesting to know if the dendrites of striatal neurons observe these borders as they often do those of striosomes (Walker et al., 1993). If they do not, then neuronal processing within the striatum may at least partly occur independently within these modules. If they do, then the spatial gradient of similarity of input patterns would be quite sharp, such that inhibitory interconnections among medium spiny neurons may act to accentuate differences in the input pattern in a fashion analogous to lateral inhibition in the visual system (Wilson 1995).

Immediate early genes in this context are themselves interesting. Further characterization of the distribution of other members of this molecular class could reveal and consolidate cell-specific differences in the effects of cortical input. The effects on IEG distributions of other striatal afferents should be compared with those of the somatosensory and motor cortex. For instance, it has been found that the expression of

Fos is activated in virtually every parvalbumin-containing GABAergic interneuron in a given matrix by stimulation of the somatosensory and motor cortex. Thus, it can be deduced that input from these cortical areas converges directly onto this class of neuron.

It may be the case, however, that different cortical areas target different classes of interneurons or even projection neurons. Such a discovery would require a restructuring of the notion of homogeneously acting cortical inputs at a microscopic level.

REFERENCES

- Akers, R.M. and H.P. Killackey (1978) Organization of corticocortical connections in the parietal cortex of the rat. *J. Comp. Neurol.* 181: 513-538.
- Albin, R.L., A.B. Young, and J.B. Penney (1989) The functional anatomy of basal ganglia disorders. *TINS* 12: 366-375.
- Alexander, G.E. and M.D. Crutcher (1990) Functional architecture of basal ganglia circuits: neural substrates of parallel processing. *TINS* 13: 266-271.
- Alexander, G.E. and M.D. Crutcher (1990) Preparation for movement: neural representations of intended direction in three motor areas of the monkey. *J. Neurophysiol.* 64: 133-150.
- Alexander, G.E., M.R. DeLong, and P.L. Strick (1986) Parallel organization of functionally segregated circuits linking basal ganglia and cortex. In *Annu.Rev.Neurosci.*, pp. 357-381.
- Alheid, G.F., L. Heimer, and R.C. Switzer (1995) The Basal Ganglia. In *Human Nervous System*, G. Paxinos, ed.,
- Aosaki, T., H. Tsubokawa, A. Ishida, K. Watanabe, A.M. Graybiel, and M. Kimura (1994) Responses of tonically active neurons in the primate's striatum undergo systematic changes during behavioral sensorimotor conditioning. *J. Neurosci.* 14: 3969-3984.
- Arikuni, T. and K. Kubota (1986) The organization of prefrontocaudate projections and their laminar origin in the macaque monkey: a retrograde study using HRP-Gel. *J. Comp. Neurol.* 244: 492-510.
- Aronin, N., K. Chase, S.M. Sagar, F.R. Sharp, and M. Difiglia (1991) N-methyl-D-aspartate receptor activation in the neostriatum increases c-Fos and Fos-related antigens selectively in medium-sized neurons. *Neurosci.* 44: 409-420.
- Asanuma, H. (1981) Microstimulation technique. In *Electrical stimulation research techniques*, pp. 61-70, Academic Press, Inc.,
- Bergman, H., T. Wichmann, and M.R. DeLong (1990) Reversal of experimental Parkinsonism by lesions of the subthalamic nucleus. *Science* 249: 1436-1438.
- Berretta, S., H.A. Robertson, and A.M. Graybiel (1992) Dopamine and glutamate agonists stimulate neuron-specific expression of fos-like protein in the striatum. *J. Neurophysiol.* 67: 767-777.
- Besson, M.J., M. Rogard, B. Zalc, and J.M. Deniau (1993) Effects of cortical electrical stimulation on c-Fos expression in the basal ganglia. *SNA* 19: 133.(Abstract)
- Bizzi, E. and P.H. Schiller (1970) Single unit activity in the frontal eye fields of unanesthetized monkeys. *Exp. Brain Res.* 10: 151-158.

- Blaustein, M.P. (1988) Calcium transport and buffering in neurons. *TINS* 11: 438-443.
- Boch, R.A. and M.E. Goldberg (1989) Participation of prefrontal neurons in the preparation of visually guided eye movements in rhesus monkey. *J. Neurophysiol.* 61: 1064-1084.
- Bon, L. and C. Lucchetti (1990) Neurons signalling the maintenance of attentive fixation in frontal area 6a β of the macaque monkey. *Exp. Brain Res.* 82: 231-233.
- Brandt, H.M. and A.V. Apkarian (1992) Biotin-dextran: a sensitive anterograde tracer for neuroanatomic studies in rat and monkey. *J. Neurosci. Meth.* 45: 35-40.
- Bray, D. (1995) Protein molecules as computational elements in living cells. *Nature* 376: 307-312.
- Brinkman, C. (1984) Supplementary motor area of the monkey's cerebral cortex; short- and long-term deficits after unilateral ablation and the effects of subsequent callosal section. *J. Neurosci.* 4: 918-929.
- Brown, L.L. (1992) Somatotopic organization in rat striatum: evidence for a combinatorial map. *Proc. Natl. Acad. Sci., U. S. A.* 89: 7403-7407.
- Bruce, C.J. and M.E. Goldberg (1985) Primate frontal eye fields. I. Single neurons discharging before saccades. *J. Neurophysiol.* 53: 603-635.
- Calabresi, P., R. Maj, A. Pisani, N.B. Mercuri, and G. Bernardi (1992) Long-term synaptic depression in the striatum: physiological and pharmacological characterization. *J. Neurosci.* 12: 4224-4233.
- Camarda, R., G. Luppino, M. Matelli, and G. Rizzolatti (1991) Cortical connections of two different eye fields in the dorsomedial frontal cortex of the macaque monkey. *SNA* 17: 459.(Abstract)
- Cavada, C. and P.S. Goldman-Rakic (1991) Topographic segregation of corticostriatal projections from posterior parietal subdivisions in the macaque monkey. *Neurosci.* 42: 683-696.
- Cenci, M.A. (1993) Transection of corticostriatal afferents reduces amphetamine- and apomorphine- induced striatal fos expression and turning behaviour in unilaterally 6-hydroxydopamine-lesioned rats. *Eur. J. Neurosci.* 5: 1062-1070.
- Chang, S.L., S.P. Squinto, and R.E. Harlan (1988) Morphine activation of c-fos expression in rat brain. *Biochem. Biophys. Res. Comm.* 157: 698-704.
- Chapin, J.K., M. Sadeq, and J.L.U. Guise (1987) Corticocortical connections within the primary somatosensory cortex of the rat. *J. Comp. Neurol.* 263: 326-346.
- Chervin, R.D., P.A. Pierce, and B.W. Connors (1988) Periodicity and directionality in the propagation of epileptiform discharges across neocortex. *J. Neurophysiol.* 60: 1695-1713.

Chevalier, G. and J.M. Deniau (1990) Disinhibition as a basic process in the expression of striatal functions. *TINS* 13: 277-280.

Cole, A.J., R.V. Bhat, C. Patt, P.F. Worley, and J.M. Baraban (1992) D₁ Dopamine receptor activation of multiple transcription factor genes in rat striatum. *J. Neurochem.* 58: 1420-1426.

Cole, A.J., D.W. Saffen, J.M. Baraban, and P.F. Worley (1989) Rapid increase of an immediate early gene messenger RNA in hippocampal neurons by synaptic NMDA receptor activation. *Nature* 340: 474-476.

Connors, B.W. (1984) Initiation of synchronized neuronal bursting in neocortex. *Nature* 310: 685-687.

Connors, B.W., R.C. Malenka, and L.R. Silva (1988) Two inhibitory postsynaptic potentials, and GABA-A and GABA-B receptor-mediated responses in neocortex of rat and cat. *J. Physiol.* 406: 443-468.

Cospito, and Kutas-Ilinsky (1981) Synaptic organization of motor corticostriatal projections in rat. *Exp. Neurol.* 72: 257-260.

Cowan, R.L. and C.J. Wilson (1994) Spontaneous firing patterns and axonal projections of single corticostriatal neurons in the rat medial agranular cortex. *J. Neurophysiol.* 71: 17-32.

Cowan, R.L., C.J. Wilson, P.C. Emson, and C.W. Heizmann (1990) Parvalbumin-containing GABAergic interneurons in the rat neostriatum. *J. Comp. Neurol.* 302: 197-205.

Deniau, J.M. and G. Chevalier (1985) Disinhibition as a basic process in the expression of striatal functions.II. The striato-nigral influence on thalamocortical cells of the ventromedial thalamic nucleus. *Brain Res.* 334: 227-233.

Desban, M., C. Gauchy, M.L. Kemel, M.J. Besson, and J. Glowinski (1989) Three-dimensional organization of the striosomal compartment and patchy distribution of striatonigral projections in the matrix of the cat caudate nucleus. *Neurosci.* 29: 551-566.

Donoghue, J.P. and M. Herkenham (1986) Neostriatal projections from individual cortical fields conform to histochemically distinct striatal compartments in the rat. *Brain Res.* 365: 397-403.

Dragunow, M., B. Logan, and R. Laverty (1991) 3,4-Methylenedioxymethamphetamine induces Fos-like proteins in rat basal ganglia: reversal with MK 801. *Eur. J. Pharmacol.* 206: 255-258.

Dragunow, M., G.S. Robertson, R.L.M. Faull, H.A. Robertson, and K. Jansen (1990) D₂ dopamine receptor antagonists induce fos and related proteins in rat striatal neurons. *Neurosci.* 37: 287-294.

Eblen, F. and A.M. Graybiel (1995) Highly restricted origin of prefrontal cortical inputs to striosomes in the macaque monkey. *J. Neurosci.* 15: 5999-6013.

Ferrier, D. (1875) Experiments on the brain of monkeys. *Philos. Trans. R. Soc. London Ser. B* 165: 433-488.

Flaherty, A.W. and A.M. Graybiel (1991) Corticostriatal transformations in the primate somatosensory system. Projections from physiologically mapped body-part representations. *J. Neurophysiol.* 66: 1249-1263.

Flaherty, A.W. and A.M. Graybiel (1991) A second input system for body representations in the primate striatal matrix. *SNA* 17: 1299.(Abstract)

Flaherty, A.W. and A.M. Graybiel (1993) Output architecture of the primate putamen. *J. Neurosci.* 13: 3222-3237.

Flaherty, A.W. and A.M. Graybiel (1993) Two input systems for body representations in the primate striatal matrix; experimental evidence in the squirrel monkey. *J. Neurosci.* 13: 1120-1137.

Fox, C.A., A.N. Andrade, D.E. Hillman, and R.C. Schwyn (1971) The spiny neurons in the primate striatum: A Golgi and electron microscopic study. *J. Hirnforsch.* 13: 181-201.

Fox, P.T., J.M. Fox, M.W. Raichle, and R.M. Burde (1985) The role of cerebral cortex in the generation of voluntary saccades: a positron emission tomographic study. *J. Neurophysiol.* 54: 348-369.

Freund, T.T., J.F. Powell, and A.D. Smith (1984) Tyrosine hydroxylase immunoreactive boutons in synaptic contact with identified striatonigral neurons, with particular reference to dendritic spines. *Neurosci.* 13: 1189-1215.

Fu, L. and R.M. Beckstead (1992) Cortical stimulation induces fos expression in striatal neurons. *Neurosci.* 46: 329-334.

Funahshi, S., C.J. Bruce, and P.S. Goldman-Rakic (1989) Mnemonic coding of visual space in the monkey's dorsolateral prefrontal cortex. *J. Neurophysiol.* 61: 331-349.

Gaymard, B., C. Pierrot-Deseilligny, and S. Rivaud (1990) Impairment of sequences of memory-guided saccades after supplementary motor area lesions. *Ann Neurol* 28: 622-626.

Gerfen, C.R. (1992) The neostriatal mosaic: multiple levels of compartmental organization. *TINS* 15: 133-139.

Gerfen, C.R., T.M. Engber, L.C. Mahan, Z. Susel, T.N. Chase, F.J. Monsma, and D.R. Sibley (1990) D1 and D2 dopamine receptor-regulated gene expression of striatonigral and striatopallidal neurons. *Science* 250: 1429-1432.

Gergen, J.A. and P.D. MacLean (1962) *A stereotaxic atlas of the squirrel monkey's brain (Saimiri sciureus)*, National Institutes of Health, Bethesda.

Giménez-Amaya, J.-M. and A.M. Graybiel (1990) Compartmental origins of the striatopallidal projection in the primate. *Neurosci.* 34: 111-126.

- Godaux, E., G. Cheron, and P. Mettens (1990) Ketamine induces failure of the oculomotor neural integrator in the cat. *Neurosci. Lett.* 116: 162-167.
- Goelet, P., V.F. Castellucci, S. Schacher, and E.R. Kandel (1986) The long and the short of long-term memory - a molecular framework. *Nature* 332: 419-422.
- Goldberg, M.E. and C.J. Bruce (1990) Primate frontal eye fields. III. Maintenance of a spatially accurate saccade signal. *J. Neurophysiol.* 64: 489-508.
- Goldberg, M.E. and M.A. Seagraves (1989) The visual and frontal cortices. In *The neurobiology of saccadic eye movements, reviews of oculomotor research*, R.H. Wurtz and M.E. Goldberg, eds., pp. 283-313, Elsevier, Amsterdam.
- Goldman, P.S. and W.J.H. Nauta (1977) An intricately patterned prefronto-caudate projection in the rhesus monkey. *J. Comp. Neurol.* 171: 369-386.
- Goldman-Rakic, P.S. (1995) Toward a circuit model of working memory and the guidance of voluntary motor action. In *Models of information processing in the basal ganglia*, J.C. Houk, J.L. Davis and D.G. Beiser, eds., pp. 131-148, MIT Press, Cambridge.
- Gould, H.J., C.G. Cusick, T.P. Pons, and J.H. Kaas (1986) The relationship of corpus callosum connections to electrical stimulation maps of motor, supplementary motor, and the frontal eye fields in owl monkeys. *J. Comp. Neurol.* 247: 297-325.
- Graveland, G.A. and M. DiFiglia (1985) The frequency and distribution of medium-sized neurons with indented nuclei in the primate and rodent striatum. *Brain Res.* 327: 308-311.
- Graybiel, A.M. (1984) Neurochemically specified subsystems in the basal ganglia. In *Ciba foundation symposium: functions of the basal ganglia*, pp. 114-149, Pitman, London.
- Graybiel, A.M. (1990) Neurotransmitters and neuromodulators in the basal ganglia. *TINS* 13: 244-254.
- Graybiel, A.M., T. Aosaki, A.W. Flaherty, and M. Kimura (1994) The basal ganglia and adaptive motor control. *Science*
- Graybiel, A.M. and M.-F. Chesselet (1984) compartmental distribution of striatal cell bodies expressing met-enkephalin-like immunoreactivity. *Proc. Natl. Acad. Sci. ,U. S. A.* 81: 7980-7984.
- Graybiel, A.M., A.W. Flaherty, and J.-M. Giménez-Amaya (1993) Striosomes and matrisomes. In *The Basal Ganglia III*, G. Bernardi and et al., eds., pp. 3-12, Plenum Press, New York.
- Graybiel, A.M., R. Moratalla, and H.A. Robertson (1990) Amphetamine and cocaine induce drug-specific activation of the c-fos gene in striosome-matrix compartments and limbic subdivisions of the rat striatum. *Proc. Natl. Acad. Sci. ,U. S. A.* 87: 6912-6916.

Graybiel, A.M. and Jr. Ragsdale, C.W. (1983) Biochemical anatomy of the striatum. In *Chemical Neuroanatomy*, P.C. Emson, ed., Raven Press, New York.

Greenberg, M.E., E.B. Ziff, and L.A. Greene (1986) Stimulation of neuronal acetylcholine receptors induces rapid gene transcription. *Science* 234: 80-83.

Gross, C.G. and M.S.A. Graziano (1990) Bimodal visual-tactile responses in the macaque putamen. *SNA 16*: 110.(Abstract)

Guitton, D., H.A. Buchtel, and R.M. Douglas (1985) Frontal lobe lesions in man causes difficulties in suppressing reflexive glances and in generating goal-directed saccades. *Exp. Brain Res.* 58: 455-472.

Hanson, P.I., T. Meyer, L. Stryer, and H. Schulman (1994) Dual role of calmodulin in autophosphorylation of multifunctional CaM kinase may underlie decoding of calcium signals. *Neuron* 12: 943-956.

Hayward, M.D., R.S. Duman, and E.J. Nestler (1990) Induction of the c-fos proto-oncogene during opiate withdrawal in the locus coeruleus and other regions of the rat brain. *Brain Res.* 525: 256-266.

Hazrati, L. and A. Parent (1992) Convergence of subthalamic and striatal efferents at pallidal level in primates: an anterograde double-labeling study with biocytin and PHA-L. *Brain Res.* 569: 336-340.

Hebb, D.O. (1949) *The organization of behavior. A neuropsychological theory*, J.Wiley, New York.

Heilig, M., J.A. Engel, and B. Soderpalm (1993) C-fos antisense in the nucleus accumbens blocks to locomotor stimulant action of cocaine. *Eur. J. Pharmacol.* 236: 339-340.

Herrling, P.L. (1985) Pharmacology of the corticocaudate excitatory postsynaptic potential in the cat: evidence for its mediation by quisqualate-or kainate-receptors. *Neurosci.* 14: 417-426.

Heurteaux, C., C. Messier, C. Destrade, and M. Lazdunski (1993) Memory processing and apamin induce immediate early gene expression in mouse brain. *Mol. Brain Res.* 18: 17-22.

Hikosaka, O. (1994) Role of basal ganglia in control of innate movements, learned behavior and cognition - a hypothesis. In *The basal ganglia IV: new ideas and data on structure and function*, G. Percheron, J.S. McKenzie and J. Féger, eds., pp. 591-598, Plenum Press, New York.

Hikosaka, O., M. Sakamoto, and S. Usui (1989) Functional properties of monkey caudate neurons. III. Activities related to expectation of target and reward. *J. Neurophysiol.* 61: 814-832.

Hikosaka, O., M. Sakamoto, and S. Usui (1989) Functional properties of monkey caudate neurons. I. Activities related to saccadic eye movements. *J. Neurophysiol.* 61: 780-798.

Hikosaka, O. and R.H. Wurtz (1983) Visual and oculomotor functions of monkey *Macaca mulatta* substantia nigra pars reticulata. 3. memory contingent visual and saccade responses. *J. Neurophysiol.* 49: 1268-1284.

Hikosaka, O. and R.H. Wurtz (1983) Visual and oculomotor functions of monkey *Macaca mulatta* substantia nigra pars reticulata. 4. Relation of substantia nigra to superior colliculus. *J. Neurophysiol.* 49: 1285-1301.

Hikosaka, O. and R.H. Wurtz (1985) Modification of saccadic eye movements by GABA-related substances. II. Effects of muscimol in monkey substantia nigra pars reticulata. *J. Neurophysiol.* 53: 292-308.

Hikosaka, O. and R.H. Wurtz (1985) Modification of saccadic eye movements by gaba-related substances. I. Effect of muscimol and bicuculine in monkey superior colliculus. *J. Neurophysiol.* 53: 266-291.

Hoeltzell, P.B. and R.W. Dykes (1979) Conductivity in the somatosensory cortex of the cat - evidence for cortical anisotropy. *Brain Res.* 177: 61-82.

Holsapple, J.W., J.B. Preston, and P.L. Strick (1991) The origin of thalamic inputs to the 'hand' representation in the primary motor cortex. *J. Neurosci.*

Houk, J.C. and J.P. Wise (1993) Outline for a theory of motor behavior: involving cooperative actions of the cerebellum, basal ganglia, and cerebral cortex. In *Natural and artificial intelligence*, P. Rudomin, M.A. Arbib and F. Cervantes-Perez, eds., Springer-Verlag, Heidelberg.

Huerta, M.F. and J.H. Kaas (1990) Supplementary eye fields as defined by intracortical microstimulation: connections in macaques. *J. Comp. Neurol.* 293: 299-330.

Hughes, P. and M. Dragunow (1995) Induction of immediate-early genes and the control of neurotransmitter-regulated gene expression within the nervous system. *Pharmacol. Rev.* 47: 133-178.

Ilinsky, I.A., M.L. Jouandet, and P.S. Goldman-Rakic (1985) Organization of the nigrothalamocortical system in the rhesus monkey. *J. Comp. Neurol.* 236: 315-330.

Illing, R.B. and A.M. Graybiel (1985) Convergence of afferents from the frontal cortex and substantia nigra onto acetylcholinesterase patches of the cat's superior colliculus. *Neurosci.* 14: 455-482.

Illing, R.B. and H. Wässle (1979) Visualization of the HRP reaction product using the polarization microscope. *Neurosci. Lett.* 13: 7-11.

Iriki, A., C. Pavlides, A. Keller, and H. Asanuma (1989) Long-term potentiation in the motor cortex. *Science* 245: 1385-1387.

Iriki, A., C. Pavlides, A. Keller, and H. Asanuma (1991) Long-term potentiation of thalamic input to the motor cortex induced by coactivation of thalamocortical and corticocortical afferents. *J. Neurophysiol.* 65: 1435-1441.

Isseroff, A., M.L. Schwarz, J.J. Dekker, and P.S. Goldman-Rakic (1984) Columnar organization of callosal and associational projections from rat frontal cortex. *Brain Res.* 293: 213-223.

Jackson, J.H. (1884) The Croonian lectures on evolution and dissolution of the nervous system. *Br. Med. J.* 1: 591-593,600-663,703-707.

Jacobs, K.M. and J.P. Donoghue (1991) Reshaping the cortical motor map by unmasking latent intracortical connections. *Science* 251: 944-947.

Jaeger, D., S. Gilman, and J.W. Aldridge (1993) Primate basal ganglia activity in a precued reaching task: preparation for movement. *Exp. Brain Res.* 95: 51-64.

Jiménez-Castellanos, J. and A.M. Graybiel (1989) Compartmental origins of striatal efferent projections in the cat. *Neurosci.* 32: 291-321.

Jones, E.G., J.D. Coulter, H. Burton, and R. Porter (1977) Cells of origin and terminal distribution of corticostriatal fibers arising in the sensory-motor cortex of monkeys. *J. Comp. Neurol.* 173: 53-80.

Jones, E.G., J.D. Coulter, and S.H.C. Hendry (1978) Intracortical connectivity of architectonic fields in the somatic sensory, motor and parietal cortex of monkeys. *J. Comp. Neurol.* 181: 291-347.

Joseph, J.P. and P. Barone (1987) Prefrontal unit activity during a delayed oculomotor task in the monkey. *Exp. Brain Res.* 67: 460-468.

Kawaguchi, Y. (1992) Large aspiny cells in the matrix of the rat neostriatum in vitro: physiological identification, relation to the compartments and excitatory postsynaptic currents. *J. Neurophysiol.* 67: 1669-1682.

Kawaguchi, Y. (1993) Physiological, morphological, and histochemical characterization of three classes of interneurons in rat neostriatum. *J. Neurosci.* 13: 4908-4923.

Kemp, J.A. and T.P.S. Powell (1970) The cortico-striate projection in the monkey. *Brain* 93: 525-546.

Kimura, M. (1990) Behaviourally contingent property of movement-related activity of the primate putamen. *J. Neurophysiol.* 61: 1277-1296.

Kita, H. (1992) Responses of globus pallidus neurons to cortical stimulation: intracellular study in the rat. *Brain Res.* 589: 84-90.

Kita, H., T. Kosaka, and C.W. Heizmann (1990) Parvalbumin-immunoreactive neurons in the rat neostriatum: a light and electron microscopic study. *Brain Res.* 536: 1-15.

Konradi, C., L.A. Kobiński, T.V. Nguyen, S. Heckers, and S.E. Hyman (1993) The cAMP-response-element-binding protein interacts, but Fos protein does not interact, with the proenkephalin enhancer in rat striatum. *Proc. Natl. Acad. Sci., U. S. A.* 90: 7005-7009.

- Korsching, S. (1993) The neurotrophic factor concept: a reexamination. *J. Neurosci.* *13*: 2739-2748.
- Kurata, K. and J. Tanji (1985) Contrasting neuronal activity in supplementary and precentral motor cortex of monkeys. II. Responses to movement triggering vs. nontriggering signals. *J. Neurophysiol.* *53*: 142-152.
- Künzle, H. (1975) Bilateral projections from precentral motor cortex to the putamen and other parts of the basal ganglia. An autoradiographic study in *Macaca fascicularis*. *Brain Res.* *88*: 195-209.
- Künzle, H. (1977) Projections from the primary somatosensory cortex to basal ganglia and thalamus in the monkey. *Exp. Brain Res.* *30*: 481-492.
- Laitinen, L.V., A.T. Bergenheim, and M.I. Hariz (1992) Leskell's posteroventral pallidotomy in the treatment of Parkinson disease. *J. Neurosurg.* *76*: 53-61.
- Lapper, S.R., Y. Smith, A.F. Sadikot, A. Parent, and J.P. Bolam (1992) Cortical input to parvalbumin-immunoreactive neurones in the putamen of the squirrel monkey. *Brain Res.* *580*: 215-224.
- Lee, K. and E.J. Tehovnik (1991) Eye position dependency of units in the dorsomedial frontal cortex. *SNA 17*: 546.(Abstract)
- Ljungberg, T., P. Apicella, and W. Schultz (1992) Responses of monkey dopamine neurons during learning of behavioral reactions. *J. Neurophysiol.* *67*: 145-163.
- Luppino, G., M. Matelli, R.M. Camarda, V. Gallese, and G. Rizzolatti (1991) Multiple representations of body movements in mesial area 6 and the adjacent cingulate cortex: an intracortical microstimulation study in the macaque monkey. *J. Comp. Neurol.* *311*: 463-482.
- MacAvoy, M.G., J.P. Gottlieb, and C.J. Bruce (1991) Smooth-pursuit eye movement representation in the primate frontal eye field. *Cereb. Ctx.* *1*: 95-102.
- Malach, R. (1994) Cortical columns as devices for maximizing neuronal diversity. *TINS* *17*: 101-106.
- Malach, R. and A.M. Graybiel (1986) Mosaic architecture of the somatic sensory-recipient sector of the cat's striatum. *J. Neurosci.* *6*: 3436-3458.
- Marsden, C.D. (1982) The mysterious motor function of the basal ganglia. *Neurology* *32*: 514-539.
- McGeorge, A.J. and R.L.M. Faull (1989) The organization of the projection from the cerebral cortex to the striatum in the rat. *Neurosci.* *29*: 503-537.

Merzenich, M.M., J.H. Kaas, J.T. Wall, M. Sur, R.J. Nelson, and D.J. Felleman (1983) Progression of change following median nerve section in the cortical representation of the hand in areas 3b and 1 in adult owl and squirrel monkeys. *Neurosci. 10*: 639-665.

Mesulam, M.-M. (1978) Tetramethyl benzidine for horseradish peroxidase neurohistochemistry: a non-carcinogenic blue reaction product with superior sensitivity for visualizing neural afferents and efferents. *J. Histochem. Cytochem. 26*: 106-117.

Mink, J.W. and W.T. Thach (1991) Basal ganglia motor control. I. Nonexclusive relation of pallidal discharge to five movement modes. *J. Neurophysiol. 65*: 273-300.

Mitz, A.R. and M. Godschalk (1989) Eye-movement representation in the frontal lobe of rhesus monkeys. *Neurosci. Lett. 106*: 157-162.

Mitz, A.R. and S.P. Wise (1987) The somatotopic organization of the supplementary motor area: intracortical microstimulation mapping. *J. Neurosci. 7*: 1010-1021.

Moratalla, R., E.A. Vickers, H.A. Robertson, B.H. Cochran, and A.M. Graybiel (1993) Coordinate expression of c-fos and jun B is induced in the rat striatum by cocaine. *J. Neurosci. 13*: 423-433.

Morgan, J.I. and T. Curran (1986) Role of ion flux in the control of c-fos expression. *Nature 322*: 552-555.

Morgan, J.I. and T. Curran (1991) Stimulus-transcription coupling in the nervous system: involvement of the inducible proto-oncogenes fos and jun. In , pp. 421-451, *Annu.Rev.Neurosci.*,

Mower, G.D. (1994) Differences in the induction of Fos protein in cat visual cortex during and after the critical period. *Mol. Brain Res. 21*: 47-54.

Murphy, T.H., P.F. Worley, and J.M. Baraban (1991) L-type voltage-sensitive calcium channels mediate synaptic activation of immediate early genes. *Neuron 7*: 625-635.

Mushiake, H., M. Inase, and J. Tanji (1990) Selective coding of motor sequence in the supplementary motor area of the monkey cerebral cortex. *Exp. Brain Res. 82*: 208-210.

Nambu, A., S. Yoshida, and K. Jinnai (1991) Movement-related activity of thalamic neurons with input from the globus pallidus and projection to the motor cortex in the monkey. *Exp. Brain Res. 84*: 279-284.

Naranjo, J.R., B. Mellstrom, M. Achaval, and P. Sassone-Corsi (1991) Molecular pathways of pain: Fos/Jun-mediated activation of a noncanonical AP-1 site in the prodynorphin gene. *Neuron 6*: 607-617.

Nelson, M.E. and J.M. Bower (1990) Brain maps and parallel computers. *TINS 13*: 403-408.

- Nudo, R.J., W.M. Jenkins, and M.M. Merzenich (1990) Repetitive microstimulation alters the cortical representation of movements in adult rats. *Somatosens. & Motor Res.* 7: 463-483.
- Palmer, A.M., P.H. Hutson, S.L. Lowe, and D.M. Bowen (1989) Extracellular concentrations of aspartate and glutamate in rat neostriatum following chemical stimulation of frontal cortex. *Exp. Brain Res.* 75: 659-663.
- Parthasarathy, H.B., S.B. Berretta, and A.M. Graybiel (1994) Cortical stimulation induces selective patterns of Jun B expression in the striatum. *SNA* 24: 406.1.(Abstract)
- Parthasarathy, H.B., J.D. Schall, and A.M. Graybiel (1992) Distributed but convergent ordering of corticostriatal projections: analysis of the frontal eye field and the supplementary eye field in the macaque monkey. *J. Neurosci.* 12: 4468-4488.
- Paxinos, G. and C. Watson (1986) *The rat brain in stereotaxic coordinates*, Academic Press, San Diego.
- Peng, Z.-C., S. Chen, M. Fusco, G. Vantini, and M. Bentivoglio (1993) Fos induction by nerve growth factor in the adult rat brain. *Brain Res.* 632: 57-67.
- Penny, G.R., S. Afsharpour, and S.T. Kitai (1986) The GAD, Leu-enkephalin, met-enkephalin, and substance P-immunoreactive neurons in the neostriatum of the rat and cat: evidence for partial population overlap. *Neurosci.* 17: 1011-1045.
- Percheron, G. and M. Fillion (1991) Parallel processing in the basal ganglia: up to a point. *TINS* 14: 55-56.
- Percheron, G., C. François, J. Yelnik, G. Fénelon, and B. Talbi (1994) The basal ganglia related system of primates: definition, description and informational analysis. In *The Basal Ganglia IV*, G. Percheron, J.S. McKenzie and J. Féger, eds., pp. 3-20, Plenum Press, New York.
- Percheron, G., J. Yelnik, and C. François (1984) The primate striato-pallido-nigral system: an integrative system for cortical information. In *The basal ganglia: structure and function*, J.S. McKenzie, R.E. Kemm and R.E. Wilcock, eds., Plenum Press, New York.
- Plenz, D. and A. Aertsen (1994) The basal ganglia: 'minimal coherence detection' in cortical activity distributions. In *The basal ganglia IV. New ideas and data on structure and function*, G. Percheron, J.S. McKenzie and J. Féger, eds., pp. 579-588, Plenum Press, New York.
- Purves, D., D.R. Riddle, and A.S. LaMantia (1992) Iterated patterns of brain circuitry (or how the cortex gets its spots). *TINS* 15: 362-368.
- Ragsdale, C.W. and A.M. Graybiel (1981) The fronto-striatal projection in the cat and monkey and its relationship to inhomogeneities established by acetylcholinesterase histochemistry. *Brain Res.* 208: 259-266.

Rajakumar, N., K. Elisevich, and B.A. Flumerfelt (1993) Biotinylated dextran: a versatile anterograde and retrograde neuronal tracer. *Brain Res.* 607: 47-53.

Ranck, J.B. (1975) Which elements are excited in electrical stimulation of mammalian central nervous system: a review. *Brain Res.* 98: 417-440.

Reiner, A., C.L. Veenman, and M.G. Honig (1993) Anterograde tracing using biotinylated dextran amine. *Neuroscience Protocols* 93-050-14-01:

Rizzolatti, G., C. Scandolara, M. Matelli, and M. Gentilucci (1981) Afferent properties of periarculate neurons in macaque monkeys. I. Somatosensory responses. *Behav. Brain Res.* 2: 125-146.

Robbins, T.W. and B.J. Everitt (1992) Functions of dopamine in the dorsal and ventral striatum. *Seminars Neurosci.* 4: 119-128.

Robertson, G.S., S.R. Vincent, and H.C. Fibinger (1989) Striatonigral projection neurons contain D1 dopamine receptor activated c-fos. *Brain Res.* 530: 346-349.

Robertson, H.A., M.R. Peterson, K. Murphy, and G.S. Robertson (1989) D₁-dopamine receptor agonists selectively activate striatal c-fos independent of rotational behaviour. *Brain Res.* 503: 346-349.

Robinson, D.A. and A.F. Fuchs (1969) Eye movements evoked by stimulation of frontal eye fields. *J. Neurophysiol.* 32: 637-648.

Robledo, P. and J. Féger (1990) Excitatory influence of rat subthalamic nucleus to substantia nigra pars reticulata and the pallidal complex: electrophysiological data. *Brain Res.* 518: 47-54.

Romo, R. and W. Schultz (1990) Dopamine neurons of the monkey midbrain: contingencies of responses to active touch during self-initiated arm movements. *J. Neurophysiol.* 63: 592-606.

Rusak, B., H.A. Robertson, W. Wisden, and S.P. Hunt (1990) Light pulses which shift rhythms induce gene expression in the suprachiasmatic nucleus. *Science* 248: 1237-1240.

Ryan, L.J. and K.B. Clark (1991) The role of the subthalamic nucleus in the response of globus pallidus neurons to stimulation of the prelimbic and agranular frontal cortices in rats. *Exp. Brain Res.* 86: 641-651.

Saint-Cyr, J.A., L.G. Ungerleider, and R. Desimone (1990) Organization of visual cortical inputs to the striatum and subsequent outputs to the pallido-nigral complex in the monkey. *J. Comp. Neurol.* 298: 129-156.

Schall, J.D. (1991) Neuronal activity related to visually guided saccadic eye movements in the supplementary motor area of rhesus monkeys. *J. Neurophysiol.* 66: 530-558.

Schall, J.D. (1991) Neuronal activity related to visually guided saccades in the frontal eye fields of rhesus monkeys: comparison with supplementary eye fields. *J. Neurophysiol.* 66: 559-579.

Schall, J.D., A. Morel, D.J. King, and C. Whalley (1991) Topography of connections between cortical visuomotor areas in the macaque. *SNA* 17: 857.(Abstract)

Schell, G.R. and P.L. Strick (1984) The origin of thalamic inputs to the arcuate premotor and supplementary motor areas. *J. Neurosci.* 4: 539-560.

Schlag, J. and M. Schlag-Rey (1987) Evidence for a supplementary eye field. *J. Neurophysiol.* 57: 179-200.

Schultz, W. (1995) The primate basal ganglia between the intention and outcome of action. In *Functions of the cortico-basal ganglia loop*, M. Kimura and A.M. Graybiel, eds., Springer-Verlag, Tokyo.

Schultz, W. and R. Romo (1992) Role of primate basal ganglia and frontal cortex in the internal generation of movements. I. Preparatory activity in the anterior striatum. *Exp. Brain Res.* 91: 363-384.

Selemon, L.D. and P.S. Goldman-Rakic (1985) Longitudinal topography and interdigitation of corticostriatal projections in the rhesus monkey. *J. Neurosci.* 5: 776-794.

Selemon, L.D. and P.S. Goldman-Rakic (1990) Topographic intermingling of striatonigral and striatopallidal neurons in the rhesus monkey. *J. Comp. Neurol.* 297: 359-376.

Sharp, F.R., M.F. Gonzalez, K. Hisanaga, W.C. Mobley, and S.M. Sagar (1989) Induction of the c-fos gene product in rat forebrain following cortical lesions and NGF injections. *Neurosci. Lett.* 100: 117-122.

Sheng, H.Z., R.D. Fields, and P.G. Nelson (1993) Specific regulation of immediate early genes by patterned neuronal activity. *J. Neurosci. Res.* 35: 459-467.

Sheng, M. and M.E. Greenberg (1990) The regulation and function of c-fos and other immediate early genes in the nervous system. *Neuron* 4: 477-485.

Sheng, M., M.A. Thompson, and M.E. Greenberg (1991) CREB: a Ca²⁺-regulated transcription factor phosphorylated by calmodulin-dependent kinases. *Science* 252: 1427-1430.

Shivers, B.D., R.E. Harlan, G.J. Romano, R.D. Howells, and D.W. Pfaff (1986) Cellular localization of preenkphalin mRNA in rat brain: gene expression in the caudate-putamen and cerebellar cortex. *Proc. Natl. Acad. Sci., U. S. A.* 83: 6221-6225.

Shook, B.L., M. Schlag-Rey, and J. Schlag (1991) Primate supplementary eye field. II. Comparative aspects of connections with the thalamus, corpus striatum, and related forebrain nuclei. *J. Comp. Neurol.* 307: 562-583.

Smith, A.D. and J.P. Bolam (1990) The neural network of the basal ganglia as revealed by the study of synaptic connections of identified neurons. *TINS* 13: 259-265.

Smith, Y., L. Hazrati, and A. Parent (1990) Efferent projections of the subthalamic nucleus in the squirrel monkey as studied by the PHA-L anterograde tracing method. *J. Comp. Neurol.* 294: 306-323.

Smith, Y., T. Wichmann, and M.R. DeLong (1994) The external pallidum and the subthalamic nucleus send convergent synaptic inputs onto single neurones in the internal pallidal segment in monkey: anatomical organization and functional significance. In *The Basal Ganglia IV*, G. Percheron, J.S. McKenzie and J. Féger, eds., pp. 51-62, Plenum Press, New York.

Smith, Y., T. Wichmann, and M.R. DeLong (1994) Synaptic innervation of neurones in the internal pallidal segment by the subthalamic nucleus and the external pallidum in monkeys. *J. Comp. Neurol.* 343: 297-318.

Snider, R.S. and J.C. Lee (1961) *A stereotaxic atlas of the monkey brain (Macaca mulatta)*, University of Chicago Press, Chicago.

Snyder-Keller, A.M. (1991) Striatal c-fos induction by drugs and stress in neonatally dopamine-depleted rats given nigral transplants: importance of NMDA activation and relevance to sensitization phenomena. *Exp. Neurol.* 113: 155-165.

Sonnenberg, J.L., F.J. Rauscher, J.I. Morgan, and T. Curran (1989) Regulation of proenkephalin by Fos and Jun. *Science* 246: 1622-1625.

Stanton, G.B., S.-Y. Deng, M.E. Goldberg, and N.T. McMullen (1989) Cytoarchitectural characteristics of the frontal eye fields in macaque monkeys. *J. Comp. Neurol.* 282: 415-427.

Stanton, G.B., M.E. Goldberg, and C.J. Bruce (1988) Frontal eye field efferents in the macaque monkey. I. Subcortical pathways and topography of striatal and thalamic terminal fields. *J. Comp. Neurol.* 271: 473-492.

Stark, P., G. Fazio, and E.S. Boyd (1962) Monopolar and bipolar stimulation of the brain. *Amer. J. Physiol.* 203: 371-3.

Strick, P.L., R.P. Dum, and N. Picard (1995) Macro-organization of the circuits connecting the basal ganglia with the cortical motor areas. In *Models of information processing in the basal ganglia*, J.C. Houk, J.L. Davis and D.G. Beiser, eds., MIT Press, Cambridge.

Sur, M., R.J. Nelson, and J.H. Kaas (1982) Representations of the body surface in cortical areas 3b and 1 of squirrel monkeys: comparisons with other primates. *J. Comp. Neurol.* 211: 177-192.

Svennilson, E., A. Torvik, R. Lowe, and L. Leskell (1960) Treatment of parkinsonism by stereotaxic thalamolesions in the pallidal region. A clinical evaluation of 81 cases. *Acta Psychiat. Neurol. Scand.* 35: 358-377.

Szabo, J. and W.M. Cowan (1984) A stereotaxic atlas of the brain of the cynomolgus monkey (*Macaca fascicularis*). *J. Comp. Neurol.* 222: 265-300.

Szekely, A.M., M.L. Barbaccia, H. Alho, and E. Costa (1989) In primary cultures of cerebellar granule cells the activation of N-methyl-D-aspartate-sensitive glutamate receptors induces c-fos mRNA expression. *Mol. Pharmacol.* 35: 401-408.

Tanji, J., H. Aizawa, K. Shima, and Y. Matsuzaka (1991) A forelimb motor task-related area rostral to the supplementary motor area. *Jpn. J. Physiol.* 41: s252.(Abstract)

Tehovnik, E.J. and K.-M. Lee (1990) Electrical stimulation of the dorsomedial frontal cortex (DMFc) of the rhesus monkey. *SNA* 16: 900.(Abstract)

Tischmeyer, W., L. Kaczmarek, M. Strauss, R. Jork, and H. Matthies (1990) Accumulation of c-fos mRNA in rat hippocampus during acquisition of a brightness discrimination. *Behav. Neural Biol.* 54: 165-171.

Tomlinson, R.D. and P.S. Bahra (1986) Combined eye-head gaze shifts in primate. II. Interactions between saccades and the vestibulo-ocular reflex. *J. Neurophysiol.* 56: 1558-1570.

Tsien, R.W., D. Lipscombe, D.V. Madison, K.R. Bley, and A.P. Fox (1988) Multiple types of neuronal calcium channels and their selective modulation. *TINS* 11: 431-438.

Uhl, G.R., B. Navia, and J. Douglas (1988) Differential expression of preproenkephalin and preprodynorphin mRNAs in striatal neurons: high levels of preproenkephalin expression depend on cerebral cortical afferents. *J. Neurosci.* 8: 4755-4764.

Veenman, C.L., A. Reiner, and M.G. Honig (1992) Biotinylated dextran amine as an anterograde tracer for single-and double-labeling studies. *J. Neurosci. Meth.* 41: 239-254.

Vogt, O. and C. Vogt (1919) Ergebnisse unserer Hirnforschung. *J. Psychol. Neurol.* 25: 277-462.

Wadman, W.J. and M.J. Gutnick (1993) Non-uniform propagation of epileptiform discharge in brain slices of rat neocortex. *Neurosci.* 52: 255-263.

Walker, R., G.W. Arbuthnott, R.W. Baughman, and A.M. Graybiel (1993) Dendritic domains of medium spiny neurons in the primate striatum: relationships to striosomal borders. *J. Comp. Neurol.* 337: 614-628.

Wan, X.S.T., F. Liang, V. Moret, M. Wiesendanger, and E.M. Rouiller (1992) Mapping of the motor pathways in rats: c-fos induction by intracortical microstimulation of the motor cortex correlated with efferent connectivity of the site of cortical stimulation. *Neurosci.* 49: 749-761.

Werner, G. (1970) The topology of the body representation in the somatic afferent pathway. In *The Neurosciences, second study program*, F.O. Scmitt, G.C. Quarton, T. Melnechuck and G. Adelman, eds., pp. 605-617, Rockefeller University Press, New York.

White, O.B., J.A. Saint-Cyr, R.D. Tomlinson, and J.A. Sharpe (1983) Ocular motor deficits in Parkinson's disease. II. Control of the saccadic and smooth pursuit systems. *Brain* 106: 571-587.

White, O.B., J.A. Saint-Cyr, R.D. Tomlinson, and J.A. Sharpe (1988) Ocular motor deficits in Parkinson's disease. III. Coordination of eye and head movements. *Brain* 111: 115-129.

Wichmann, T., M.S. Baron, and M.R. DeLong (1994) Local inactivation of the sensorimotor territories of the internal segment of the globus pallidus and the subthalamic nucleus alleviates Parkinsonian motor signs in MPTP treated monkeys. In *The Basal Ganglia IV*, G. Percheron, J.S. McKenzie and J. Féger, eds., pp. 357-363, Plenum Press, New York.

Wickens, J. and R. Köster (1995) Cellular models of reinforcement. In *Models of information processing in the basal ganglia*, J.C. Houk, J.L. Davis and D.G. Beiser, eds., pp. 188-214, MIT Press, Cambridge.

Wickens, J.R., M.E. Alexander, and R. Miller (1991) Two dynamic modes of striatal function under dopaminergic-cholinergic control: simulation and analysis of a model. *Synapse* 8: 1-12.

Wilson, C.J. (1990) Basal Ganglia. In *The synaptic organization of the brain*, Vol. 3rd, G.M. Shepherd, ed., pp. 279-316, Oxford University Press, Oxford.

Wilson, C.J. (1993) The generation of natural firing patterns in neostriatal neurons. In *Chemical signalling in the basal ganglia. Progress in Brain Research*, G.W. Arbuthnott and P.C. Emson, eds.,

Wilson, C.J. (1995) The contribution of cortical neurons to the firing pattern of striatal spiny neurons. In *Models of information processing in the basal ganglia*, J.C. Houk, J.L. Davis and D.G. Beiser, eds., MIT Press, Cambridge, MA.

Wisden, W., M.L. Errington, S. Williams, S.B. Dunnett, C. Waters, D. Hitchcock, G. Evans, T.V.P. Bliss, and S.P. Hunt (1990) Differential expression of immediate early genes in the hippocampus and spinal cord. *Neuron* 4: 603-614.

Woolsey, C.N., P.H. Settlage, D.R. Meyer, W. Sencer, T.P. Hamuy, and A.M. Travis (1952) Patterns of localization in precentral and "supplementary" motor areas and their relation to the concept of a premotor area. *Res. Publ. Assoc. Res. Nerv. Ment. Dis.* 30: 238-264.

Yelnik, J., C. François, G. Percheron, and D. Tande (1991) Morphological taxonomy of the neurons of the primate striatum. *J. Comp. Neurol.* 313: 273-294.

Yeomans, J.S. (1990) *Principles of brain stimulation*, Oxford University Press, New York.

Yeterian, E.H. and G.W. Van Hoesen (1978) Cortico-striate projections in the rhesus monkey: the organization of certain cortico-caudate connections. *Brain Res.* 139: 43-63.

Young, S.T., L.J. Porrino, and M.J. Iadarola (1991) Cocaine induces striatal c-Fos-immunoreactive proteins via dopaminergic D₁ receptors. Proc. Natl. Acad. Sci. ,U. S. A. 88: 1291-1295.

APPENDIX. Excitation Of The Motor Cortex Induces Fos, Jun B, And NGFI-A In The Rat Striatum.*

INTRODUCTION

Descriptions of neurological disorders related to the basal ganglia first implicated this neural system in motor control (reviewed in Marsden, 1982). However, such disorders, when compared to those involving primary motor areas or cerebellar nuclei make it clear that the basal ganglia is not functioning at a low level in the process of converting sensation, perception, or intention to action. Rather, growing evidence from lesion studies, pharmacological manipulations, and single unit recording implicate the basal ganglia in so-called 'adaptive motor control', 'context-dependent motor tasks' and 'reward-related behaviour' (Robbins and Everitt, 1992; Graybiel et al., 1994; Hikosaka, 1994).

All of these rather loose definitions share the property of learned response. In neural terms, such learning is often thought of in terms of plasticity of neural connections and synaptic efficacies. In recent years, attention has focused on a possible role for immediate early genes (IEGs) in mediating the transition between short-term changes in second messenger levels and longer-term alterations in neuronal properties (Goelet et al., 1986). IEGs code for a class of transcriptionally activated DNA binding effector molecules (reviewed in Sheng and Greenberg, 1990; Morgan and Curran, 1991; Hughes and Dragunow, 1995).

A plethora of experiments have examined the role of different neurotransmitter systems on the expression of IEGs in the striatum. Extensive studies have focused on the dopaminergic system, for which a variety of pharmacological manipulations have been shown to affect induction of IEGs (Robertson et al., 1989,1990; Dragunow et al., 1990; Graybiel et al., 1990; Young et al., 1991; Cole et al., 1992; Moratalla et al., 1993) . Similar experiments have implicated opiates (Chang et al., 1988; Hayward et al., 1990)

* Experiments performed in collaboration with Dr. Sabina Berretta.

and glutamate (Aronin et al., 1991; Synder-Keller, 1991; Berretta et al., 1992; Cenci et al., 1993) in the regulation of these genes in the striatum. The sum of these experiments suggest that the interactions of neurotransmitters within the corpus striatum, arguably the center of information processing in the basal ganglia, regulate the expression of these genes in particular populations of neurons to ultimately influence the flow of information through the striatum.

As a first step in testing this notion directly, we asked whether a direct afferent pathway, rather than a neurotransmitter system, could affect IEG expression in the striatum. We examined the effect of stimulating the motor cortex, an area which sends strong input to the basal ganglia on a set of IEGs (Fos, Fos B, Jun B, c-Jun, and NGFI-A) in the striatum. We used two complementary methods to stimulate motor cortex in awake, freely moving rats: (1) electrical microstimulation and (2) local intracortical blockade of GABA_A receptor function by epidural application of picrotoxin. Electrical microstimulation has the advantage that we could accurately control placement of the stimulus and manipulate the patterns of stimulation. However, the imposed stimulus probably activates neurons that would never normally be coactivated, and also passing fibers, both ortho- and antidromically. Chemical stimulation by local pharmacological blockade of GABAergic function unmasks endogenous cortical activity, and thus may be a more natural mode of cortical activation. However, this paradigm offers less fine control of the stimulation site, and we could not control the pattern of stimulation. For reasons which are discussed, using picrotoxin-induced cortical activation to elicit IEG expression in the striatum proved to be a much more robust method in our hands. For this reason, we confined full analysis of the phenotypic distribution and the pharmacological blockade of the IEG induction to those cases involving chemical stimulation. Using the two methods of cortical activation in parallel, we hope to come a step closer to understanding the influence of cortical afferents on neurons in the striatum.

METHODS

General preoperative treatment for rat experiments. In order to minimize stress-induced effects, the rats were brought to the experimental room at least 2 hrs before any treatment.

Electrical microstimulation of the motor cortex in anesthetized rats. Rats were anesthetized with Nembutal (50 mg/kg, supplemented as needed) and the motor cortex exposed. The dura mater was opened and a site from which parallel bipolar stimulation could elicit movements at low current intensity thresholds was found. Stimulation (40 msec trains, 4 trains/sec, 250 pps, 0.2 msec p.w., biphasic, 300-500 μ amp for 1 hour, unless otherwise noted) was followed by a 1 hour survival time.

Electrical microstimulation of the motor cortex in awake rats. The motor cortex of ketamine-xylazine-anaesthetized rats (50 mg/kg ketamine and 10 mg/kg xylazine i.p.) was exposed. In some cases, the motor cortex was mapped by low intensity microstimulation to identify somatotopy by movements. We based implantation of electrodes in subsequent experiments on stereotaxic coordinates derived from these maps. Low impedance tungsten electrodes made from 0.003'' bare diameter teflon-coated tungsten wire (A-M Systems) were implanted at chosen sites, the exposed dura mater was covered with Vaseline, and the electrodes were fixed in place with dental cement. One day later, electrical microstimulation (40 msec trains, 4 trains/sec, 250 pps, 0.2 msec p.w., biphasic, 50-400 μ Amps) for 1 hour (unless otherwise noted) was followed by a 1 hour survival time.

Picrotoxin application on cerebral cortex. The rats were anaesthetized (50 mg/kg ketamine and 10 mg/kg xylazine) and placed on a stereotaxic device (Kopf). A hole (ca. 2 mm diameter, centered at A0.5, L1.5 from Bregma, Paxinos and Watson, 1986) was drilled in the skull. A small plastic well, with a cap, was fixed to the skull with dental cement and filled with 0.9% saline. The wound was sutured, the rat allowed to recover for 1 day, the saline solution removed and 0.3 mM picrotoxin was put into the well for 2 hours (unless otherwise noted), after which, the animal was perfused. During drug application, the rats were closely observed for movements elicited.

Perfusion. Overdose of Nembutal (150 mg/kg) was followed by transcardial perfusion with 4% paraformaldehyde in 0.1M sodium cacodylate buffer (pH. 7.4). Brain were

removed, postfixed for approximately 1 hour, and then placed in a cacodylate-buffered solution of 20% glycerol for a minimum of 12 hours.

Immunohistochemistry. 30 or 15 μm coronal sections were cut on a sliding microtome and the free-floating sections were later processed for immunohistochemistry, using antibodies against c-Fos (Oncogene Science Ab-2, 1:200 and 1:500), ChAT (Incstar, 1:2000), parvalbumin (Sigma, 1:1000), met-enkephalin (Incstar, 1:1000), calretinin (Swant, 1:500), Jun B and NGFI-A (1:12000) antiserum (1:3000 and 1:10,000) from Dr. R. Bravo. Sections were treated with 10% methanol and 3% hydrogen peroxide to increase cellular membrane permeability and to inhibit endogenous peroxidases, then incubated with 5% normal secondary serum, followed by overnight incubation at 4°C in primary antibody in phosphate-buffered saline with 0.2% triton X-100 (PBS-Tx). After incubation with biotinylated secondary antibody, sections were processed with avidin-biotin kits (Vector) and visualized with nickel-enhanced DAB. Double-labeling immunohistochemistry was performed serially, with overnight washing in PBS-Tx followed by blocking steps in hydrogen peroxide, avidin, and biotin between the two procedures. BSA was substituted throughout for normal secondary serum. The first antigen was visualized with nickel-enhanced DAB (black reaction product), the second with cacodylate-buffered DAB (brown reaction product). For double-labeling of enkephalin and Fos antigens, the Fos was revealed as a black reaction product with an immunogold procedure for the secondary antibody (4 hours in Jansen gold-conjugated secondary antibody 1:50, followed by several rinses in 1% sodium acetate and then 20 minute incubations in Intense-M silver intensification kit as necessary). Histochemistry to detect NADPH-diaphorase was performed after DAB immunolabeling of Fos.

Biocom image analysis

Single immunolabeling: IEGs counting. For each IEG studied (Fos, NGFI-A, Jun B), sample sections from cases treated with 0.3 mM picrotoxin (n=10), and cases treated with 0.3 mM picrotoxin and 1 mg/kg MK-801 (n=10) were selected and immunostained at the same time. For each IEG a section from a representative case was used as a reference to establish a threshold: the contrast and luminosity were adjusted so that only darkly stained

nuclei would be counted. Then, for each case, the two sections that showed the most intense induction were selected and the number of labeled nuclei over threshold counted. The resulting number of nuclei for each treatment was averaged. A t-test was performed to evaluate the significance of differences between treatments.

Double immunolabeling to detect Fos with markers for specific neuronal subtypes.
We performed double label immunohistochemistry to establish in which striatal neuron subtypes application of picrotoxin to the motor cortex induced Fos expression.

Interneurons: Sections double labeled with Fos and with a marker for striatal interneurons (ACh, PVB, Calretinin, NADPH-diaphorase) that showed the highest induction of these IEGs were selected. We then drew the region of the striatum that showed induction. Inside this areas we counted neurons that only showed labeling with the marker for the interneuron and neurons that showed labeling with both the marker for interneuron and the IEG under study. In some cases, in order to obtain a comparison between double labeled nuclei and distribution of the IEG induction, nuclei labeled with Fos were counted as well.

Projection neurons: To mark striatal projections neurons we used antibodies against enkephalin or dynorphin. From the sections in which either Fos were expressed most intensely, we counted neurons that expressed Fos alone and neurons that expressed both Fos and either enkephalin or dynorphin.

RESULTS

Electrical stimulation.

The advantage of using electrical stimulation to explore cortically-driven immediate early gene expression is inherent in the ability to alter the patterns of stimulation, both spatially and temporally. This however, turned out to be less than a simple matter.

Three other groups have reported that electrical stimulation of the rodent motor cortex induces c-Fos in the striatum. They reported the following parameters:

REFERENCE	Intratrains Freq	Train Freq	Train dur	pulse type and width	Stim dur	Post-stim survival	Intensity	Electrode arrangement	Anesthesia
Besson et al. 1993	250 pps	4 Hz	40 msec	?	60 min	30 min	?	bipolar 1.5 mm apart	sodium pentobarbital
Fu & Beckstead 1991	100 pps	5 Hz	20 msec	biphasic 0.5msec	15 min	0,30, 90,180 min	subthreshold of generalized convulsions	bipolar 4 mm apart	sodium pentobarbital
Wan et al. 1992	400 pps	0.5 Hz	30 msec	0.4 msec	90 min	30 min	current needed for movement (sometimes contra limb also moved (30-600 microamps)	1 electrode	none

With these studies in mind, we designed our experiments to follow parameters very similar to those of Besson et al. (1993). Robust expression of Fos was reliably obtained by high frequency stimulation (0.2 msec p.w., biphasic, 250 pps in 40 msec trains, 4 trains/sec for 1 hour) through a parallel bipolar arrangement of electrodes separated by 1.5 mm (see Table A.1A, Cases R5-R7). The field of effective stimulation was thus complex, as the path of least resistance between the electrodes depends on the arrangement of the elements between them.

Of the many stimulus parameters, we were most interested in the area of stimulation, the pulse frequency within a train, and the train frequency necessary to elicit reliable IEG induction. We began our experiments in anesthetized animals, but later switched to using preimplanted electrodes in unrestrained, awake animals.

Table A.1 is a partial list of experiments conducted over a two year period. Because the immunohistochemical procedures were evolving over that time, it was virtually impossible to compare the results quantitatively, except in those experiments which were done close together. Therefore, we have simply indicated the general level of IEG induction and we did not attempt a quantitative comparison among all the animals.

Area of Induction. In Nembutal-anesthetized animals, stimulus intensities of 300-500 microamps induced Fos-like-immunoreactivity in the dorsolateral striatum. We found that within this set of conditions, the distance between the two electrodes was a critical variable influencing both the volume and density of striatal induction (Fig. A.1). The same stimulation intensity delivered between electrodes spaced 0.5 mm apart as compared to 1.0 mm, or 1.0 mm as compared to 1.5 mm, induced Fos in a much smaller area and much more sparsely.

Pulse and train frequency. After establishing that very low train frequencies (0.67 Hz = one train every four seconds) were ineffective in the induction of Fos in the striatum of Nembutal-anesthetized animals (cases R1-R4), we began using awake animals to do the remainder of our experiment. This switch simplified the interpretation of results by removing interference of anesthesia. However, new complexities were introduced.

While in Nembutal-anesthetized animals, it was a simple matter to use rather high currents to reliably elicit a strong well-localized movement, in awake animals, stimulation at a constant current led either to movement habituation or at the other extreme, to generalized seizures. In the case of rapid habituation, no induction of Fos and very sparse Jun B was observed (cases R20-R22). This is perhaps not surprising since many corticofugal neurons send collaterals to the striatum before descending further and movements would be a reliable index of having activated those neurons. However, stimulation at a constant current, which initially induced a discrete movement, often caused an increased activity which resulted in generalized motor seizures and extensive IEG expression throughout the striatum (cases R55-R63). These current thresholds varied from animal to animal, and were probably related to the configuration of the electrodes

with respect to the cortical layers and areas, which we were unable to control precisely. Jun B induction in the striatum appeared to be much more sensitive to spreading seizure activity in the cortex than was Fos.

Thus, to achieve focal induction in the striatum, reflecting the known topography of the dorsolateral “motor” striatum, it was necessary to constantly monitor and vary the current intensity to maintain a strong discrete body movement (R39-R47). Strong bilateral induction was usually observed only when the stimulated movement at least intermittently included the contralateral limb (R48-R52). Figure A.4a shows the typical overall pattern of Fos induction after electrical stimulation.

Lowering the train frequency from 4 Hz to 1 Hz diminished but did not completely abolish induction of Fos and Jun B in the striatum, whether we conserved the number of pulses (train duration = 160 msec; # pulses = 40/sec; R34,R35 but not R28,R29) or kept the train size constant (# pulses = 10/sec;R36,R37, but not R30). In contrast, changing the stimulus to a constant series of pulses at 10 Hz (#pulses = 10/sec;R24-R27) was not an effective stimulus. At 40 Hz (R38), however, a continuous series of pulses was effective in eliciting focal induction in the lateral striatum (Fig.A.2)

Cortical lesion. It has been suggested that lesions of the cerebral cortex activate the expression of Fos in the striatum (Sharp et al., 1989). In our paradigm, we observed a somewhat inverse effect. In all cases where the surgical procedure (application of dental acrylic or skull screws) inadvertently caused cortical lesions, little or no Fos induction was observed (R22,23,28,30,32,33,37,39,40).

Chemical stimulation.

Because of the difficulties in controlling the intensity of electrical stimulation in awake animals, and because we were limited by our apparatus in our ability to do large numbers of animals simultaneously to overcome variability, we searched for an alternative method of exciting the cortex with which we could efficiently pursue the role of cortical afferents in immediate early gene regulation.

In 20 rats, epidural application of the GABA_A receptor antagonist picrotoxin to a small region of the motor cortex proved a robust method for inducing IEGs in the dorsolateral striatum. The overall pattern of induction was very similar in cases for which electrical stimulation was successful in inducing striatal IEGs (Figs.A.3, A.4A and A.4B).

The distribution of these IEGs in the striatum after control experiments in which picrotoxin was applied to a more rostral or more caudal portion of the cortex was different from the one observed after stimulation of the motor cortex (not shown). Furthermore in one case in which the motor cortex had suffered a severe hemorrhage, the application of picrotoxin did not induce any IEGs in the striatum. In the normal cases, histological analysis by Nissl staining did not show any apparent damage of the cortex or of other parts of the brain.

Behavior. Approximately 15 minutes after application of picrotoxin to the motor cortex, the rats showed motor tics that involved either the forelimb or the hindlimb or both. The tics had a frequency of about 26.3/min (2.28 sec between tics) and did not interfere with the spontaneous behavior of the animals that, in most cases, could sleep, groom, drink and feed themselves. The motor tics continued for the entire duration of the treatment (2 hrs and 15 min.).

Induction of immediate early genes in the striatum: The most intense induction of Fos, Jun B and NGFI-A was found in the rostral dorsolateral region of the striatum, in a pattern very similar for all the IEGs (Fig A.6). The distribution in this region very often showed a core of induction, in which there was a high density of neurons expressing IEGs, and a more sparse area of induction that formed a halo around the core. Some sparse labeling was also found in more caudal parts of the striatum. In some cases labeled nuclei in the most caudal part of the striatum were found in clusters and in a rim around the GPe. In the ventral striatum and in the nucleus accumbens induction of Jun B was very strong whereas the induction of Fos, and NGFI-A was less consistent.

Concentration Curve. As shown in Fig. A.5, decreasing concentrations of picrotoxin (0.3, 0.1, 0.05, 0.03, 0.01, 0.005 mM) induced decreasing number of striatal neurons to express Fos. A sharp change was found between 0.1 and 0.05 mM, which had a mean of

171.0 (69.0 Std. Error) and 9.3 (16.16 Std. Error) respectively; some induction was still found up to a concentration of 0.01 mM whereas 0.005 mM induced no Fos.

Induction of immediate early genes in other structures: Cortex. In the treated hemisphere, layers II, III, V and VI showed massive induction, in layer IV the induction was less intense or absent. This distribution was found for all the IEGs studied; however, in most cases the induction in layer III was extremely weak for Jun B while it was very strong for Fos, and NGFI-A. Similarly, in most cases studied, layer V did not contain Jun B-positive nuclei, but showed a weak induction of the other genes. In all cases a very intense induction was found to correspond with the area of picrotoxin application in a shape of a "wedge" (Fig A.4B). The contralateral cortex did not show induction (not shown).

Of the other basal ganglia-related structures (Table A.2), the globus pallidus, entopeduncular nucleus, substantia nigra and subthalamic nucleus, showed a very consistent and selective pattern of activation. In the globus pallidus a few Fos-positive nuclei, and even fewer Jun B-positive nuclei, were found in the central region but no other IEGs were expressed; the entopeduncular nucleus, substantia nigra and subthalamic nucleus consistently showed induction of Fos and NGFI-A but not of Jun B. The parafascicular and the centromedian nuclei of the thalamus showed a strong induction of Fos but induction of other IEGs was much weaker and less consistent. Only very rarely was Fos induction found in the ventrolateral nucleus. In the amygdala, the central and basolateral nuclei showed strong induction of Fos and Jun B but not of NGFI-A.

Induction of Fos in striatal subpopulations: In order to investigate the phenotypic distribution of striatal neurons in which IEGs were induced, we used a double immunohistochemistry method with antisera that correspond to different neurochemical markers. We chose to assess the distribution of Fos because of its low constitutive expression in the striatum. Antisera against enkephalin and dynorphin were used to label striatal projection neurons. Antisera against parvalbumin and calretinin label GABAergic interneurons; choline acetyl transferase (Chat) is expressed by large aspiny cholinergic striatal interneurons. Histochemistry for NADPH-diaphorase was used to detect striatal interneurons that contain neuropeptide Y, somatostatin and nitric oxide synthase.

We found that the majority of neurons expressing Fos were enkephalinergic (70-80%) whereas only 7% contained dynorphin. The Fos labeled nuclei expressing these two markers were typically found in the region of densest induction. In particular, neurons that showed colocalization of Fos and dynorphin were always found in the core of the region of induction.

As can be seen in Fig.A.7, the second largest population of striatal neurons expressing Fos were GABAergic parvalbumin-containing interneurons. Up to 22% of Fos-positive nuclei were found in parvalbumin-containing neurons. If a region of the striatum that contained not only the densest area of Fos induction but also a periphery of more sparse induction was considered, the population of parvalbumin positive neurons that expressed Fos reached 78%. If only the area of densest induction was considered, this percentage increased to 88%.

A much smaller percentage (2-4%) of Fos positive neurons were expressed by NADPH-positive interneurons. These neurons were characteristically found within the peripheral areas of Fos induction and, in fact, showed a tendency to be distributed in a larger area as compared to the Fos-positive/parvalbumin-containing interneurons. Within this larger perimeter, 43.7% of NADPH-diaphorase neurons expressed Fos. This percentage dropped to 32% in the area of densest induction of Fos.

The distributions of Fos-positive parvalbumin and NADPH-diaphorase expressing neurons expressing Fos were, therefore, sharply contrasted with the pattern of enkephalin and dynorphin neurons expressing Fos in response to motor cortex activation.

Virtually no cholinergic or calretinin-containing interneurons were found to express Fos.

Glutamate receptors blocking. Rats were divided in three groups: one control group (p+v) received picrotoxin on the motor cortex and the vehicle used for MK-801 (saline) systemically; the second control group (v+m) received saline on the motor cortex and MK-801 (1 mg/kg) systemically; the third group (p+m) received picrotoxin on the motor cortex and MK-801 (1 mg/kg) systemically. Injection of MK-801 by itself (v+m) did not induce IEGs in the striatum.

In the experimental group (p+m), systemic injection of the NMDA glutamate receptor antagonist MK-801 (1 mg/kg; i.p.) partially blocked the induction of Fos, Jun B and NGFI-A in the striatum. However, as can be seen in Fig A.10, these IEGs were not affected by MK-801 in the same measure.

For total Fos expression in the dorsal striatum, the differences were highly significant between cases treated with picrotoxin and the vehicle for MK-801 and cases treated with picrotoxin and MK-801 (Fig.A.10). In the ventral part of the striatum the difference was still significant but was not so extreme, due probably to a greater variance (not shown).

For NGFI-A the difference between the groups v+p and p+m did not reach significance in the dorsal striatum. However, it was significant if calculated over the entire striatum (Fig.A.10) or in the ventral striatum by itself (not shown).

For Jun B the group p+m did show a substantial decrease in the induction in the dorsal striatum, as well as in ventral regions. It can be seen in Fig A.10 that this decrease is quite consistent but does not reach significance.

Notably, in the cerebral cortex, induction of Fos in areas not directly exposed to picrotoxin was completely abolished by systemic administration of MK-801. The induction of Jun B and NGFI-A in the cortex was reduced by not completely absent.

DISCUSSION

We have used two complementary methods to activate the motor cortex in rats in order to elicit the expression of immediate early genes in the striatum. The first, electrical stimulation of sites in the motor cortex through parallel bipolar electrodes, induced immediate early genes in the topographically correct dorsolateral region of the striatum (Cospito and Kultas-Illinsky, 1981; Donoghue and Herkenham, 1986; McGeorge and Faull, 1989; Brown, 1992), however the stimulus was difficult to control in awake animals. The second, local epidural application of the GABA_A antagonist picrotoxin to a 2.3 mm diameter area of the motor cortex, also induced immediate early genes in the dorsolateral striatum. This method proved more reliable and had the advantage of being less invasive of the cortex.

We used picrotoxin-induced activation of the cortex to study the induction of Fos, Jun B, and NGFI-A in the dorsolateral striatum. In addition, Fos and NGFI-A, but not Jun B were induced in the target structures of the striatum, the globus pallidus, the substantia nigra, and the entopeduncular nucleus. All three genes were induced in similar patterns. The induction of all three genes was reduced, by systemic administration of the NMDA antagonist, MK-801. However, this reduction reached significance only in the case of Fos and NGFI-A, because of a larger variability for Jun B.

Finally, we examined the phenotypic pattern of expression of Fos in the striatum. Of the projection neurons, Fos was found predominantly in enkephalinergic neurons. Of the interneurons, only parvalbumin and NADPH-diaphorase containing neurons expressed Fos in response to cortical activation.

Induction of immediate early genes. *In vitro* studies have demonstrated that the induction of immediate early genes can be regulated by calcium- or cAMP-mediated phosphorylation of the transcription factor CREB, which in turn binds to the enhancer elements (CRE) present on these genes (Morgan and Curran, 1986; Sheng and Greenberg,

1990; Sheng et al., 1991). The most parsimonious explanation for the cortically-driven induction of immediate early genes in the striatum is that glutamate from cortical terminals is released (Palmer et al., 1989) and causes sufficient depolarization of the postsynaptic striatal neuron for a sustained calcium rise through voltage-gated calcium channels at the soma. The resultant calcium rise would then trigger calcium/calmodulin-dependent kinases to phosphorylate CREB. P-CREB (the phosphorylated form) binding enhances transcription of IEGs, and subsequent translational events would culminate in the accumulation of protein which we visualize via immunohistochemistry. Even this minimalist cascade presents serious complexities, particularly when one considers the dynamic interactions among the various enzymes and substrates (Bray, 1995). It has been hypothesized for *in vitro* systems that the regulatory cascades may have resonant properties responsive to particular input frequencies (Sheng et al., 1993). Furthermore, because each cortical neuron gives only a few terminals to a given striatal neuron and because certain regions of the motor cortex converge on the same striatal neurons, whereas other regions, which could be adjacent, diverge, it is conceivable that the distance between electrodes, the surface of the area stimulated, and the location of each electrode will be determinant factors.

If we assume, as in the case of cultured cortical neurons, that the L-type calcium channels are responsible for the calcium influx necessary for IEG induction (Murphy et al. 1991), then certain predictions can be made. Because a given striatal neuron receives inputs from many cortical neurons, each only weakly effective, and because the majority of striatal neurons (i.e. projection neurons) are dominated by an inward-rectifier that shunts depolarization, at least a few hundred cortical cells would have to fire over roughly a 25 msec time scale (Wilson, 1995) in order to activate these high threshold-calcium channels.

Other relevant features of L-type calcium channels include an extremely slow rate of inactivation ($\tau \sim 0.5$ sec) and a voltage-sensitivity of inactivation below the range for activation (Tsien et al., 1988). Thus, in principle, calcium influx through L-type channels would be maintained for the duration of the somatic depolarization and would taper off on the order of 0.5 sec. However, considering the complexities of internal calcium

buffering within neurons, it would not be surprising if the effective calcium concentrations were more transient (Blaustein, 1988). Therefore trains of stimulation would be probably most effective when the train interval is less than 0.5 sec.

Calmodulin and calcium/calmodulin-dependent kinases, also thought to be important players in this scenario, exhibit interesting frequency-dependent properties of their own. Because of cooperative binding effects, kinase activity is greatly enhanced by calcium spike frequency, and displays a half-maximum of 0.5 calcium spikes/sec (Hanson et al., 1994).

Less still is known about the dynamics of CREB phosphorylation, IEG transcription, and subsequent translation, which requires at least 30 min (Cole et al., 1989; Graybiel et al., 1990). Long periods of stimulation may be required to prevent degradation or feedback and so maintain the levels of protein expression required for immunohistochemical detection. In conclusion, on the basis of only the calcium-dependent part of the cascade leading to eventual IEG induction, one might well imagine that an optimal stimulus would be one which caused bursts of cortical activity (on the order of 25 msec) to depolarize sufficiently striatal neurons for activation of L-type calcium channels. These bursts would ideally be spaced less than 500 msec apart in order to cooperatively influence calcium/calmodulin-dependent kinase activity (Fig. A.10).

Electrical stimulation. The parallel bipolar electrode configuration we chose was the most successful for eliciting IEG induction in the striatum, but was not ideal for studying the effects of stimulus area, because the resultant intensity profile was a complex function of placement with respect to neuronal elements, intraelectrode distance, and current intensity (Stark, 1962; Ranck, 1975; Hoeltzell, 1979; Asanuma, 1981; Yeomans, 1990). Furthermore, because the distribution of corticostriatal neurons and their terminations is nonuniform (Wilson, 1995), the variable of intraelectrode distance was itself confounded by the placement with respect to cortical areas. Even so, within the anterior motor cortex, we did observe a consistent relationship between intraelectrode distance and IEG induction. As shown in Fig A.1, increments of 0.5 mm determined a

noticeable difference in the intensity of induction of IEGs in cases that had been stimulated with the same current intensity. This supports our hypothesis that the induction of IEGs in a given striatal neuron heavily depends on the number of cortical neurons activated.

Our results concerning the frequency-dependence of IEG expression are consistent with the above argument. Continuous low frequency stimulation (10 pps), which stimulated movement, did not induce the expression of Fos or Jun B in the striatum. Continuous higher frequency stimulation at 40 pps, was more successful. It should be noted that this frequency is approximately that reported by Calabresi et al (1992) for LTD threshold in the striatum. Finally, one 250 pps train/ sec (either 40 msec trains so that train length was conserved or 160 msec trains so that number of pulses was conserved) was much less effective than four trains/sec, but not completely ineffective in inducing IEGs. One glaring problem with these experiments is that stimulation intensity is determined by the maintenance of a consistent, visible, discrete movement. It is well known, and was observed by us, that frequency, train duration and intensity of stimulation interact to produce behavioral effects (Yeomans, 1990). Although this does not pose a problem for false negatives involving continuous low frequency stimulation (which theoretically would require higher currents to induce movement), it does pose a problem for false negatives involving longer trains.

In general, the problem of spreading cortical excitation seriously limited these experiments. In fact, stimuli which were potentially epileptogenic were much more likely to induce IEGs in the striatum. Normal stimulation parameters for which we had to repeatedly increase the current to counteract habituation and continuous 10 pps stimulation were less effective than continuous 40 pps stimulation (which was quite sensitive to current and for which movements were not timelocked to the stimulus) and normal parameters for which we had to alternatively raise and lower the current to prevent more general seizure. This might very well be because these stimuli were equally "potentiating" the excitatory intracortical connections as well as the corticostriatal connections. At the frequencies used, synaptic potentiation is undoubtedly playing some

role in the observed response to electrical stimulation (Iriki et al., 1989, 1991; Nudo et al., 1990; Jacobs and Donoghue, 1991).

Chemical stimulation. The cerebral cortex contains dense reciprocal long- and short-range excitatory connections (Akers and Killackey, 1978; Chapin et al., 1987; Isseroff et al., 1984). It appears that an equally strong network of inhibitory neurons controls the spread of excitation in the cortex, probably by acting at GABA_A receptors. Bath application of GABA_A antagonists, such as bicuculline or picrotoxin, inhibit the fast inhibitory postsynaptic potentials which normally overlap with the excitatory postsynaptic potentials (e.p.s.p.) evoked by local stimulation. (Connors et al., 1988). If the concentrations applied are sufficient to block most of these receptors, external stimuli result in spreading bursts of regenerating activity that appear to originate from neurons in the deep cortical layers which are capable of intrinsic bursting (Connors, 1984). These waves of activity proceed across the cortex at a rate of approximately 0.07 m/s. This velocity appears to be limited by the threshold for synchronous activation of neuronal aggregates within the cortex (Chervin et al., 1988; Wadman and Gutnick, 1993).

In our experiments, the continuous infusion of picrotoxin into a local area of the cerebral cortex probably disinhibits that area and a small area of the surround, determined by the concentration gradient resulting from diffusion. The waves of excitation sweeping across this area would be stopped at this border by inhibitory interneurons receiving this excitation and controlling its spread, unhindered by the picrotoxin-blockade of GABAergic synapses.

At a theoretical rate of 0.07 m/s, such a wave would travel from one end of the 2.3 mm opening to the other in approximately 30 msec. This time scale is roughly equivalent to that of a corticostriatal e.p.s.p. and thus a range in which depolarization by individual corticostriatal synapses could summate (Wilson, 1995). As observed by the resulting motor activity, these waves recurred approximately every 2 seconds (with a wide standard deviation of 0.87 seconds), and thus is within the timescale proposed necessary for IEG induction.

The superior reliability of this method with respect to electrical stimulation probably stems from the fact that we are relying on endogenous cortical activity. To successfully artificially excite neuronal elements by electrical stimulation, positioning of the stimulus with respect to these elements becomes critical. Furthermore, electrical stimulation will indiscriminately activate all neurons, including inhibitory interneurons, which may then impede the resulting excitation.

NMDA receptors. Having built a simple hypothesis which relies solely on glutamate-induced depolarization reaching the soma of a given striatal neuron to induce voltage-gated influx of calcium, we now reach the problem that systemic administration of a NMDA receptor antagonist does block the striatal induction of IEGs.

Systemic administration, by definition means that the drug could be acting anywhere within the nervous system to affect the ultimate results of our experiments. In light of the fact that the corticostriatal excitatory postsynaptic potential is thought not to be mediated by NMDA receptors (Herrling, 1985), it is most likely that MK-801 is acting intracortically to suppress sufficient excitation of corticostriatal neurons. In support of this suggestion, IEG induction in cerebral cortical areas outside the immediate area of picrotoxin application was greatly reduced or abolished by MK-801. However, animals which had received MK-801, still exhibited motor tics after application of picrotoxin, so the issue is more complex and awaits local application of glutamate antagonists within the CNS to be resolved.

We did attempt intrastriatal injection of MK-801 but found by exposure of sections to film after injection of tritiated MK-801, that the substance largely disappears from the area 10 minutes after injection (data not shown), and thus would have to be continuously infused in order to be valuable for these experiments.

IEGs and function. Evidence is accumulating which suggests that transcription factor IEGs play a physiological role in the normal functioning of the nervous system. In the

mouse hippocampus, for example, increased expression of c-fos and c-jun mRNAs has been observed during learning of a bar-pressing task (Heurteaux et al., 1993). Increased c-fos mRNA levels have also been observed in the rat hippocampus after training to attain foot-shock-motivated brightness discrimination (Tischmeyer et al., 1990). There are many other examples of correlation between IEG induction and learning. However, issues of stress and arousal state confound many of these studies and a causal role has yet to be established (Hughes and Dragunow, 1995). Interestingly, recent experiments with c-fos antisense suggest a role in controlling motor functions of the basal ganglia. Injections of c-fos antisense into the nucleus accumbens can block the stimulatory effect of cocaine on locomotor activity (Helig et al., 1993).

More and more evidence is accumulating to support a role for the striatum in conditioned learning. If the striatum is in fact a storage place for certain forms of memory, one would expect, as in the case of the hippocampus, that long term changes in neuronal connections be manifested in altered gene regulation. In this case, all neurons in the striatum probably would not be affected equally by one type of afferent input. Indeed, while striatonigral cells are known to receive cortical input (Freund et al., 1984) and the majority of striatonigral cells are thought to contain substance P and dynorphin (Graybiel and Ragsdale, 1983; Gerfen et al., 1990), we have found that cortical afferents do not induce the expression of Fos in these neurons. Instead, the other type of projection neuron, the enkephalinergic neuron, strongly expresses the majority of cortically-driven Fos in the striatum. Furthermore, a differential effect on the spatial distribution of interneurons in which Fos is induced has been found. We have, of course, only examined the complete induction profile of one immediate early gene. Undoubtedly, other genes will have other expression patterns. Such a scheme of cortical regulation of gene expression, in combination with the interactions of other afferent systems could be one of the keys to understanding long-term effects of inputs to the striatum on its neural processing.

Complex and diversified effects of motor cortex activation on the expression of IEGs was also found in other structures such as the thalamus, the nucleus accumbens and the target structures of the striatum. In the reticular nucleus of the thalamus, there was

strong induction of NGFI-A and Fos, but not of Jun B. In the nucleus accumbens, there was an intense induction of Jun B and NGFI-A, whereas Fos was much weaker and less consistently induced. In the target structures of the striatum, Fos and NGFI-A were always induced, but never Jun B. These differences indicate that the effects on gene regulation by cortical activity are very selective and much more complex than could be predicted by the assessment of a simple excitatory postsynaptic potential caused by glutamate release.

Table A.1. Summary of electrical stimulation experiments. Unless otherwise noted on the side-bar descriptions, all experiments had the same stimulation parameters: 40 msec trains, 4 trains per second, 250 pps within a train, biphasic, 0.2 msec pulse width per phase. Listed in part **A** are the experiments conducted as acute procedures, using Nembutal anesthesia. Included are all cases in which the train frequency was lowered to 0.067 trains/sec (one train every four seconds) and in which no induction was seen. The remainder of the experiments, listed in parts **B**, **C**, and **D** were performed on awake rats, in the cortices of which we had previously implanted electrodes. They are divided in to the following groups: **B**) experiments in which practically no Fos and only very sparse Jun B was induced in the dorsolateral motor-cortex recipient quadrant. Included in this category are cases in which the stimulation was applied for shorter periods, cases in which stimulation induced rapid habituation, cases in which stimulation parameters were changed to continuous low frequency, and some of the cases in which standard parameters were used and in which the train frequency was reduced to one per second. **C**) experiments in which Fos and Jun B were induced in the dorsolateral quadrant. Included in this category are cases in which train frequency was reduced to one per second, cases in which stimulation was changed to continuous intermediate frequency, and cases in which standard parameters were used. **D**) experiments in which Jun B (and often Fos) was strongly induced throughout the striatum. Included in this category are cases in which stimulation induced generalized seizures or strong bilateral movements of the forelimbs. * = sparse, ** = strong, well localized, ***= strong throughout, G = generalized seizure occurred, W = movement was weak or habituating, N = no seizure (normal), U = unknown, C = rhythmic movements included contralateral limb, Str = striatum, stim = stimulus.

A. Electrical stimulation to induce Fos in rats, anesthetized with Nembutal

	Case	distance between electrodes	coordinates	intensity (range) μ A	stim duration	total survival time	movements	Fos induction in the striatum
one train every four seconds	R1 (HP15)	1.5 mm	MI (A-1,A1; L2; H1.7)	300-350	1.5 hrs	2 hrs.	forelimb	none
	R2 (HP16a)	1.5 mm	MI (central)	500	1 hr	2 hrs	forelimb	none
	R3 (HP16b)	1.5 mm	MI (central)	500	1 hr	2 hrs	forelimb and whisker	none
	R4 (HP16c)	1.5 mm	MI (rostral)	50	1 hr	2 hrs	whisker	none
	R5 (HP17a)	1.5 mm	MI (central)	500	1 hr	1.5 hrs	forelimb	lateral striatum**
	R6 (HP17b)	1.5	MI (central)	500	1hr	2 hrs	forelimb	lateral striatum**
	R7 (HP18a)	1.5	MI (central)	500	1 hr	2 hrs	whiskers	lateral striatum**
	R8 (HP22a)	0.5	MI (A0,A2;L2.5;H1.4)	300	1 hr	2 hrs	forelimb	lateral striatum *
standard parameters	R9 (HP22b)	0.5	SI (P0.3,P2.3; L4.1;H1.3)	300	1 hr	2 hrs	none	0
	R10 (HP23a)	1	MI (A0.7,A2.7, L2.4,H1.4)	300	1 hr	2 hrs	forelimb flexion	lateral striatum **
	R11 (HP23b)	1	MI(A0.4,A2.5; L2.4; H1.5)	500	1 hr	2 hrs	forelimb flexion	lateral striatum**
	R12 (HP25a)	1	A1.7,A3.7; L0.4; H3.0	500	1 hr	2 hrs	bilateral whiskers	medial striatum**
	R13 (HP25b)	1	MI (P0.5,A1.5; L2;H1.3)	500	1 hr	2 hrs	forelimb	lateral striatum*
	R14 (HP26a)	1	A1.7,A3.7 L0.4;1.0	500	1 hr	2 hrs		medial striatum**
	R15 (HP26b)	1.5	A2.6,A4.6, L0.5, H3.0	500	1 hr	2 hrs		medial striatum**
	R16 (HP26c)	1.5	A2.7,A4.7; L3.0; H3.0	500	1 hr	2 hrs	faint whisker twitches	medial striatum***

C. Cases in which electrical stimulation induced Fos in the topographically correct region of the striatum

	Case	distance between electrodes (mm)	coordinates	intensity (lowest) μ A	intensity (highest) μ A	stim duration (min)	total survival time (min)	Fos (Str)	Jun B (Str)	Seizure?	Cortical lesion?	movements
one train per second (40 msec)	R34 (HPSB245)	2	A0.5,A2.5; L3; H2	110	130	60	120	*	*	N		proximal forelimb and head
	R35 (HPSB243)	2	A0.5,A2.5; L3; H2	120	150	60	120	*	**	W		very small forelimb mvmts
	R36 (HPSB246)	2	A0.5,A2.5; L3; H2	70	90	60	120	*	0	N		forelimb and head
cont. 40 pps	R37 (HPSB248)	2	A0.5,A2.5; L3; H2	110	140	60	120	*	**	N	Y	forelimb and head
	R38 (HPSB241)	2	A0.5,A2.5; L3; H2	55	70	60	120	**	**	W		intermittent hand tremor, some head (30 min)
	R39 (HPSB238)	2	A0.5,A2.5; L3; H2	60	135	60	120	*	0	W	Y	discrete hand clenching movements (weak) throughout
standard parameters, well controlled movement	R40 (HPSB250)	2	A0.5,A2.5; L3; H2	70	100	60	120	*	0	N	Y	forelimb and head
	R41 (HPSB204)	2	A0.5,A2.5; L3; H2	50	50	60	120	*	*	N		consistent distal forelimb (45 min)
	R42 (HPSB155)	1.5	A0.5,A2; L3;H2.4;H2	40	60	120	120	*	*	N		forelimb and head
	R43 (HPSB110)	1.6	A0.5; L1.L2.6; H0.7	400	400	60	120	*	**	N		forelimb and whiskers
	R44 (HPSB126)	2.5	A2, A4.5; L3;H2	200	200	60	120	*	**	N		forelimb and head
	R45 (HPSB151)	1.5	A0.5,A2; L3;H?	65	90	120	120	*	**	N		forelimb and head (30 min)
	R46 (HPSB233)	2	A0.5,A2.5; L3; H2	75	95	60	120	**	**	N		forelimb/hand
R47 (HPSB154)	3	P1.A2; L2.L2.5; 3; H2	80	140	120	120	**	**	N		hindlimb and forelimb	
standard parameters; spreading excitation to ipsilateral limbs	R48 (HPSB235)	2	A0.5,A2.5; L3; H2	130	150	60	120	**	**	C		both forelimbs (proximal) and head
	R49 (HPSB105)	3	A0.5;L1.L4; H1.6	200	400	60	120	**	**	C		both forelimbs
	R50 (HPSB109)	1.6	A0.5; L1.L2.6; H1.7	100	400	60	120	**	**	C		both forelimbs
	R51 (HPSB142)	2	A0.5,A2.5; L3; H2.5	75	110	120	120	**	**	C		both forelimbs and head
	R52 (HPSB152)	1.5	A0.5,A2.5; L3; H?	90	100	120	120	**	**	C		both forelimbs and head
stimulation triggered 60/100 pps	R53 (HPSB153)	1.5	A0.5,A1.5; L3.L3.5; H2.1	50	68	120	120	**	**	G		both forelimbs and head
	R54 (HPSB203)	2	A0.5,A2.5; L3;H2	70	130	60	120	**	**	G		forelimb

D. Cases in which electrical stimulation induced Jun B (and usually Fos) throughout the striatum

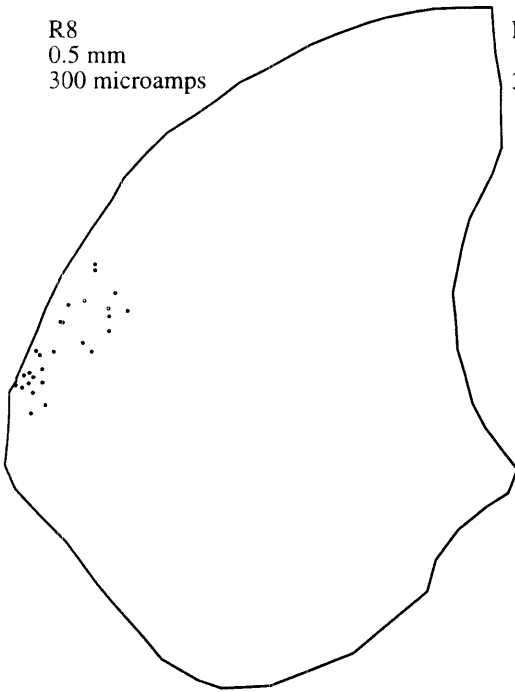
	Case	distance between electrodes (mm)	coordinates	intensity (lowest) μ A	intensity (highest) μ A	stim duration (min)	total survival time (min)	Fos (Str)	Jun B (Str)	Seizure?	Cortical lesion?	movements
short stimulation period, with spreading excitation	R55 (HPSB058)	2	A0.A2; L=2 H1.8	200	200	10	70	*	***	C		both forelimbs
	R56 (HPSB130)	2.5	A0. A2.5; L1.5:H1.7	150	200	30	120	*	***	G		whiskers
	R57 (HPSB057)	1.5	A0. A1.5; L2; H=1.8	150	150	30	90	***	***	C		both forelimbs
	R58 (HPSB128)	2.5	A2. A4.5; L3:H2	200	200	40	120	***	***	G		forelimb
standard parameters	R59 (HPSB115)	2	A0.5; L1.L3; H1.7	200	200	60	120	*	***	?		forelimb flexion
	R60 (HP29A)	2	M1. H0.7	200	200	60	120	**	***	C		both forelimbs
	R61 (HPSB117)	2	A0.5; L1.L3; H1.7	200	200	60	120	***	***	G		forelimb
	R62 (HPSB127)	2.5	A2. A4.5; L3:H2	200	200	60	120	***	***	G		forelimb
	R63 (HPSB206)	2	A0.5.A2.5; L3:H2	40	90	60	120	***	***	G		forelimb

Table. A.2. Summary of IEG induction observed in the forebrain after application of picrotoxin to the motor cortex. Number of * symbols indicates relative amount of induction observed.

Structure	Fos Jun B NGFI-A		
Caudoputamen	***	***	****
Cortex	****	***	*****
Nucleus Accumbens	*	****	***
Globus Pallidus	*	-	*
Entopeduncular Nucleus	**	-	**
Substantia Nigra	**	-	*
Subthalamic Nucleus	***	-	**
Thalamus	***	*	***
Amygdala	**	**	*

Figure A.1. Transverse sections through the caudoputamen representing cases for which different intraelectrode distances were used to electrically stimulate the motor cortex. Induction of Fos in the striatum by electrical stimulation depends on the distance between parallel bipolar electrodes placed in the motor cortex. Identical stimulation parameters were conserved between R8 and R10 and electrode distance was varied (R8 = 0.5 mm, R10 = 1.0 mm). Likewise, between R11 and R7 all conditions were identical except electrode distance (R11 = 1.0mm, R7 = 1.5 mm). Because these animals were anesthetized during the stimulation procedure, there is little or no induction observed along the medial edge of the striatum, as observed bilaterally in animals stimulated while awake (see Fig. A.2). Sections with the greatest number of Fos-positive nuclei were chosen and all visible nuclei were charted at 5x on the Eutectics imaging system.

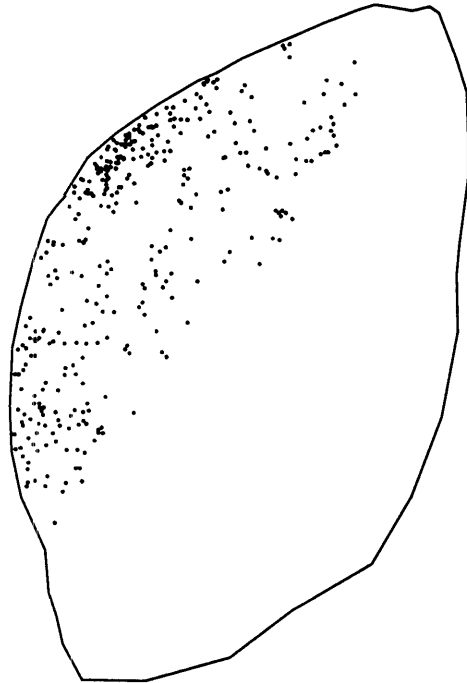
R8
0.5 mm
300 microamps



R10
1.0 mm
300 microamps



R11
1.0 mm
500 microamps



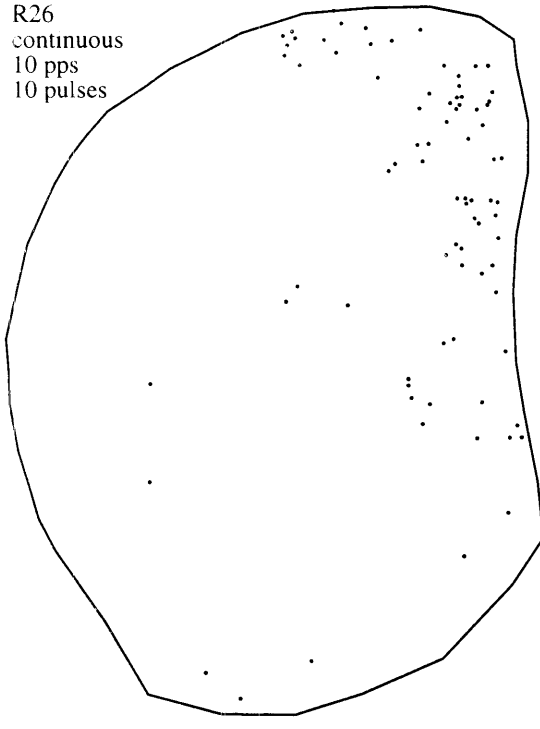
R7
1.5 mm
500 microamps



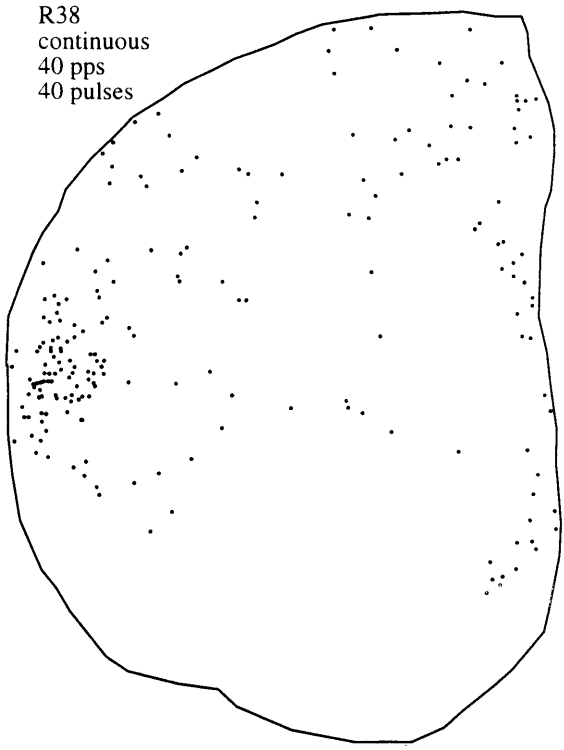
1 mm

Figure A.2. Transverse sections through the caudoputamen representing cases for which different stimulation parameters were tested. All conditions of electrical stimulation in awake rats caused the induction of Fos along the medial edge of the striatum. This was observed bilaterally (not shown) and was probably stress-related. However, stimulation of the forelimb representation of motor cortex at continuous low frequency (R26, 10 pps) did not induce Fos expression in the topographically correct lateral quadrant. Continuous stimulation at higher frequency (40 pps, R38) was more effective, as was high frequency stimulation grouped in trains (R34 and R37). Sections with the greatest number of Fos-positive nuclei were chosen and all visible nuclei were charted at 5x on the Eutectics imaging system.

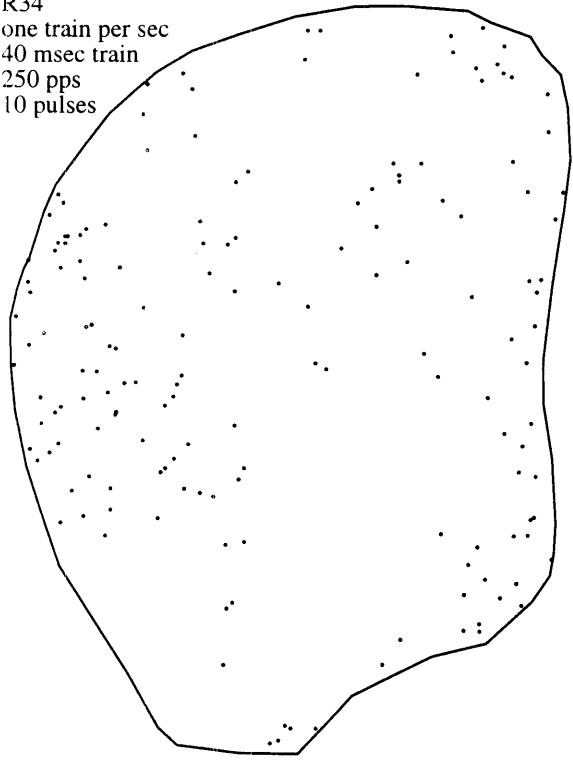
R26
continuous
10 pps
10 pulses



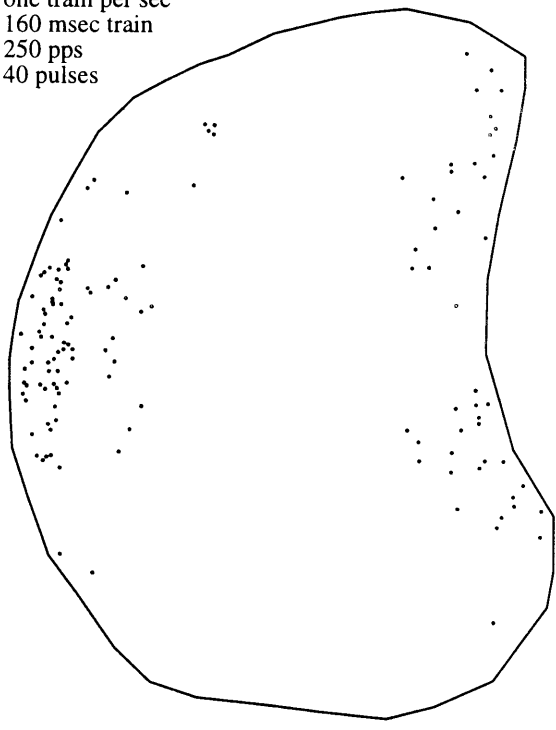
R38
continuous
40 pps
40 pulses



R34
one train per sec
40 msec train
250 pps
10 pulses



R37
one train per sec
160 msec train
250 pps
40 pulses



1 mm

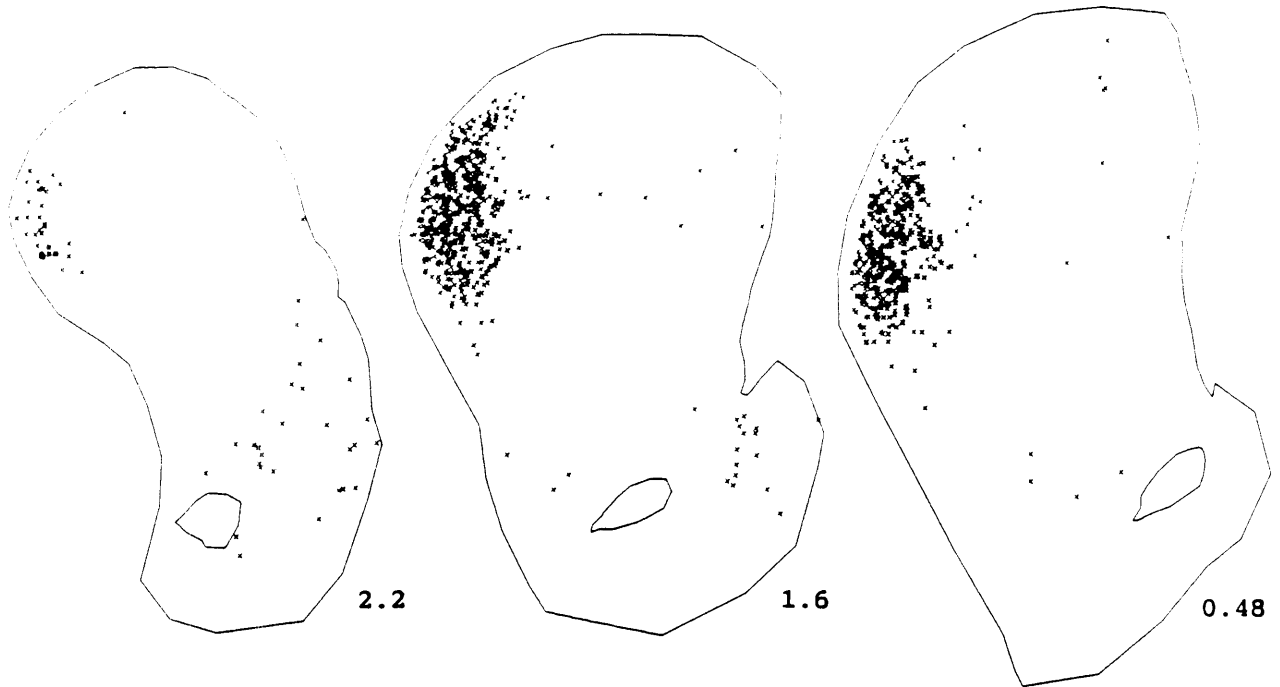
Figure A.3a. Activation of the motor cortex by electrical stimulation induced the expression of Fos in the dorsolateral caudoputamen.



Figure A.3b. Activation of the motor cortex by local epidural application of the GABA_A antagonist picrotoxin induced the expression of Fos in a pattern quite similar to the pattern of expression induced by electrical stimulation of the motor cortex (compare with Fig. A.3a., case R42). The wedge of Fos induction in the dorsal cortex, which includes all layers, is somewhat sharper in the case of non-invasive epidural picrotoxin application (shown here) as compared to electrical stimulation via implanted electrodes (Fig. A.3a).



Figure A.4a. A series of transverse sections illustrating the pattern of Fos expression induced in the striatum by electrical stimulation of the motor cortex in a representative case (R51). Numbers below each section indicate the approximate anteroposterior distance of the section from bregma (Paxinos and Watson 1986). Sections were charted on the Biocom imaging system, to include only nuclei stained above a certain threshold value (see methods).

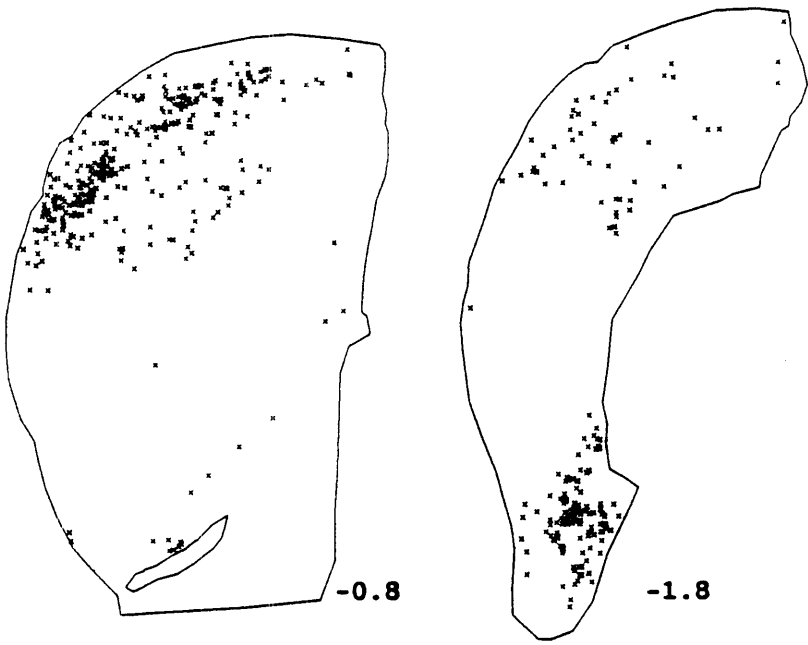
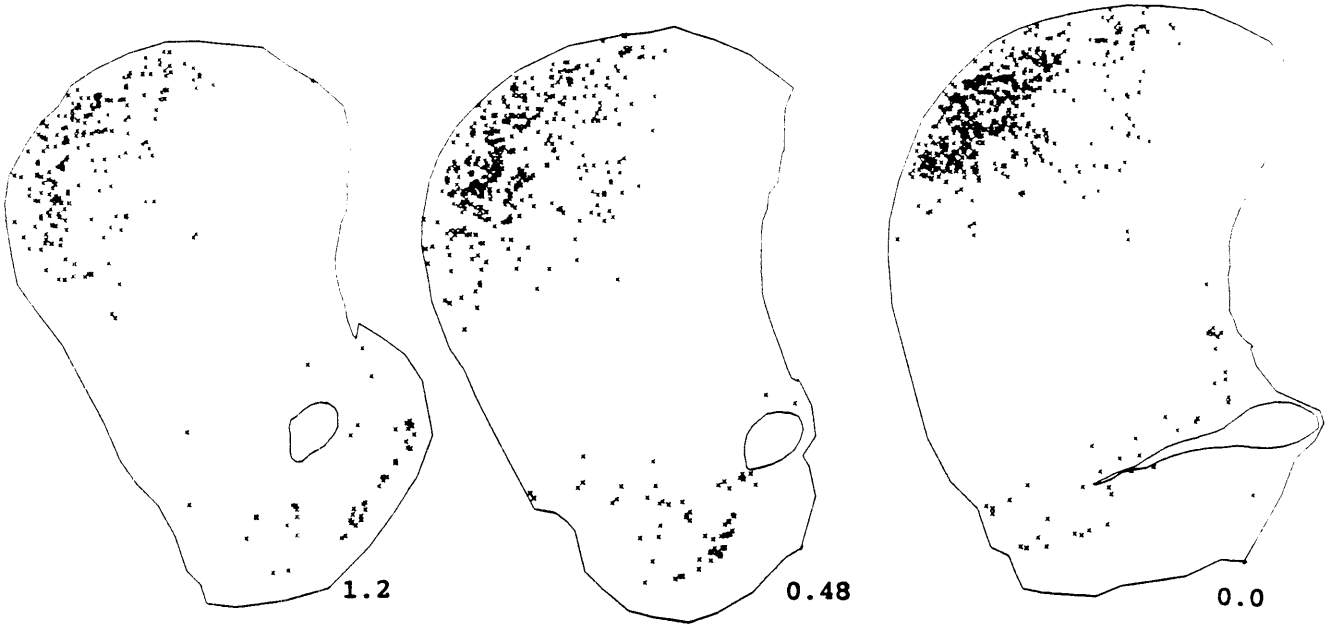


electrical stimulation

FOS-li

1000 Microns

Figure A.4b. A series of transverse sections illustrating the pattern of Fos expression induced in the striatum by epidural application of picrotoxin to the motor cortex in a representative case. Numbers below each section indicate the approximate anteroposterior distance of the section from bregma (Paxinos and Watson 1986). Sections were charted on the Biocom imaging system, to include only nuclei stained above a certain threshold value (see methods).



picrotoxin

FOS-li

1000 Microns

Figure A.5. Application of picrotoxin to the motor cortex resulted in an induction of Fos which was dependent on the concentration of picrotoxin tested. **A.** Concentrations of picrotoxin below 0.05 mM did not induce the expression of Fos in the striatum. 0.1 mM was of intermediate effectiveness as compared to 0.3 mM. **B.** Transverse sections through representative cases in which the concentration of picrotoxin applied to the motor cortex was varied. Sections were charted using the Biocom imaging system, to include only nuclei stained above a certain threshold intensity (see methods).

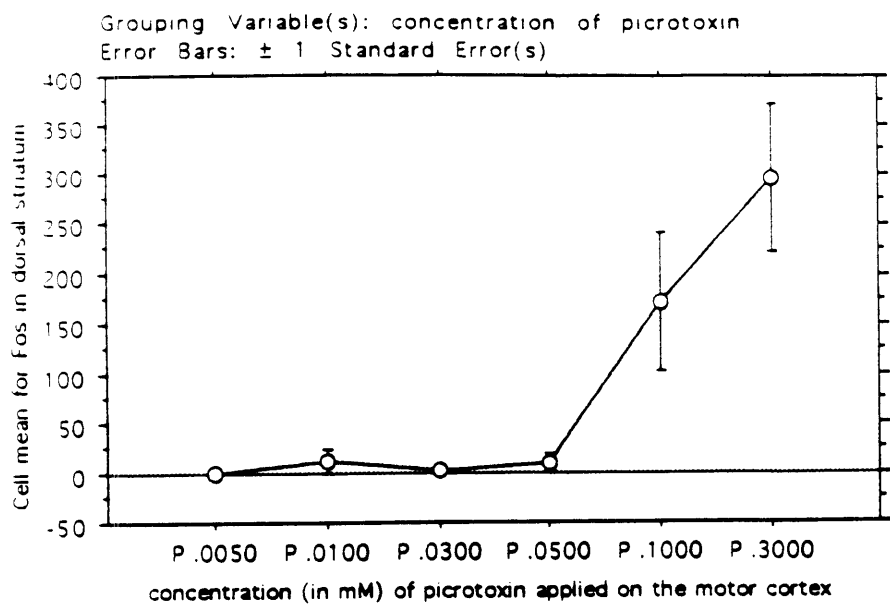
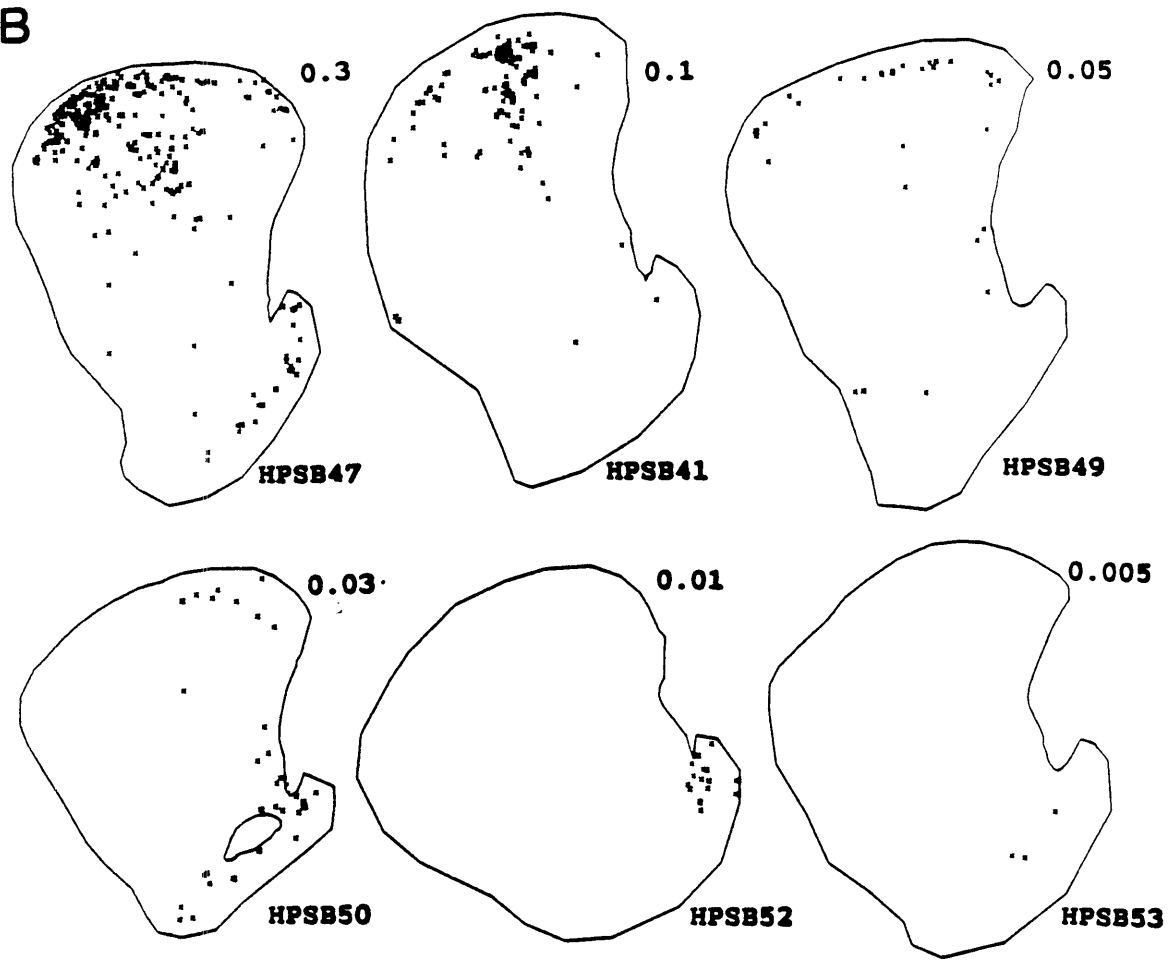
A**B**

Figure A.6. Transverse sections through two representative cases (**A** and **B**) comparing the distribution of different immediate early genes induced by application of picrotoxin to the motor cortex. Sections were charted using the Biocom imaging system, to include only nuclei stained above a certain threshold intensity (see methods).

Fos

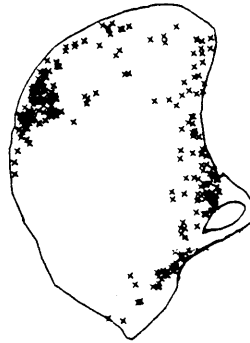
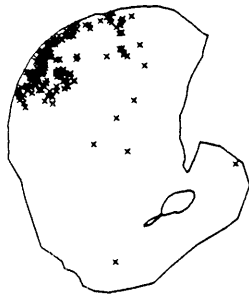
Jun B

NGFI-A

A



B



picrotoxin

1000 Microns

Figure A.7. Distribution of striatal neurons expressing Fos in response to epidural application of picrotoxin to the motor cortex. The majority of the Fos-positive nuclei are found in enkephalinergic neurons. Parvalbumin-containing neurons are much more sparsely distributed in the striatum, but were found to express most of the remaining Fos. NADPH-diaphorase-containing interneurons and dynorphin-containing projection neurons make up the remainder of the population of neurons in which Fos was induced. Note that no Fos induction was observed in calretinin-containing or cholinergic interneurons.

Distribution of striatal neurons expressing Fos after picrotoxin-induced activation of the cortex

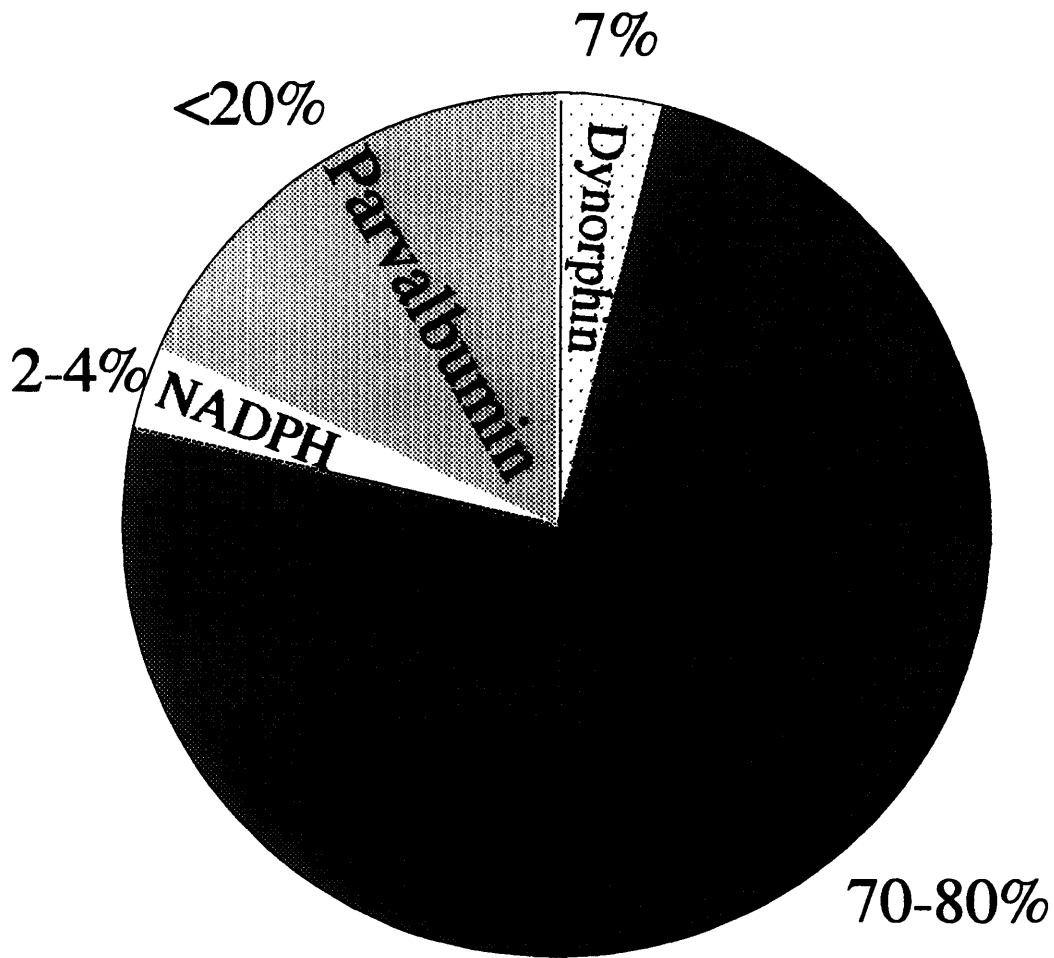


Figure A.8. Epidural application of picrotoxin to the motor cortex induces Fos in only certain types of striatal interneurons. Photomicrographs illustrate the colocalization of Fos with antigenic markers of different striatal neurons. Double-labeled neurons are indicated by arrows, Fos-positive nuclei alone are indicated by arrowheads, and neurons not containing Fos are indicated by curved arrows. Most of the parvalbumin-containing neurons (**A**) within the field of Fos induction strongly expressed Fos. Many NADPH-diaphorase-containing neurons also expressed Fos (**D**). In contrast, Fos was never expressed by cholinergic (**B**) or calretinin-containing (**C**) interneurons. Scale bar is 20 microns.

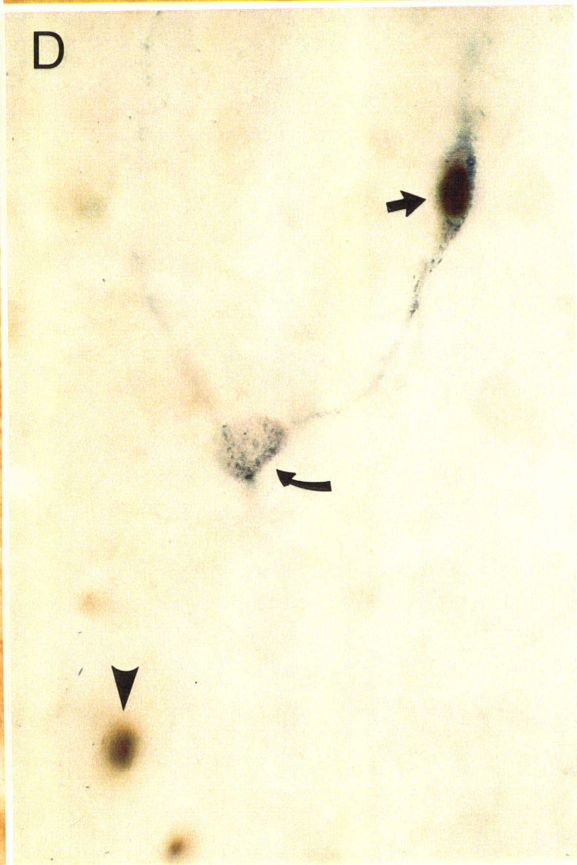
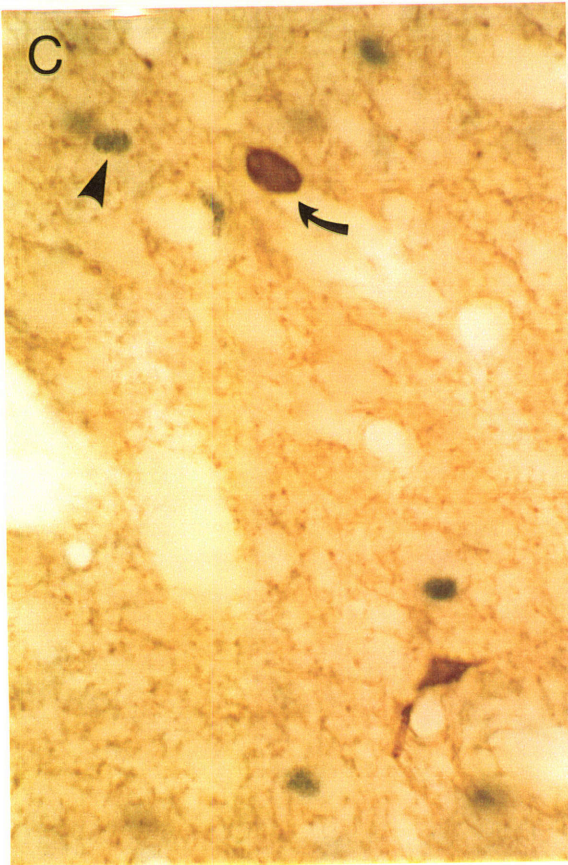
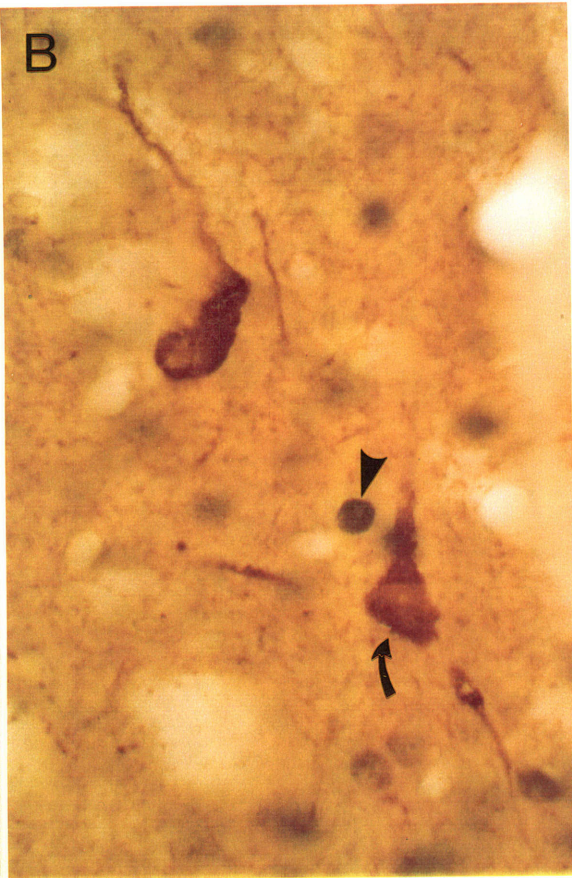
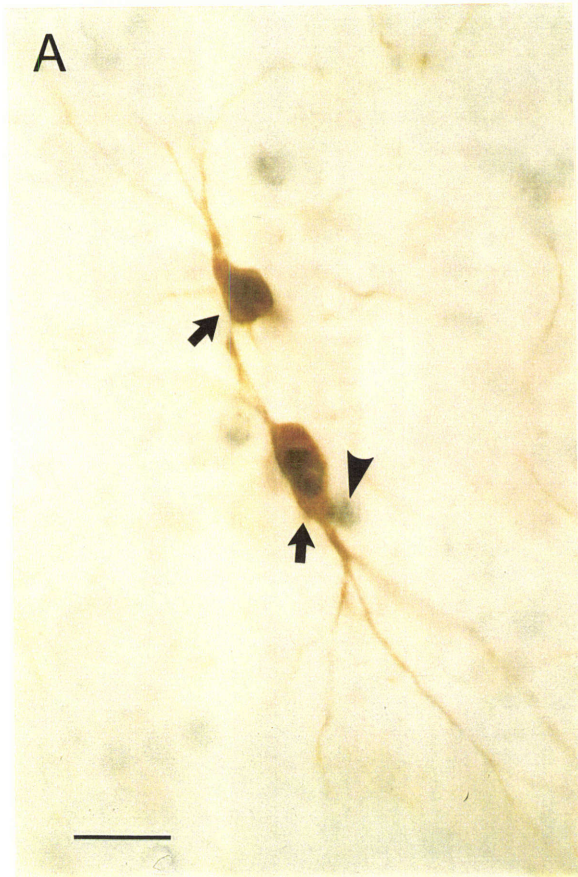


Figure A.9. Epidural application of picrotoxin to the motor cortex induces Fos in only certain types of striatal projection neurons. Photomicrographs illustrate the colocalization of Fos with antigenic markers of different striatal neurons. Double-labeled neurons are indicated by arrows, Fos-positive nuclei alone are indicated by arrowheads, and neurons not containing Fos are indicated by curved arrows. **A.** All Fos-positive nuclei (black dots) in this field are found in enkephalinergic neurons (brown), although some not all enkephalinergic neurons expressed Fos. **B.** Dynorphin-containing neurons rarely expressed Fos. In this field, the two clearly visible dynorphin-containing neurons (brown) have unstained nuclei. Scale bar is 20 microns.

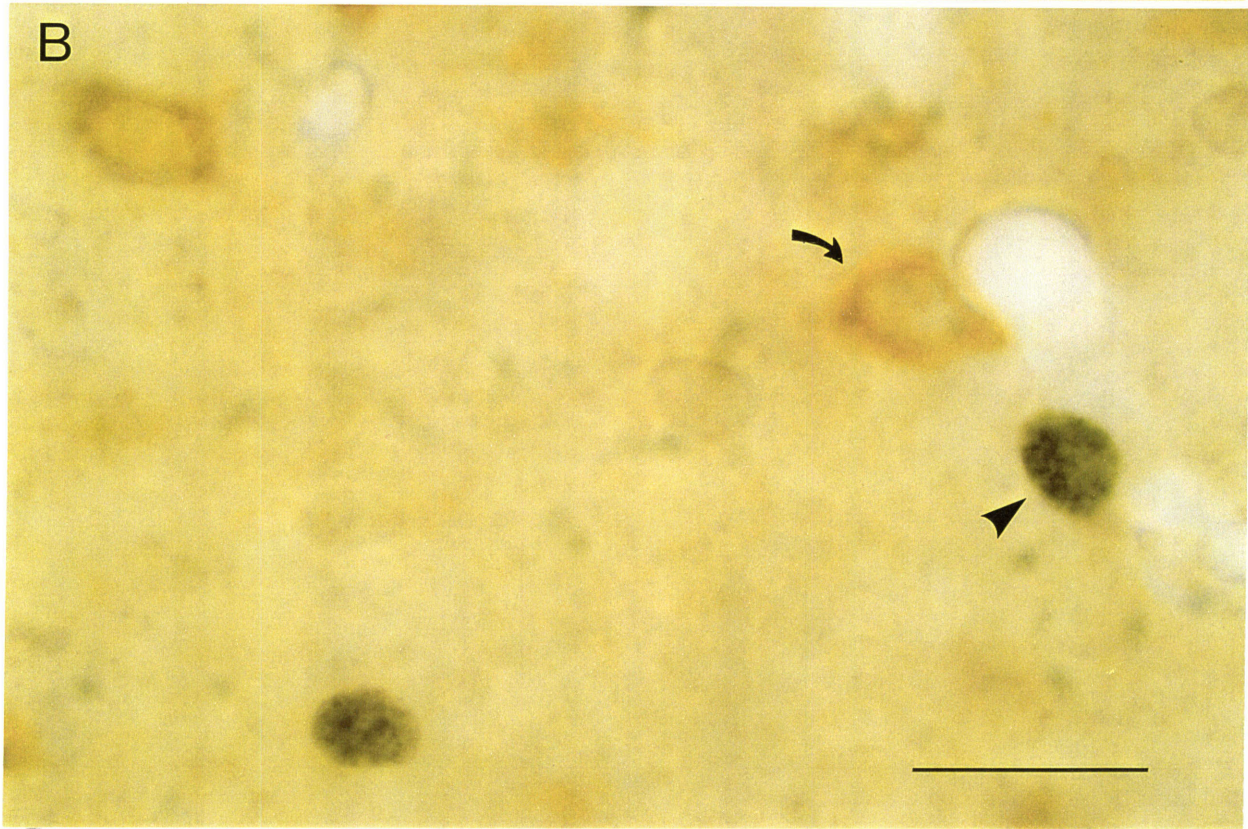
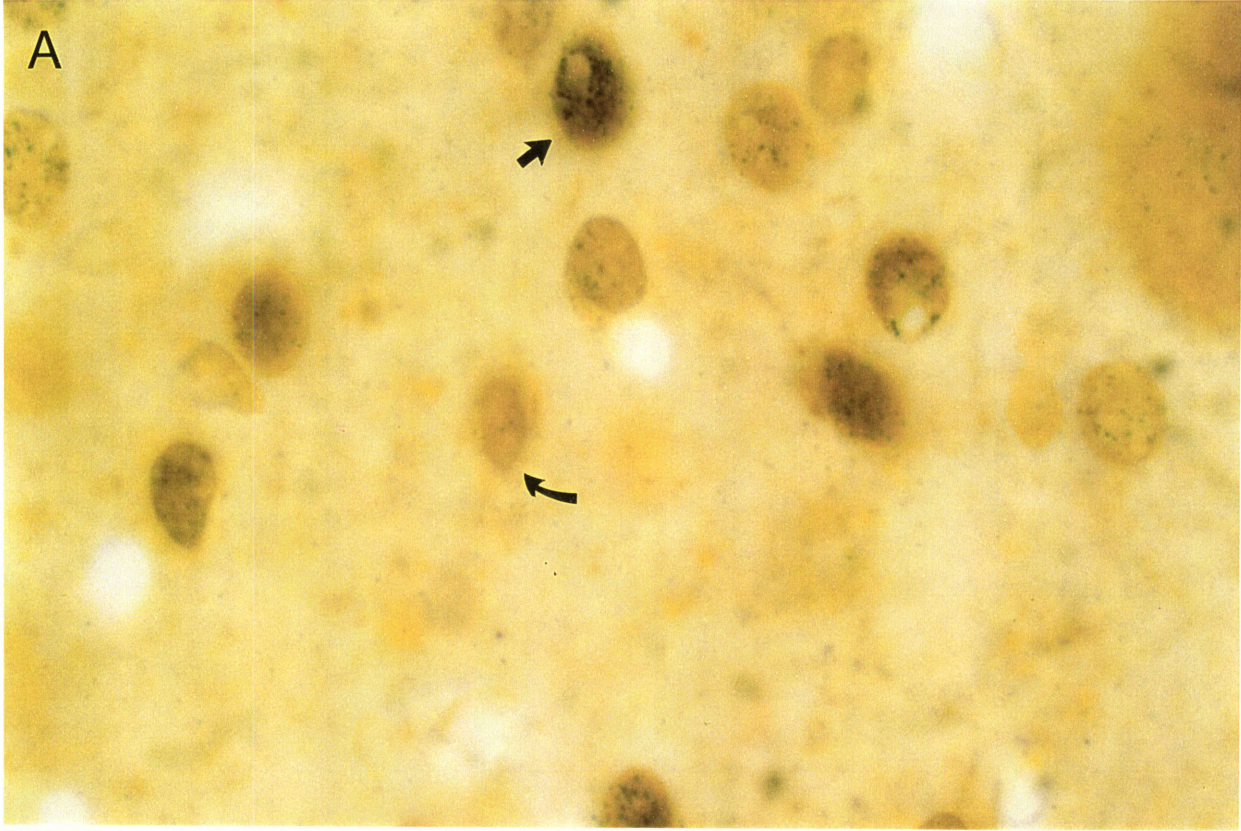


Figure A.10. Bar graph showing the effect of systemic administration of the NMDA antagonist MK-801 on the induction of immediate early genes in the striatum by the application of picrotoxin to the motor cortex. Induction of all immediate early genes was reduced by MK-801 (dense dot pattern) as compared to controls (sparse dot pattern). v+p = systemic administration of vehicle, m+p = systemic administration of MK-801.

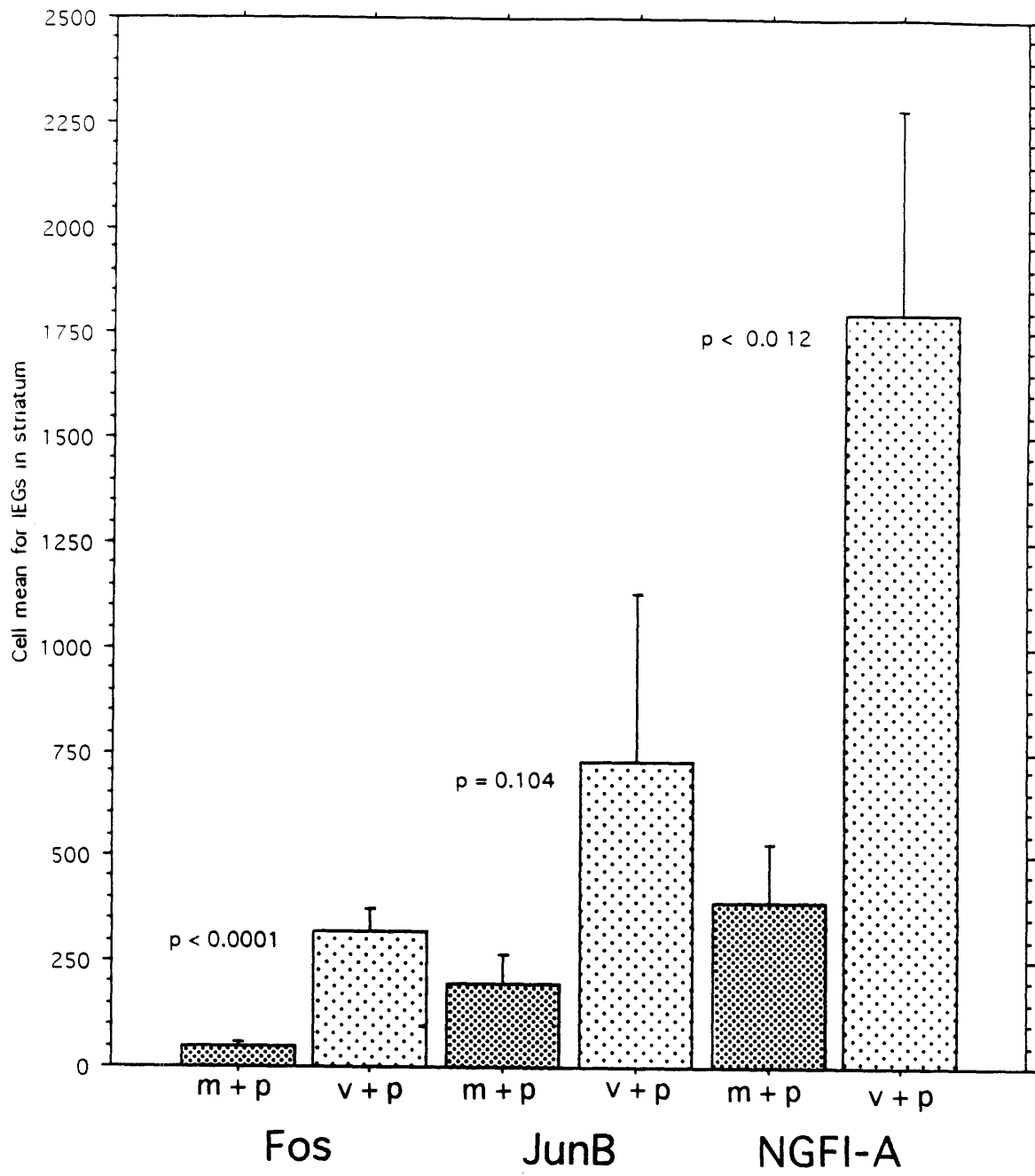


Figure A.11. Illustration of a possible route by which cortical activity affects the induction of immediate early genes in striatal neurons. Summation of glutamatergic depolarization at corticostriatal synapses leads to depolarization of the striatal neuron and opening of voltage-gated calcium channels. Calcium accumulates sufficiently to cause calcium/calmodulin-dependent phosphorylation of the DNA-binding protein, CREB, which can then enhance the expression of *c-fos*. *Lower left:* Diagram modified from Hanson et al. (1994) showing the cooperative effect of calcium/calmodulin on the kinase activity. Rapid discharge bursts cause the repeated longer duration calcium spikes which cause the augmentation of calcium/calmodulin-dependent kinase activity.

